THERMODYNAMIC AND KINETIC PARAMETERS THAT EXPLAIN CRYSTALLIZATION AND SOLUBILITY OF PHARMACEUTICAL COCRYSTALS

by

Sarah Jean Bethune

A dissertation submitted in partial fulfillment
of the requirements for the degree of
Doctor of Philosophy
(Pharmaceutical Sciences)
in The University of Michigan
2009

Doctoral Committee:

Associate Professor Naír Rodríguez-Hornedo, Chair
Professor Gordon L. Amidon
Professor David E. Smith
Associate Professor Adam J. Matzger
Associate Professor Steven P. Schwendeman
Research Professor Gregory E. Amidon

Dedicated to my mom who always taught me to strive for excellence

ACKNOWLEDGEMENTS

I would like to take this opportunity to thank those who helped make this thesis and my five years at the University of Michigan a reality. I am grateful for everyone's dedication and support throughout these five years. First and foremost, I thank my research advisor, Dr. Naír Rodríguez-Hornedo. She is the model of inspiration! Her excitement about supramolecular chemistry convinced me to come to this university and ultimately join her lab. She has been a terrific mentor, I have profound respect for her and her research, and I hope to always be her colleague and friend. I would like to acknowledge my dissertation committee, Dr. Gordon Amidon, Dr. David Smith, Dr. Greg Amidon, Dr. Adam Matzger, and Dr. Steve Schwendeman, for their insightful discussions and suggestions.

This doctoral research was made possible by financial contributions from the Rackham Graduate School Board of Regents Fellowship, the Pharmacological Sciences Training Program (GM07767 from NIGMS), the American Foundation for Pharmaceutical Education Fellowship, and the Warner Lambert/Park Davis College of Pharmacy fellowship.

My interest for science began with classes from Dr. Mark Vitha and Dr. Nita Pandit at the Drake University. Their scientific passion plus canny ability to lead a well-rounded life has been imparted onto me, and I will be forever grateful. If I become a professor some day, I hope to influence my students as positively as they influenced me.

I am very grateful for discussions about solution complexation with Dr. Kenneth Connors from the University of Wisconsin. His expertise helped to enhance the analysis and discussion in my first paper published in *Crystal Growth & Design* (Chapter 2). I'd like to say a special thanks to past and present members of the Rodríguez lab: Barbara Rodríguez Spong, Kurt Seefeldt, Adivaraha (Jay) Jayasankar, Sreenivas Reddy, Dave Good, Chinmay Maheshwari, Phil Zocharski, Neal Huang, and Lilly Roy. I have great memories of working, laughing, and revising papers together. I would like to particularly like to thank Jay, who joined the department at the same time as I did. My graduate research experience would not have been as rewarding, enriching, or as fun without him.

The love and support from my family and friends have encouraged me throughout these five years. My mom and dad were always there for me and instilled the value of an education at an early age. My sister has always been there for me if I need to talk, no matter what time of the day. I would like to thank my friends—Kendra, Amberlyn, Tasneem, Carrie, Chris, and Nick—who have provided much needed outlets along the way, whether it's a late night Arby's milkshake, a new card game, or a ride in a truck to take my mind off of research for a bit. Most of all, I thank my husband, Matt, for his utmost love and patience as I complete my degree. He has been here for me through all my times of laughing and crying; he has helped me slow down and appreciate the small yet significant moments in life; he celebrated every achievement throughout education and beyond; and he has waited to start his post-education goals until I finished mine. I am eternally grateful to have you in my life. I love you.

Finally, a note to the reader: parts or sections of the chapters presented in this dissertation have been published in the following articles:

- Nehm, S.; Rodríguez-Spong, B.; Rodríguez-Hornedo, N. Phase Solubility Diagrams of Cocrystals Are Explained by Solubility Product and Solution Complexation. *Cryst. Growth Des*. **2006**, 6, 592-600.
- Rodríguez-Hornedo, N.; Nehm, S; Seefeldt, K.; Pagán, Y.; Falkiewicz, C. Reaction Crystallization of Pharmaceutical Molecular Complexes. *Mol. Pharm*. **2006**, 3, 362-367.
- Rodríguez-Hornedo, N.; Nehm, S. J.; Jayasankar, A. Cocrystals: Design, Properties and Formation Mechanisms. In *Encyclopedia of PharmaceuticalTechnology,* 3rd ed.; Swarbrick, J., Eds.; Informa Health Care: New York, **2006**, pp.615-635.
- Rodríguez-Hornedo, N.; Nehm, S.; Jayasankar, A. Process Analytical Technologies to Analyze and Control Crystallization. *Am. Pharm. Rev.* **2007**, 10, 46-55.
- Reddy, L.S.; Bethune, S.; Kampf, J.; Rodríguez-Hornedo, N. Cocrystals and Salts of Gabapentin: pH-dependent cocrystal stability and solubility. *Cryst. Growth Des*. **2009**, 9, 378-385.

TABLE OF CONTENTS

LIST OF FIGURES

LIST OF TABLES

CHAPTER ONE

INTRODUCTION

Background and Significance

The design of pharmaceutical crystals that possess different molecular components is valuable to control pharmaceutical properties of solids without changing covalent bonds. Cocrystals, multiple component crystals, often rely on hydrogen-bonded assemblies between neutral molecules of the active pharmaceutical ingredient (API) and other components with well-defined stoichiometries (Etter 1991; Caira 1992; Desiraju 1995; Nangia and Desiraju 1998; Byrn, Pfeiffer et al. 1999; Aakeroy, Beatty et al. 2002; Almarsson and Zaworotko 2004; Wenger and Bernstein 2008). Therefore, cocrystals increase the diversity of solid-state forms of an API even for non-ionizable APIs, and enhance pharmaceutical properties by modification of chemical stability, moisture uptake, mechanical behavior, solubility, dissolution rate, and bioavailability (Remenar, Morissette et al. 2003; Rodríguez-Spong, Zocharski et al. 2003; Childs, Chyall et al. 2004; Rodríguez-Spong, Price et al. 2004; Zocharski, Nehm et al. 2004; Rodríguez-Spong 2005; Trask, Motherwell et al. 2005; Nehm, Rodríguez-Spong et al. 2006).

Families of API cocrystals are being designed and prepared by applying molecular recognition, thermodynamic, and kinetic principles to build hydrogen-bonded molecular assemblies of multiple components. Cocrystals are gaining much interest

because the resulting new crystal forms of APIs many times have different pharmaceutical, physical, and chemical properties compared to the original API.

This chapter will introduce cocrystals, including the criteria for selecting cocrystal formers. The next section will focus on the pharmaceutical properties that can be tailored for an API, including the solubility dependence of a cocrystal on the second component concentration and in some cases on pH. The final two sections are devoted to the solution and solid-state approaches to designing cocrystals and understanding the kinetics and mechanisms behind cocrystallization. It will conclude with research objectives and model compounds referred to throughout the thesis.

Cocrystal Design

Cocrystals are multiple component systems where intermolecular interactions (including hydrogen bonds, van der Waals, and π-π interactions) and favorable geometries lead to a self-assembled supramolecular network. Cocrystals offer the advantage of generating solid forms of APIs even when they lack ionizable functional groups and in this way produce materials with a large range of properties that are not available in single API solid phases (polymorphs and amorphous forms), or in API solvates, or salt forms. Solvates are compounds where one of the components is liquid at room temperature, such as a hydrate. In a crystalline salt, the interactions are mostly electrostatic, and the components are ionized. A pharmaceutical cocrystal contains an API and a coformer molecule(s), both of which typically exist in the neutral state and interact by hydrogen bonding or by other non-covalent bonds. (A few cocrystals have been synthesized in which the API is ionized, but the coformer is still non-ionized

(Childs and Hardcastle 2007; Reddy, Bethune et al. 2009).) The term cocrystal generally refers to components that in their pure states are solids at room temperature (Almarsson and Zaworotko 2004; Aakeroy and Salmon 2005). Cocrystals may include two or more different components and in most cases to date, two and three component systems are reported with the latter being mostly cocrystalline solvates, e.g. theophylline-5-fluorouracil hydrate (Zaitu, Miwa et al. 1995), carbamazepine-4-aminobenzoic acid hydrate (McMahon, Bis et al. 2005), and tetroxoprim-sulfametrole methanolate (Caira, Bettinetti et al. 2003). Table 1 presents some examples of pharmaceutical cocrystals and solvated cocrystals.

Table 1.1. Examples of pharmaceutical cocrystals. Crystal structures not yet deposited into the Cambridge Structural Database will not have a REFCODE.

API	Cocrystal Former	Ratio (API:Ligand)	REFCODE	Reference
Carbamazepine	Nicotinamide	1:1	UNEZES	(Fleischman, Kuduva et al. 2003)
	Saccharin	1:1	UNEZAO	(Fleischman, Kuduva et al. 2003)
	4-aminobenzoic acid	2:1	XAQRAJ	(Zaworotko et al 2006)
	4-aminobenzoic acid-hydrate	2:1:1	XAQREN	(Zaworotko et al. 2006)
	Succinic acid	2:1		(Childs, Rodríguez-Hornedo et al. 2008)
	Salicylic acid	1:1		(Childs, Rodríguez-Hornedo et al. 2008)
	Fumaric acid	2:1		(Childs, Rodríguez-Hornedo et al. 2008)
	Oxalic acid	2:1		(Childs, Rodríguez-Hornedo et al. 2008)
	Glutaric acid	1:1		(Childs, Rodríguez-Hornedo et al. 2008)
	Malonic acid	2:1		(Childs, Rodríguez-Hornedo et al. 2008)
Itraconazole	Succinic acid	2:1	IKEQEU	(Remenar, Morissette et al. 2003)
	Malic acid	2:1		(Remenar, Morissette et al. 2003)
	Tartaric acid	2:1		(Remenar, Morissette et al. 2003)
Piroxicam	Succinic acid	2:1	DIKCIK	(Childs and Hardcastle 2007)
	1-hydroxy-2-naphthoic acid	1:1	DIKCOQ	(Childs and Hardcastle 2007)
	Caprylic acid	1:1	DIKCUW	(Childs and Hardcastle 2007)
	Benzoic acid	1:1	DIKDOR	(Childs and Hardcastle 2007)

Table 1.1. (continued)

Caffeine	Oxalic acid	2:1	GANXUP	(Trask, Motherwell et al. 2005)
	Malonic acid	2:1	GANYAW	(Trask, Motherwell et al. 2005)
	Maleic acid	2:1, 1:1	GANYIE, GANYEA	(Trask, Motherwell et al. 2005)
	Glutaric acid	1:1 (Forms I, II)	EXUQUJ	(Trask, Motherwell et al. 2005)
	Barbital	2:1	CAFBAR20	(Craven and Gartland 1974)
	Sulfaproxyline	1:1	VIGVOW	(Ghosh, Basak et al. 1991)
	Acetylsalicylic acid	1:1	VUGMIT	(Caira 1992)
	4-aminosalicylic acid	1:1	VUGMOZ	(Caira 1992)
	2-aminobenzoic acid	1:1	SORWEB	(Caira 1991)
	4-aminobenzoic acid	1:1	SORWIF	(Caira 1991)
Theophylline	5-fluorouracil monohydrate	2:1	ZAYLOA	(Zaitu, Miwa et al. 1995)
	Phenobarbital	2:1	THOPBA	(Nakao, Fujii et al. 1977)
	Acetaminophen	1:1	KIGLUI	(Childs, Stahly et al. 2007)
	Glutaric acid	1:1	XEJXIU	(Trask, Motherwell et al. 2006)
	Salicylic acid	1:1	KIGLES	(Childs, Stahly et al. 2007)
	Malonic acid	1:1	XEJXAM	(Trask, Motherwell et al. 2006)
Lamivudine	4-quinolinone	1:1		(Bhatt, Azim et al. 2009)
	Zidovudine hydrate	1:1:1		(Bhatt, Azim et al. 2009)

The field of crystal engineering has focused on understanding the intermolecular interactions and connectivities that lead to the construction of supermolecules or extended architectures. Because of its strength and directionality, the hydrogen bond has been the most important interaction in cocrystal formation (Etter 1990; Etter and Reutzel 1991; Desiraju 2002; Wenger and Bernstein 2008). By studying the hydrogen bond patterns in crystalline solids, valuable knowledge is gained to identify hydrogen-bond preferences and reliable synthons that lead to cocrystal formation (Leiserowitz and Schmidt 1969; Etter 1990; Desiraju 1995; Aakeroy, Beatty et al. 2002; Wenger and Bernstein 2008). The frequency of hydrogen bond motifs and other important interactions in crystal lattices can be studied by using the Cambridge Structural Database (CSD) by searching for specific molecules, functional groups, and synthons (Etter and

Reutzel 1991; Nangia and Desiraju 1998; Allen 2002). Some commonly found synthons are shown in Figure 1.1.

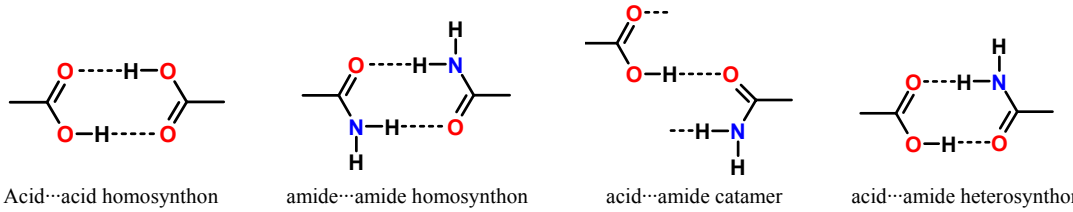

Figure 1.1. Common synthons found between carboxylic acid and amide functional groups.

Guidelines for preferred hydrogen bond patterns in crystals based on rigorous analysis of hydrogen bonds and packing motifs have been developed by Donohue (Donohue 1952) and Etter (Etter 1991). These include: (a) all acidic hydrogens available in a molecule will be used in hydrogen bonding in the crystal structure of that compound (Donohue 1952), (b) all good acceptors will be used in hydrogen bonding when there are available hydrogen-bond donors (Etter 1991), and (c) the best hydrogen-bond donor and the best hydrogen-bond acceptor will preferentially form hydrogen bonds to one another (Etter 1991). Etter also considered a variety of reasons for which this behavior does not occur. These include the presence of multiple competitive hydrogen-bond sites, conformational freedom, steric hindrances, or competing dipolar or ionic forces. These general principles nevertheless establish the basis for predicting likely and unlikely structures.

These principles of cocrystal formation were applied to the design of cocrystals of carbamazepine, an API which has the reliable carboxamide synthon (Figure 1.2).

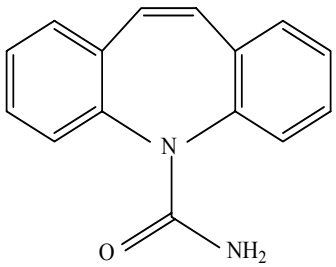

Figure 1.2. Chemical structure of carbamazepine.

Carbamazepine (CBZ) is of interest because of its low water solubility and its well-known four polymorphs (Himes, Mighell et al. 1981; Reboul, Cristau et al. 1981; Lowes, Caira et al. 1987; Murphy, Rodríguez-Cintron et al. 2002; Grzesiak, Lang et al. 2003) and solvates (water and acetone solvates) (Terrence, Sax et al. 1983; McMahon, Timmins et al. 1996; Kobayashi, Ito et al. 2000; Fleischman, Kuduva et al. 2003). The crystal packing of CBZ in polymorphs and solvates shows the formation of cyclic dimers, with the carboxamide unit acting as both a hydrogen bond donor and acceptor. The differences among the polymorphic crystal forms lie in the packing of the dimer units as illustrated in Figure 1.3 for the monoclinic (form III) and trigonal (form II) polymorphs. Ribbons of carboxamide dimers are not observed in CBZ polymorphs because the azepine ring sterically hinders the exterior amide hydrogen bond donor and acceptor.

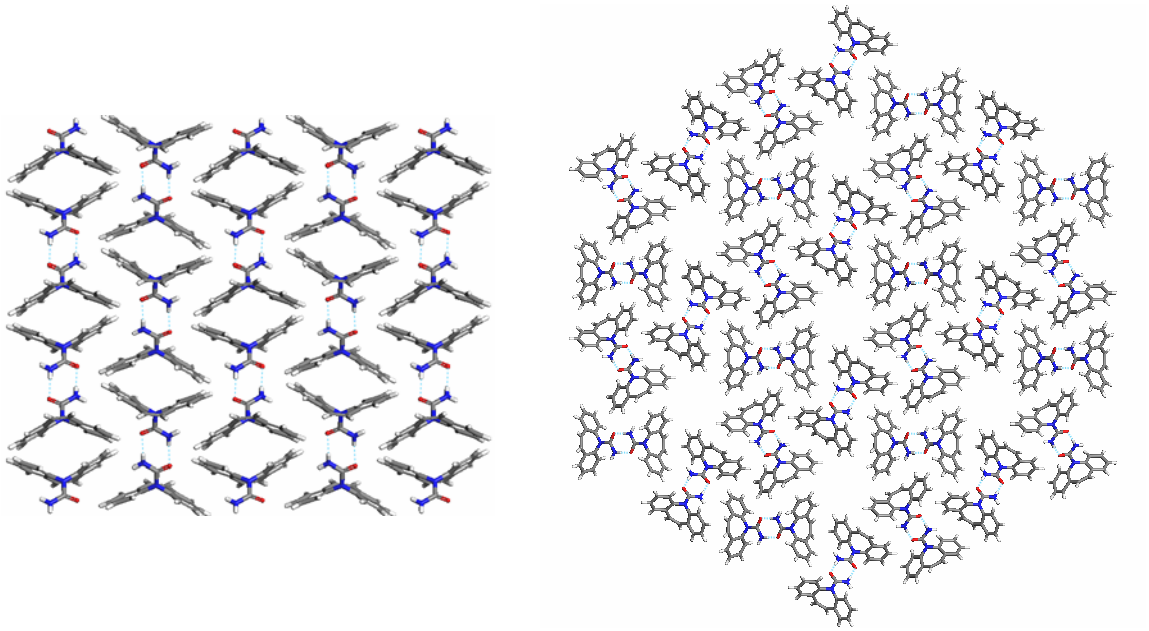

(a) (b)

Figure 1.3. Packing diagrams of carbamazepine anhydrous polymorphs, (a) monoclinic, form III and (b) trigonal, form II (Grzesiak, Lang et al. 2003).

Examination of the crystal structures of solvates reveals hydrogen-bonding arrangements that can be applied to cocrystal formation. In many solvates, the solvent molecule is hydrogen-bonded to the API molecule, as shown for water or acetone in the CBZ structures in Figure 1.4 a-b. The solvent molecule is connected by the *exterior* N–H…O hydrogen bond and occupies the space between two pairs of CBZ carboxamide homodimers. These solvates of CBZ confirm that the propensity of an API molecule to form solvates is related to molecular structures, hydrogen bond patterns, and crystal packing (Morris, Griesser et al.; Khankari and Grant 1995; Nangia and Desiraju 1998; Bingham, Hughes et al. 2001; Infantes and Motherwell 2002; Gillon, Feeder et al. 2003).

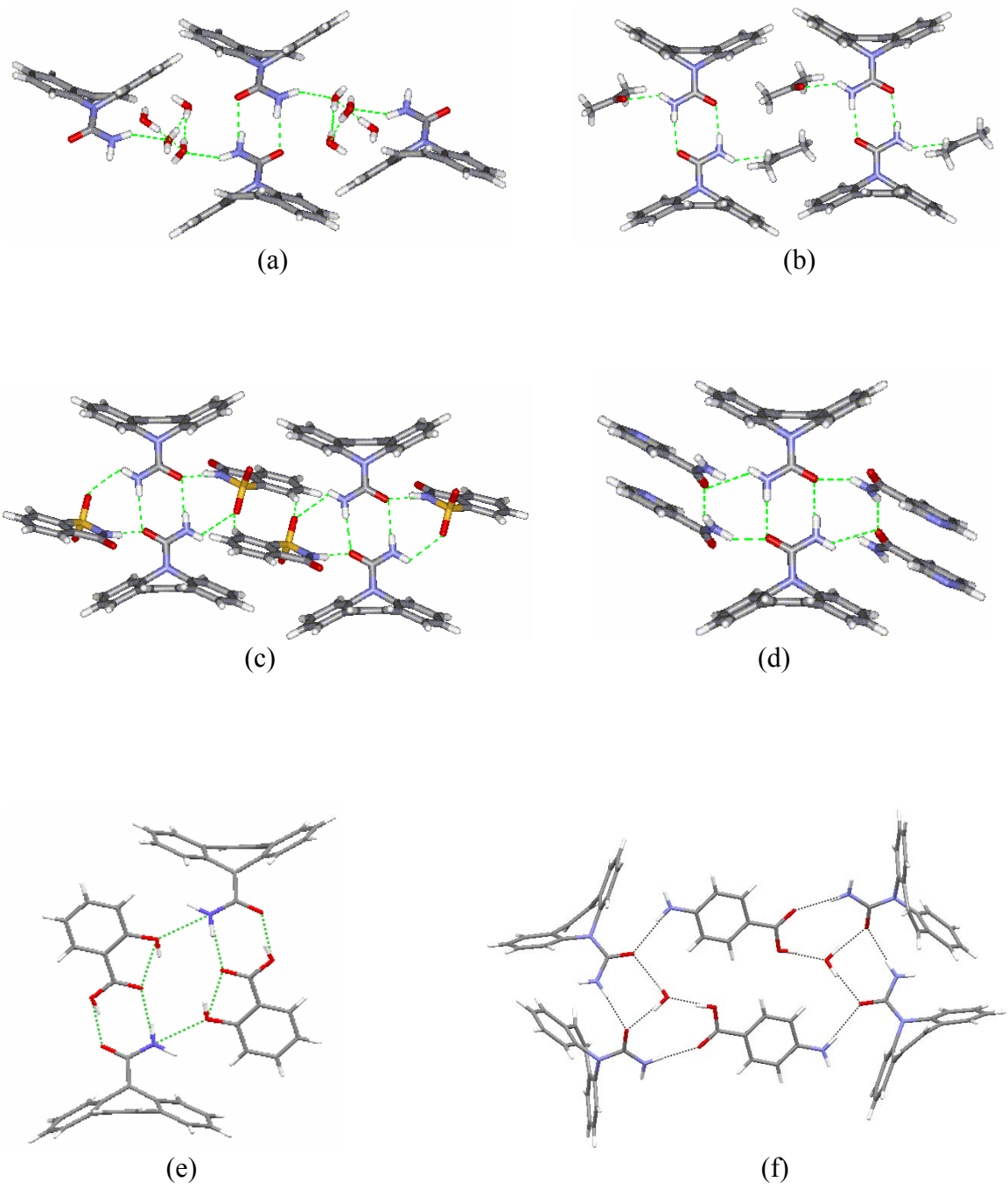

Figure 1.4. Molecular interactions in carbamazepine cocrystals and solvates, (a) dihydrate, (b) acetone solvate, (c) carbamazepine-saccharin, (d) carbamazepine-nicotinamide, (e) carbamazepine-salicylic acid, and (f) carbamazepine-4-aminobenzoic acid hydrate. (Fleischman, Kuduva et al. 2003), (McMahon, Bis et al. 2005), and (Childs, Rodríguez-Hornedo et al. 2008).

Supramolecular design strategies were utilized to prepare CBZ cocrystals using this moiety as the primary supramolecular synthon where interactions either retain (strategy I) or disrupt carboxamide dimer formation (strategy II) (Fleischman, Kuduva et al. 2003). Strategy I maintains the carboxamide homosynthon and uses the exterior hydrogen bond donor and acceptor sites. Strategy II forms a heterodimer by hydrogen bonds between the carboxamide and carboxylic groups.

Figure 1.4c-d shows how carbamazepine can form cocrystals by strategy I with saccharin or nicotinamide that retain the carboxamide dimer and hydrogen bond instead with the exterior donor/acceptor groups. This pattern is similar to those observed in the water and acetone solvates. In strategy II, carboxylic acids such as salicylic acid and 4-aminobenzoic acid cocrystals of CBZ replace the carboxamide dimer with an amide-carboxylic acid dimer (Figure 1.4e-f). Given that these cocrystals significantly alter intermolecular associations and modify crystal packing, physical and pharmaceutical properties will consequently be affected.

Cocrystals as a Means of Controlling Material Properties

The value of cocrystals with pharmaceutical components lies in the ability to tailor the functionality of materials. Pharmaceutical scientists often consider alternative solid state forms to a free drug compound, such as polymorphs or salts, to improve pharmaceutical properties. In contrast to polymorphs, that have the same chemical composition, cocrystals do not, implying that greater changes in materials properties could be introduced compared with polymorphs. Some compounds do not possess ionizable functional groups, eliminating salts as an option for drug formulation. If

cocrystals can alter pharmaceutical properties, they could become viable alternatives for drug product formulations. Properties that relate to pharmaceutical performance and that can be controlled by cocrystal formation include melting point, hygroscopicity, chemical stability, dissolution, solubility, mechanical properties, and bioavailability. Over the past few years, numerous examples have been published in which pharmaceutical properties of cocrystals have been presented and a selection is highlighted below.

Hydrate Formation

APIs can be cocrystallized with coformers such that the API will not form a hydrate or a solvate. Since cocrystals are supramolecular assemblies and are designed based on functional groups and hydrogen bond complementarity, solvate formation that relies on this complementarity will be inhibited by the formation of cocrystals, given that the intermolecular interactions between the API and coformer are stronger than between the API and solvent molecule. An example of this is the stability of carbamazepine cocrystals (nicotinamide or saccharin) when exposed to high relative humidities (Rodríguez-Spong, Zocharski et al. 2003; Rodríguez-Spong 2005). Even though the pure carbamazepine anhydrous crystal transforms to carbamazepine dihydrate when exposed to high relative humidities (Figure 1.5), the cocrystals do not (Rodríguez-Spong 2005).

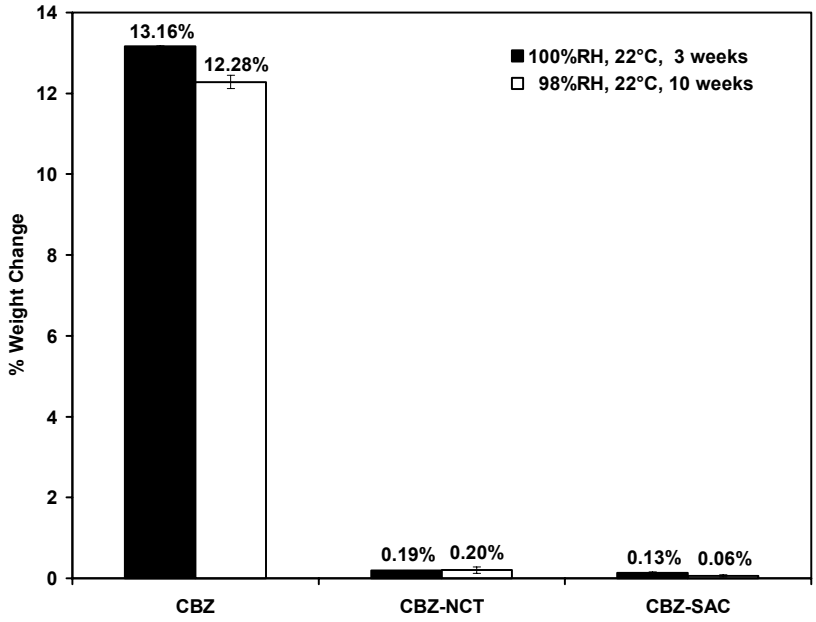

Figure 1.5. Moisture uptake of CBZ-NCT, CBZ-SAC, and CBZ(III) at room temperature for three weeks at 100% RH or 10 weeks at 98% RH. Equilibration time represents the rate of transformation from CBZ(III) to CBZ(D). (Adapted from (Rodríguez-Spong 2005)).

A similar study on caffeine shows that the caffeine-oxalic acid cocrystal did not transform to caffeine hydrate under high relative humidity for seven weeks. However, other caffeine cocrystals dissociated and consequently, the hydrated form of the API resulted (Trask, Motherwell et al. 2005).

Chemical Stability

Cocrystal formation can also improve the chemical stability of an API when chemical reactivity requires that reactant molecules be in suitable positions in the solid state. For example, the single component CBZ polymorphs degrade by solid-state photochemical reaction, where a cyclobutyl dimer is one of the main decomposition products (Matsuda, Akazawa et al. 1994; Rodríguez-Spong 2005). Formation of the

cyclobutyl dimer requires alignment and a distance between azepine rings of less than or equal to 4.1 Å. CBZ cocrystal formation with saccharin and nicotinamide inhibits photodegradation of CBZ by altering the molecular arrangements in the solid state such that the distance between the azepine rings is more than 4.1 Å, thereby preventing photodegradation (Rodríguez-Spong 2005).

Dissolution Rate

Dissolution rates of various API cocrystals have been reported. The intrinsic dissolution rates of CBZ-NCT and CBZ-SAC cocrystals in water are 1.7 and 2.3 times that of CBZ(D) (Rodríguez-Spong 2005) and close to that of the single component anhydrous CBZ(III) (Murphy, Rodríguez-Cintron et al. 2002).

Itraconazole (ITZ), an antifungal agent, is an API with very low water solubility so it is marketed as the amorphous form to increase oral bioavailability. Remenar et al. (Remenar, Morissette et al. 2003) synthesized four cocrystals with a stoichiometry of 2:1 (drug:ligand) where the ligand was fumaric acid, succinic acid, malic acid, and tartaric acid. The powder dissolution rate in 0.1N HCl at 25˚C of these four cocrystals was compared to the crystalline and amorphous forms of itraconazole. The cocrystals have 4- to 20-fold higher dissolution profiles than pure crystal itraconazole, and the L-tartaric acid and L-malic acid cocrystals have dissolution profiles similar to the amorphous itraconazole (Remenar, Morissette et al. 2003).

Childs et al. (Childs, Chyall et al. 2004) formulated crystalline complexes with a salt form of an API with carboxylic acids. The antidepressant, fluoxetine hydrochloride, was cocrystallized with benzoic acid, succinic acid, and fumaric acid where the chloride

ion acts as a hydrogen bond acceptor for the carboxylic acid groups of the three ligands. Intrinsic dissolution studies were carried out at 10˚C because at 25˚C, the rates were so rapid that the dissolution rates of the cocrystals could not be distinguished from one another. The fumaric acid 2:1 complex had a similar dissolution rate to that of the crystalline fluoxetine hydrochloride, but the dissolution rate for the benzoic acid 1:1 complex was half that of fluoxetine hydrochloride. Fluoxetine hydrochloride-succinic acid 2:1 complex had approximately three times higher dissolution rate, but the dissolution was so fast that an accurate value was difficult to measure (Childs, Chyall et al. 2004).

Remenar et al. (Remenar, Peterson et al. 2007) reported dissolution rates of celecoxib-nicotinamide higher than celecoxib form III. When cocrystal was blended with 2% SDS and PVP, 90% of the cocrystal dissolved within 5 minutes, a rate significantly higher than celecoxib III blended with the same excipients and was very similar to amorphous celecoxib blended in the same manner (Remenar, Peterson et al. 2007).

Indomethacin-saccharin cocrystal had a greater than 50 times increase in dissolution rate in a 200mM phosphate buffer (pH 7.4) compared to γ-indomethacin, the most stable polymorph (Basavoju, Bostrom et al. 2008). It was interesting to note that when lower concentrations of buffer were used, the cocrystal did not achieve as high of a dissolution rate and conversion to amorphous and α-indomethacin occurred.

Cocrystal Solubility

Cocrystal solubility is dependent on cocrystal component concentration, solution complexation, and ionization when one or more components are ionizable. Mathematical

models have been developed that describe the solubility of binary cocrystals with non-ionizable components based on the equilibria between cocrystal and cocrystal components in solution (Nehm, Rodríguez-Spong et al. 2006). Chapters 2, 3, 5, and 6 will fully discuss the effects of cocrystal dissociation, solution complexation, and ionization on the phase equilibria.

Solubility was examined for a series of nine cocrystals of an Amgen compound (AMG 517) (Stanton and Bak 2008), although the results resemble powder dissolution studies and conversion to a more stable form was observed for some cocrystals. Three cocrystals with AMG 517 (trans-cinnamic acid, 2,5-dihydroxybenzoic acid, and 2-hydroxycaproic acid) had lower solubility values than the free base, while cocrystals with glutaric acid, glycolic acid, sorbic acid, trans-2-hexanoic acid, and L(+)-lactic acid, and benzoic acid resulted in higher concentrations after 24 hours compared to the free base even if transformation was observed by XRPD.

Bioavailability

If cocrystals are going to be a viable alternative for solid state forms of a drug, bioavailability studies need to be performed. Two manuscripts have been recently published that report the first bioavailability studies using cocrystals. McNamara et al reported a 1:1 cocrystal of 2-[4-(4-chloro-2-fluorophenoxy)phenyl]pyrimidine-4-carboxamide with glutaric acid that had a dissolution rate 18 times higher than the pure API (McNamara, Childs et al. 2006). Bioavailability studies revealed the cocrystal attained approximately three times higher plasma concentrations for the same dose in dogs (McNamara, Childs et al. 2006).

During formulation of an Amgen compound (AMG 517), a cocrystal of the API formed with sorbic acid, an ingredient in the suspending agent (Bak, Gore et al. 2008). The cocrystal exhibited better dissolution and bioavailability than the free API. Pharmacokinetic studies in rats revealed that similar plasma levels were achieved with only 30mg/kg dose of the cocrystal as with 500mg/kg dose of the free API (Bak, Gore et al. 2008).

Carbamazepine-saccharin was reported to yield slightly higher plasma levels when compared to dosing carbamazepine monoclinic, form III, although the authors reported that the increase was not statistically significant (Hickey, Peterson et al. 2006).

Cocrystal Synthesis

Throughout the cocrystalline literature, numerous solution-mediated and solid-state mediated methods have been used to synthesize cocrystals. Current solution-mediated methods to synthesize cocrystals include slow evaporation (Caira 1991; Etter and Reutzel 1991; Ghosh, Basak et al. 1991; Fleischman, Kuduva et al. 2003; Walsh, Bradner et al. 2003; Childs, Chyall et al. 2004) from solutions with equimolar or stoichiometric concentrations of cocrystal components and solvo-thermal methods (Bettinetti, Caira et al. 2000; Rodríguez-Spong 2005), with the former being more common. These processes, however, suffer from the risk of crystallizing the single component phases, thereby reducing the possibility of forming the multiple component crystalline phase. As a result of these empirically based approaches, a very large number of experimental conditions are often tested (Morissette, Almarsson et al. 2004) and

transferability to larger scale crystallization processes is limited. A more rational solution-mediated approach has been designed and is explained in detail in chapter 4.

Cocrystallization can occur during storage of solid blends of cocrystal components and deliquescent additive (Jayasankar, Good et al. 2007). Cocrystallization in these blends is facilitated by moisture sorbed due to deliquescence of additive at relative humidities above the deliquescent relative humidity (DRH). It is hypothesized that the water sorbed by the deliquescent material creates a medium for the cocrystal components to dissolve. The rate of cocrystal formation depends on the rates of moisture sorption, dissolution of cocrystal components and rate of nucleation and growth from solution phase.

Cocrystal formation in the solid state is based on mechanical activation of materials by processes such as grinding or milling and examples of cocrystals formed by these processes are abundant (Etter 1990; Etter 1991; Etter and Reutzel 1991; Etter, Reutzel et al. 1993; Caira, Nassimbeni et al. 1995; Pedireddi, Jones et al. 1996; Oguchi, Kazama et al. 2000; Trask and Jones 2005; Trask, Motherwell et al. 2005; Jayasankar, Somwangthanaroj et al. 2006; Childs, Rodríguez-Hornedo et al. 2008). The addition of small drops of solvent is becoming increasingly common in the cocrystal grinding literature (Trask, Motherwell et al. 2004; Wenger and Bernstein 2008).

Since grinding is a highly energetic process, cocrystal formation by cogrinding reactants proceeds through the formation of amorphous or disordered phases by the reactants. This has been shown in studies with anhydrous form III carbamazepine (CBZ(III)) and saccharin (SAC) (Jayasankar, Somwangthanaroj et al. 2006). Faster rate of cocrystal formation was observed during cogrinding at room temperature.

Interestingly, carbamazepine-nicotinamide and carbamazepine-saccharin were shown to spontaneously form under a variety of storage conditions even when the two components were not ground together, suggesting that transformation from single components to multi-components was thermodynamically favorable (Maheshwari, Jayasankar et al. 2009).

Differential scanning calorimetry has recently been shown to be an efficient thermal method to synthesize cocrystals *in situ* (Lu, Rodríguez-Hornedo et al. 2008). Sixteen out of twenty cocrystals of carbamazepine, theophylline, caffeine, and sulfamethazine were formed. The heating rate appeared to affect the rate and extent of cocrystal formation, and solid phases were confirmed by variable temperature XRD.

Research Objectives

Cocrystals are becoming increasingly important as a means of controlling the properties of pharmaceutical solids by designing multiple component molecular networks that introduce the desired functionality. Because cocrystal design is based on supramolecular synthesis, it provides a powerful approach for the proactive discovery of novel pharmaceutical solid phases. Application of the fundamental concepts presented in this thesis explains pharmaceutical properties of cocrystals, in particular solubility, dissolution, and stability. These results are essential for the pharmaceutical scientist to anticipate the formation of cocrystals during pharmaceutical processes, to develop reliable methods for cocrystal discovery and production, and to predict solubility and dissolution trends.

The following are the specific objectives for the proposed research:

- To demonstrate that cocrystal solubility can be explained by equilibria including
  - Cocrystal dissociation
  - Solution complexation
  - Ionization

- To identify crystallization and stability regions where selective isolation of either single or multiple component phases can occur.

- To develop efficient and scalable cocrystal screening methods and to design cocrystallization processes using more environmentally friendly solvents.

- To study the relationship between cocrystal composition, solubility, dissolution, and stability as a function of pH

Model Compounds

Carbamazepine (CBZ, 5H-Dibenz[b,f]azepine-5-carboxamide) (Figure 1) has four known anhydrous polymorphs and also exists as a dihydrate when exposed to moisture (Kobayashi, Ito et al. 2000). The most stable anhydrous form at room temperature, monoclinic (CBZ(III)), has an aqueous solubility of 1.6mM at 25°C (Murphy, Rodríguez-Cintron et al. 2002) and the dihydrate has a solubility of 0.508mM at 25°C (Rodríguez-Spong 2005). CBZ is used in the treatment of seizures and is marketed as Tegretol®.

In 2003, 13 cocrystals of carbamazepine were synthesized and characterized (Fleischman, Kuduva et al. 2003). The cocrystal formers included: acetone, DMSO, benzoquinone, terephthalaldehyde, saccharin, nicotinamide, acetic acid, formic acid, butyric acid, trimesic acid, 5-nitroisophthalic acid, adamantane-1,3,5,7-tetracarboxylic acid, and formamide. In 2008, 27 cocrystals of carbamazepine were synthesized and characterized (Childs, Rodríguez-Hornedo et al. 2008). The cocrystal formers were pharmaceutically accepted and included: succinic acid, benzoic acid, ketoglutaric acid,

maleic acid, glutaric acid, molonic acid, oxalic acid, adipic acid, camphoric acid, 4-hydroxybenzoic acid, salicylic acid, 1-hydroxy-2-naphthoic acid, DL-tartaric acid, L-tartaric acid, glycolic acid, fumaric acid, DL-malic acid, and L-malic acid.

Four carbamazepine cocrystals—CBZ-nicotinamide, CBZ-saccharin, CBZ-4-aminobenzoic acid, and CBZ-salicylic acid—have been studied in greater detail throughout this thesis. Nicotinamide (NCT, pyridine-3-carboxylic acid amide) also known as vitamin B_3, is shown in Figure 1.6. NCT is non-covalently bonded to CBZ through C = O ··· H – H hydrogen bonds (Figure 1.4d). Crystal packing reveals π···π interactions between the CBZ and NCT molecules (Fleischman, Kuduva et al. 2003).

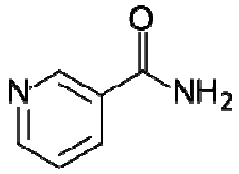

Figure 1.6. Chemical structure of nicotinamide.

Saccharin (SAC, 2,3-dihydroxy-1,2-benzisothiazol-3-one-1,1-dioxide) (Figure 1.7) is an ionizable compound with a $pK_a = 1.8$. In the cocrystal, saccharin acts as a hydrogen bond donor and acceptor. SAC forms a N – H ··· O hydrogen bond to the carbamazepine carbonyl, and the saccharin sulfonyl group forms a S = O ··· H – N hydrogen bond with carbamazepine (Figure 1.4c).

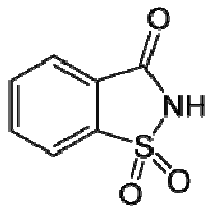

Figure 1.7. Chemical structure of saccharin.

4-aminobenzoic acid (4ABA) (Figure 1.8) is an amphoteric compound with the amine pK_a = 2.6 and the acid pK_a = 4.8. In the 2:1 hydrated cocrystal (Figure 1.4f), carbamazepine forms a C = O ··· H – N hydrogen bond to 4ABA and a O – H ··· O hydrogen bond to a water molecule.

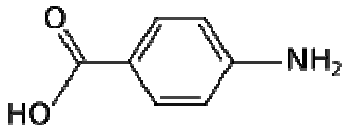

Figure 1.8. Chemical structure of 4-aminobenzoic acid.

Finally, salicylic acid (SLC, 2-hydroxybenzoic acid) (Figure 1.9) is an ionizable compound with a pK_a = 2.98. SLC is non-covalently bonded to CBZ through C = O ··· H – N and O - H ··· O = C hydrogen bonds (Figure 1.4e).

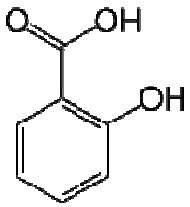

Figure 1.9. Chemical structure of salicylic acid.

References

Aakeroy, C. B., A. M. Beatty, et al. (2002). "A High-Yielding Supramolecular Reaction." *Journal of the American Chemical Society* **124**: 14425-14432.

Aakeroy, C. B. and D. J. Salmon (2005). "Building co-crystals with molecular sense and supramolecular sensibility." *Crystal Engineering Communication* **7**: 439-448.

Allen, F. H. (2002). "The Cambridge Structural Database: a quarter of a million crystal structures and rising." *Acta Crystallographica* **B58**: 380-388.

Almarsson, O. and M. J. Zaworotko (2004). "Crystal engineering of the composition of pharmaceutical phases. Do pharmaceutical co-crystals represent a new path to improved medicines?" *Chemical Communications*: 1889-1896.

Bak, A., A. Gore, et al. (2008). "The co-crystal approach to improve the exposure of a water insoluble compound: AMG 517 sorbic acid cocrystal characterization and pharmacokinetics." *Journal of Pharmaceutical Sciences* **97**: 3942-3956.

Basavoju, S., D. Bostrom, et al. (2008). "Indomethacin-saccharin cocrystal: design, synthesis and preliminary pharmaceutical characterization." *Pharmaceutical Research* **25**: 530-541.

Bettinetti, G., M. R. Caira, et al. (2000). "Structure and Solid-State Chemistry of Anhydrous and Hydrated Crystal Forms of the Trimethoprim-Sulfamethoxypyridazine 1:1 Molecular Complex." *Journal of Pharmaceutical Sciences* **89**: 478-489.

Bhatt, P., Y. Azim, et al. (2009). "Co-crystals of the anti-HIV drugs lamivudine and zidovudine." *Crystal Growth & Design* (published online Dec. 2008).

Bingham, A. L., D. S. Hughes, et al. (2001). "Over one hundred solvates of sulfathiazole." *Chemical Communications* **7**: 603-604.

Byrn, S. R., R. R. Pfeiffer, et al. (1999). Drugs as Molecular Solids. *Solid-State Chemistry of Drugs*. West Lafayette, IN, SSCI.

Caira, M. R. (1991). "Molecular complexes of sulfonamides. Part 1. 1:1 complexes between sulfadimidine [4-amino-N-(4,6-dimethyl-2-pyrimidinyl)benzenesulfonamide] and 2- and 4-aminobenzoic acids." *Journal of Crystallographic and Spectroscopic Research* **21**: 641-648.

Caira, M. R. (1992). "Molecular complexes of sulfonamides. 2. 1:1 complexes between drug molecules: sulfadimidine-acetylsalicylic acid and sulfadimidine-4-aminosalicylic acid." *Journal of Crystallographic and Spectroscopic Research* **22**: 193-200.

Caira, M. R., G. Bettinetti, et al. (2003). "Order-Disorder Enantiotropy, Monotropy, and Isostructurality in a Tetroxoprim-Sulfametrole 1:1 Molecular Complex: Crystallographic and Thermal Studies." *Journal of Pharmaceutical Sciences* **92** (11): 2164-2176.

Caira, M. R., L. R. Nassimbeni, et al. (1995). "Selective formation of hydrogen bonded cocrystals between a sulfonamide and aromatic carboxylic acids in the solid state." *Journal of the Chemical Society, Perkin Transactions 2*: 2213-2216.

Childs, S. L., L. J. Chyall, et al. (2004). "Crystal Engineering Approach to Forming Cocrystals of Amine Hydrochlorides with Organic Acids. Molecular Complexes of Fluoxetine Hydrochloride with Benzoic, Succinic, and Fumaric Acids." *Journal of the American Chemical Society* **126**: 13335-13342.

Childs, S. L. and K. I. Hardcastle (2007). "Cocrystals of piroxicam with carboxylic acids." *Crystal Growth & Design* **7**: 1291-1304.

Childs, S. L., N. Rodríguez-Hornedo, et al. (2008). "Screening strategies based on solubility and solution composition generate pharmaceutically acceptable cocrystals of carbamazepine." *Crystal Engineering Communications* **10**: 856-864.

Childs, S. L., G. P. Stahly, et al. (2007). "The salt-cocrystal continuum: the influence of crystal structure on ionization state." *Molecular Pharmaceutics* **4**: 323-338.

Craven, B. M. and G. L. Gartland (1974). "The 2:1 Crystal Complex of 5,5-diethylbarbituric Acid (Barbital) and Caffeine." *Acta Crystallographica* **B30**: 1191-1195.

Desiraju, G. R. (1995). "Supramolecular Synthons in Crystal Engineering--A New Organic Synthesis." *Angewandte Chemie International Edition in English* **34**: 2311-2327.

Desiraju, G. R. (2002). "Hydrogen Bridges in Crystal Engineering: Interactions without Borders." *Accounts of Chemical Research* **35**: 565-573.

Donohue, J. (1952). "The Hydrogen Bond in Organic Crystals." *Journal of Physical Chemistry* **56**: 502-510.

Etter, M. C. (1990). "Encoding and Decoding Hydrogen-Bond Patterns of Organic Compounds." *Accounts of Chemical Research* **23**: 120-126.

Etter, M. C. (1991). "Hydrogen Bonds as Design Elements in Organic Chemistry." *Journal of Physical Chemistry* **95**: 4601-4610.

Etter, M. C. (1991). "Hydrogen bonds as design elements in organic chemistry." *J. Phys. Chem.* **95**: 4601 - 4610.

Etter, M. C. and S. M. Reutzel (1991). "Hydrogen Bond Directed Cocrystallization and Molecular Recognition Properties of Acyclic Imides." *Journal of the American Chemical Society* **113**: 2586-2598.

Etter, M. C., S. M. Reutzel, et al. (1993). "Self-organization of adenine and thymine in the solid state." *J. Am. Chem. Soc.* **115**: 4411-4412.

Fleischman, S. G., S. S. Kuduva, et al. (2003). "Crystal Engineering of the Composition of Pharmaceutical Phases: Multiple-Component Crystalline Solids Involving Carbamazepine." *Crystal Growth & Design* **3**: 909-919.

Ghosh, M., A. K. Basak, et al. (1991). "Structure and Conformation of the 1:1 Molecular Complex of Sulfaproxyline-Caffeine." *Acta Crystallographica* **C47**: 577-580.

Gillon, A. L., N. Feeder, et al. (2003). "Hydration in molecular crystals--a Cambridge Structural Database analysis." *Crystal Growth and Design* **3**: 663-673.

Grzesiak, A. L., M. Lang, et al. (2003). "Comparison of the four anhydrous polymorphs of carbamazepine and the crystal structure of form I." *Journal of Pharmaceutical Sciences* **92**: 2260-2271.

Hickey, M. B., M. L. Peterson, et al. (2006). "Performance comparison of a co-crystal of carbamazepine with marketed product." *European Journal of Pharmaceutical Sciences* **67**: 112-119.

Himes, V. L., A. D. Mighell, et al. (1981). "Structure of carbamazepine-5H-benz[b.f]azepine-5-carboxamide." *Acta Crystallographica* **B37**: 2242-2245.

Infantes, L. and S. Motherwell (2002). "Water clusters in organic molecular crystals." *Crystal Engineering Communications* **4**: 454-461.

Jayasankar, A., D. J. Good, et al. (2007). "Mechanisms by which moisture generates cocrystals." *Molecular Pharmaceutics* **4**: 360-372.

Jayasankar, A., A. Somwangthanaroj, et al. (2006). "Cocrystal formation during cogrinding and storage is mediated by amorphous phase." *Pharmaceutical Research* **23**: 2381-2392.

Khankari, R. K. and D. J. W. Grant (1995). "Pharmaceutical Hydrates." *Thermochemica Acta* **248**: 61-79.

Kobayashi, Y., S. Ito, et al. (2000). "Physicochemical properties and bioavailability of carbamazepine polymorphs and dihydrate." *International Journal of Pharmaceutics* **193**: 137-146.

Leiserowitz, L. and G. M. J. Schmidt (1969). "Molecular Packing Modes. Part III. Primary Amides." *Journal of the Chemical Society (A): Inorganic, Physical, Theoretical*: 2372-2382.

Lowes, M. M. J., M. R. Caira, et al. (1987). "Physicochemical properties and X-ray structural studies of the trigonal polymorph of carbamazepine." *Journal of Pharmaceutical Sciences* **76**: 744-752.

Lu, E., N. Rodríguez-Hornedo, et al. (2008). "A rapid thermal method for cocrystal screening." *Crystal Engineering Communications* **10**: 665-668.

Maheshwari, C., A. Jayasankar, et al. (2009). "Factors that influence the spontaneous formation of of pharmaceutical cocrystals by simply mixing solid reactants." *Crystal Engineering Communications* (published online Nov. 2008).

Matsuda, Y., R. Akazawa, et al. (1994). "Pharmaceutical Evaluation of Carbamazepine Modifications--Comparitive-Study for Photostability of Carbamazepine Polymorphs by Using Fourier-Transformed Reflection-Absorption Infrared-Spectroscopy and Colorimetric Measurement." *Journal of Pharmacy and Pharmacology* **46**: 162-167.

McMahon, J. A., J. A. Bis, et al. (2005). "Crystal engineering of the composition of pharmaceutical phases 3. Primary amide supramolecular heterosynthons and their role in design of pharmaceutical cocrystals." *Z. Kristallogr* **220**: 340-350.

McMahon, L. E., P. Timmins, et al. (1996). "Characterization of Dihydrates Prepared from Carbamazepine Polymorphs." *Journal of Pharmaceutical Sciences* **85**: 1064-1069.

McNamara, D. P., S. L. Childs, et al. (2006). "Use of a glutaric acid cocrystal to improve oral bioavailability of a low solubility API." *Pharmaceutical Research* **23**: 1888-1897.

Morissette, S. L., O. Almarsson, et al. (2004). "High-throughput crystallization: polymorphs, salts, co-crystals and solvates of pharmaceutical solids." *Advanced Drug Delivery Reviews* **56**: 275-300.

Morris, K. R., U. J. Griesser, et al. personal communication.

Murphy, D., F. Rodríguez-Cintron, et al. (2002). "Solution-mediated phase transformation of anhydrous to dihydrate carbamazepine and the effect of lattice disorder." *International Journal of Pharmaceutics* **246**: 121-134.

Nakao, S., S. Fujii, et al. (1977). "The Crystal and Molecular Structure of the 2:1 Molecular Complex of Theophylline with Phenobarbital." *Acta Crystallographica* **B33**: 1373-1378.

Nangia, A. and G. R. Desiraju (1998). "Supramolecular Synthons and Pattern Recognition." *Topics in Current Chemistry* **198**: 57-95.

Nehm, S., B. Rodríguez-Spong, et al. (2006). "Phase Solubility Diagrams of Cocrystals Are Explained by Solubility Product and Solution Complexation." *Crystal Growth & Design* **6**: 592-600.

Oguchi, T., K. Kazama, et al. (2000). "Specific complexation of ursodeoxycholic acid with guest compounds induced by co-grinding." *Physical Chemistry Chemical Physics* **2**: 2815-2820.

Pedireddi, V. R., W. Jones, et al. (1996). "Creation of crystalline supramolecular arrays: a comparison of co-crystal formation from solution and by solid-state grinding." *Chemical Communications*: 987-988.

Reboul, J. P., B. Cristau, et al. (1981). "5H-5-Dibenzyl[b,f]azepinecarboxamide (carbamazepine)." *Acta Crystallographica* **B37**: 1844-1848.

Reddy, L. S., S. J. Bethune, et al. (2009). "Cocrystals and Salts of Gabapentin: pH dependent cocrystal stability and solubility." *Crystal Growth & Design* (published online Dec 2008).

Remenar, J. F., S. L. Morissette, et al. (2003). "Crystal Engineering of Novel Cocrystals of a Triazole Drug with 1,4-Dicarboxylic Acids." *Journal of the American Chemical Society* **125**: 8456-8457.

Remenar, J. F., M. L. Peterson, et al. (2007). "Celecoxib:Nicotinamide Dissociation: Using excipients to capture the cocrystal's potential." *Molecular Pharmaceutics* **4**: 386-400.

Rodríguez-Spong, B. (2005). Enhancing the Pharmaceutical Behavior of Poorly Soluble Drugs Through the Formation of Cocrystals and Mesophases, Ph.D. Thesis, University of Michigan.

Rodríguez-Spong, B., C. P. Price, et al. (2004). "General principles of pharmaceutical solid polymorphism: A supramolecular perspective." *Advanced Drug Delivery Reviews* **56**: 241-274.

Rodríguez-Spong, B., P. Zocharski, et al. (2003). "Enhancing the Pharmaceutical Behavior of Carbamazepine Through the Formation of Cocrystals " *The AAPS Journal* **5**: Abstract M1298.

Stanton, M. and A. Bak (2008). "Physicochemical Properties of Pharmaceutical Co-crystals: A Case Study of Ten AMG 517 Co-Crystals." *Crystal Growth & Design* **8**: 3856-3862.

Terrence, C. F., M. Sax, et al. (1983). "Effect of Baclofen enantiomorphs on the spinal trigeminal nucleus and steric similarites of carbamazepine." *Pharmacology* **27**: 85-94.

Trask, A. and W. Jones (2005). "Crystal engineering of organic cocrystals by the solid-state grinding approach." *Top. Curr. Chem.* **254**: 41-70.

Trask, A., W. D. S. Motherwell, et al. (2006). "Physical Stability Enhancement of Theophylline Via Cocrystallization." *International Journal of Pharmaceutics* **320**: 114-123.

Trask, A., V., W. D. S. Motherwell, et al. (2004). "Solvent-drop grinding: green polymorph control of cocrystallisation." *Chemical Communications*: 890-891.

Trask, A. V., W. D. S. Motherwell, et al. (2005). "Pharmaceutical Cocrystallization: Engineering a Remedy for Caffeine Hydration." *Crystal Growth & Design* **5**: 1013-1021.

Walsh, R. D. B., M. W. Bradner, et al. (2003). "Crystal Engineering of the Composition of Pharmaceutical Phases." *Chemical Communications*: 186-187.

Wenger, M. and J. Bernstein (2008). "An alternate crystal form of gabapentin: a cocrystal with oxalic acid." *Crystal Growth & Design* **8**: 1595-1598.

Zaitu, S., Y. Miwa, et al. (1995). "A 2:1 Molecular Complex of Theophylline and 5-Fluorouracil as the Monohydrate." *Acta Crystallographica* **C51**: 1857-1859.

Zocharski, P., S. Nehm, et al. (2004). "Can Solubility Products Explain Cocrystal Solubility and Predict Crystallization Conditions?" *The AAPS Journal* **6**: Abstract R6192.

CHAPTER TWO

PHASE SOLUBILITY DIAGRAMS OF COCRYSTALS ARE EXPLAINED BY SOLUBILITY PRODUCT AND SOLUTION COMPLEXATION

Introduction

Molecular interactions responsible for the formation of molecular complexes of active pharmaceutical ingredients (APIs) with other compounds are important not only because of the ability to control pharmaceutical properties without changing covalent bonds (Higuchi and Zuck 1953; Higuchi and Zuck 1953; Higuchi and Connors 1965; Higuchi and Pitman 1973), but also because they can be used in the design of new materials (Leiserowitz and Schmidt 1969; Etter 1990; Desiraju 1995; Aakeroy, Beatty et al. 2003). In recent years, advances in crystal engineering and supramolecular chemisty have motivated research on the design of pharmaceutical materials by directing molecular assembly of different components in the crystalline state to form cocrystals (Amai, Endo et al. 1998; Bettinetti, Caira et al. 2000; Brader, Sukumar et al. 2002; Fleischman, Kuduva et al. 2003; Remenar, Morissette et al. 2003; Walsh, Bradner et al. 2003; Childs, Chyall et al. 2004; Trask, Motherwell et al. 2005). Pharmaceutical properties of some cocrystals have also been reported such as solubility, dissolution rate, hygroscopicity, and chemical stability (Rodríguez-Spong, Zocharski et al. 2003; Zocharski, Nehm et al. 2004; Rodríguez-Spong 2005; Trask, Motherwell et al. 2005). The purpose of the studies

presented in this manuscript is to explain the solubility behavior of cocrystals in solutions of cocrystal components.

Molecular recognition phenomena that give rise to complexation in solution was the focus of research by Higuchi and co-workers in the 1950s(Higuchi and Zuck 1953; Higuchi and Zuck 1953; Kostenbauder and Higuchi 1956; Higuchi and Bolton 1959) and is the subject of various reviews (Higuchi and Connors 1965; Grant and Higuchi 1990). Much of this fundamental work was geared towards understanding the mechanisms of complex formation and determining the relative influence of intermolecular interactions in solutions (hydrogen bonds, charge-transfer forces, and other electrostatic and induction forces) that favored complex formation. This early work was concerned with improving the aqueous solubility of poorly water soluble compounds via solution complexation (Higuchi and Zuck 1953; Higuchi and Zuck 1953) and mathematical models were developed to evaluate complexation behavior from solubility studies of API in solutions of ligand. As a result, fewer publications address insoluble molecular complexes that formed during this phase solubility studies of API crystals (Higuchi and Zuck 1953; Kostenbauder and Higuchi 1956; Higuchi and Pitman 1973). It is noted that the terms molecular complex, solid-state complex, and molecular compound have been used in the pharmaceutical literature since the 1950s, while the term cocrystal is found in the more recent literature.

In this report we develop models that describe the solubility of binary cocrystals with nonionizable components, by taking into consideration the equilibria between cocrystal and cocrystal components in solution. We demonstrate that (1) the solubility of a 1:1 cocrystal *AB* is described by a solubility product, (2) the cocrystal solubility is

increased by a constant value when there is 1:1 solution complexation, and (3) the cocrystal solubility goes through a minimum value when there are 1:1 and 1:2 solution complexes. Thus a graphical representation of the cocrystal solubility dependence on ligand concentration will serve as a diagnostic tool for the stoichiometry of solution complexes. Experimental results for the solubility of carbamazepine-nicotinamide 1:1 cocrystal in organic solvents are analyzed in terms of the theoretical arguments developed. Solubility products and complexation constants are also determined.

These findings have practical applications in the development of crystallization methods for cocrystal screening and in the formulation of solutions with ingredients that can form cocrystals.

Fundamentals

Solubility product of cocrystals

The solubility of a binary cocrystal of API (*A*) and ligand or cocrystal component (*B*), of composition A_aB_b where the cocrystal components do not ionize or form complexes in solution, is given by the equilibrium reaction

$$A_aB_{b\ solid} \rightleftharpoons aA_{solution} + bB_{solution} \quad (1)$$

Subscripts refer to the stoichiometric number of molecules of *A* or *B* in the complex. The equilibrium constant for this reaction is given by

$$K_{eq} = \frac{a_A^a a_B^b}{a_{AB}} \quad (2)$$

and is proportional to the thermodynamic activity product of the cocrystal components. If the activity of the solid is equal to 1 or is constant, the cocrystal solubility can be described by a solubility product

$$K_{\text{sp}} = a_A^a a_B^b \approx [A]^a [B]^b \tag{3}$$

where $[A]$ and $[B]$ are the molar concentrations of each cocrystal component at equilibrium, as long as the activity coefficients are unity. This approximation applies to dilute solutions and for practical purposes will be used in this manuscript to calculate material balances and solution compositions.

If a binary cocrystal of 1:1 stoichiometry dissolves in pure solvent into its individual components without further complexation or ionization to form a saturated solution, the mass balance for each component in solution can be expressed in terms of the molar solubility of the cocrystal, S

$$[A] = S \quad \text{and} \quad [B] = S, \tag{4}$$

and substituting these in the solubility product equation (3) gives

$$\mathrm{K_{sp}} = S^2 \quad \text{and} \quad S = (\mathrm{K_{sp}})^{1/2} \tag{5}$$

Equations 4 and 5 apply only to solutions of stoichiometric composition when the solution molar ratio is the same as that of the cocrystal.

For non-stoichiometric solution compositions, let C be the excess concentration of ligand so the mass balances when excess B is added become

$$[A] = S \quad \text{and} \quad [B] = S + C, \tag{6}$$

and therefore,

$$\mathrm{K_{sp}} = S(S + C) \tag{7}$$

In the case where a large excess of ligand is present, such that $C >> S$, then

$$S \approx K_{sp} / C\,. \tag{8}$$

A quadratic equation must otherwise be solved, and gives

$$S = \frac{-C + \sqrt{C^2 + 4K_{sp}}}{2} \tag{9}$$

This equation predicts that addition of either cocrystal component to a solution in excess of S decreases the cocrystal solubility when the preceding conditions apply.

A plot of the solubility of cocrystal AB as a function of total ligand in solution according to equation (9) is shown in Figure 2.1.

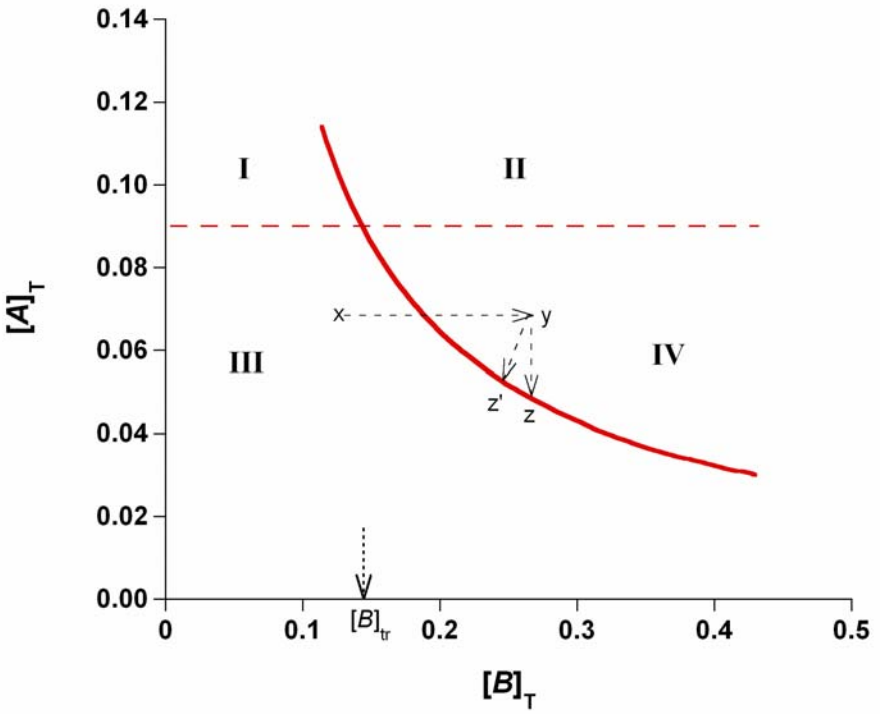

Figure 2.1: Effect of ligand concentration on the solubility of cocrystal AB (solid line) and the solubility of single component crystal A (dashed line) calculated from equation (9) with K_{sp} = 0.0129 M^2, and S_A= 0.09 M. The transition ligand concentration $[B]_{tr}$, occurs when the solubility of A equals the solubility of AB.

Here, $[A]_T = S$ and $[B]_T = S + C$ as shown in equation (6), and the subscript "T" stands for total concentration. This solubility behavior resembles that of the common ion effect in the case of sparingly soluble salts. But in contrast with the case of salts and that of

solvates where analogous equilibria have been considered (Shefter and Higuchi 1963; Tomazic and Nancollas 1979; Nielsen and Toft 1984; Rodríguez-Clemente 1989; Khankari and Grant 1995) cocrystals dissociate into primary components (at least two different molecules) that can crystallize as single component phases.

Also shown in Figure 2.1 is the solubility of single component crystal of *A*, as a function of cocrystal component or ligand (*B*) concentration in solution. This phase diagram is based on the following assumptions: (1) *A* is less soluble than *B*, (2) *A* is less soluble than *AB* in stoichiometric solutions (with respect to *AB*), (3) there is no complexation or ionization of cocrystal components in solution, and (4) the solubility of *A* is independent of the concentration of *B* in solution. Under these considerations, the solubility curves of cocrystal and single component crystal intersect. Therefore, there is a cocrystal component concentration in solution, $[B]_{tr}$, at which the solubility of cocrystal *AB* is equal to the solubility of crystal *A* and above which the solubility of cocrystal *AB* is less soluble than crystal *A*.

The transition concentration of cocrystal component can be predicted by substituting the single component crystal solubility, S_A, for the cocrystal solubility, *S*, in equation (7) and rearranging to give

$$C_{tr} = \frac{K_{sp} - S_A^2}{S_A} \tag{10}$$

where C_{tr} is the excess concentration of cocrystal component at the transition concentration, and the total concentration of cocrystal component at the transition, $[B]_{tr}$, is given by

$$[B]_{tr} = S + C_{tr} = S + \frac{K_{sp} - S_A^2}{S_A} \tag{11}$$

where S is the solubility of cocrystal under stoichiometric conditions. This equation predicts that $[B]_{tr}$ increases as the solubility of A decreases or as K_{sp} increases, as shown in Figure 2.2.

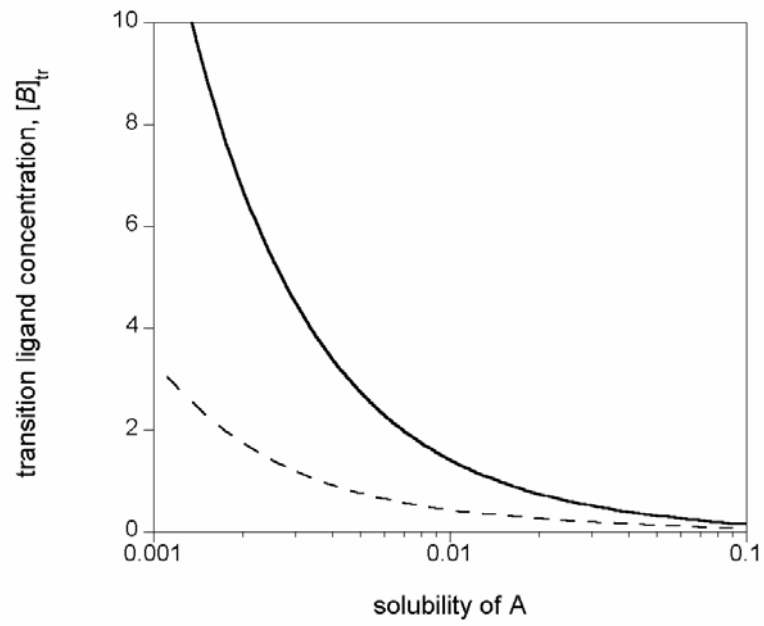

Figure 2.2: The transition ligand concentration as a function of the solubility of the single component crystal, S_A, calculated from equation (11) with values of K_{sp} = 0.0129 M^2 (solid line) and K_{sp} = 0.0032 M^2 (dashed line).

The phase diagram which includes the solubilities of cocrystal and single component crystal, Figure 2.1, also defines four domains representing regions of kinetic and thermodynamic control for the dissolution or crystallization of the single and multi-component phases. Domain I is supersaturated with respect to A but undersaturated with respect to cocrystal AB. Both A and AB are supersaturated in domain II, but undersaturated in domain III. Domain IV is supersaturated with respect to AB but is undersaturated with respect to A. A theoretical plot such as this indicates regions of

thermodynamic stability and which form(s) will dissolve or have the potential to crystallize. This information is important for the development of screening methods for the crystallization of cocrystals, identifying conditions where phase transformations between crystal and cocrystal occur, and controlling or preventing the crystallization of cocrystal in solutions of cocrystal components.

Figure 2.1 also illustrates the path of a solution that is initially undersaturated with respect to *A* and *AB* at point *x* and goes through saturated ($[A]_T = S_{AB}$) and supersaturated ($[A]_T > S_{AB}$) states with respect to *AB* as the ligand concentration in solution increases to point *y*. The driving force for crystallization is the supersaturation, or difference in chemical potential between *y* and *z*. Since crystallization of *AB* will reduce [*B*], the reaction will proceed until a saturated state at *z'* is reached.

While the decrease in cocrystal solubility with increasing ligand concentration provides a means for identifying conditions for preparing cocrystals, the path shown in Figure 2.1, *x* to *y* to *z'*, predicts the unexpected crystallization of *AB* from a formulation of compound *A* in solutions of *B* if only the solubility of *A* is considered during development. For instance, in the case where an API (*A*) is formulated in an undersaturated solution of composition *x* addition of excipient *B* to the solution at a composition *y* may result in crystallization of cocrystal *AB*, since the concentration *y* in domain IV is supersaturated with respect to the cocrystal.

Effect of complex formation in solution on the solubility of cocrystals AB (1:1)

1:1 Solution complexation

When dissolution of a 1:1 cocrystal of an API (*A*) and ligand (*B*) leads to 1:1 complex formation in solution, the equilibrium reactions are

$$AB_{solid} \overset{K_{sp}}{\rightleftharpoons} A_{soln} + B_{soln} \tag{12}$$

$$A_{soln} + B_{soln} \overset{K_{11}}{\rightleftharpoons} AB_{soln} \tag{13}$$

Equilibrium constants for these reactions are the solubility product

$$K_{sp} = [A][B] \tag{14}$$

and the binding constant for the 1:1 complex formed in solution

$$K_{11} = \frac{[AB]}{[A][B]} = \frac{[AB]}{K_{sp}} \tag{15}$$

From the mass balances for *A* and *B* in solution

$$[A]_T = [A] + [AB] \tag{16}$$

$$[B]_T = [B] + [AB] \tag{17}$$

[*AB*] is the solution concentration of complex and according to Equation (15) is

$$[AB] = K_{11}K_{sp} \tag{18}$$

Thus the solution concentration of complex is fixed by the coupled equilibria. This presents an unusual and interesting condition.

Substituting equations (14) and (18) into equations (16) and (17) one obtains

$$[A]_T = \frac{K_{sp}}{[B]} + K_{11}K_{sp} \tag{19}$$

$$[\mathrm{B}]_\mathrm{T} = [\mathrm{B}] + \mathrm{K}_{11}\mathrm{K}_{\mathrm{sp}} \tag{20}$$

$[A]_\mathrm{T}$ is the solubility of cocrystal *AB*, when measuring total *A* in solutions under the equilibrium conditions described in equation (1). By combining the above equations, the cocrystal solubility can be expressed in terms of the total ligand concentration, $[B]_\mathrm{T}$ according to

$$[A]_T = \frac{K_{sp}}{[B]_T - K_{11}K_{sp}} + K_{11}K_{sp} \tag{21}$$

If $\mathrm{K}_{11}\mathrm{K}_{\mathrm{sp}} << [B]_\mathrm{T}$, then

$$[A]_T = \frac{K_{sp}}{[B]_T} + K_{11}K_{sp} \tag{22}$$

Therefore, both K_{sp} and K_{11} can be evaluated from a plot of $[A]_\mathrm{T}$ versus $1/[\mathrm{B}]_\mathrm{T}$. If there are no higher order complexes in solution, this plot is linear with

slope = K_{sp}

and

intercept = $\mathrm{K}_{11}\mathrm{K}_{\mathrm{sp}}$

under the conditions $\mathrm{K}_{11}\mathrm{K}_{\mathrm{sp}} << [B]_\mathrm{T}$.

Equation (22) predicts that cocrystal solubility decreases with increasing ligand concentrations and that cocrystal solubility is higher by a constant value, the product of K_{11} and K_{sp}, compared to the case where there is no solution complexation. This is shown in the lower two curves of Figure 2.3a. The top two curves represent conditions with higher order complexes, 1:2, and are discussed in the following section.

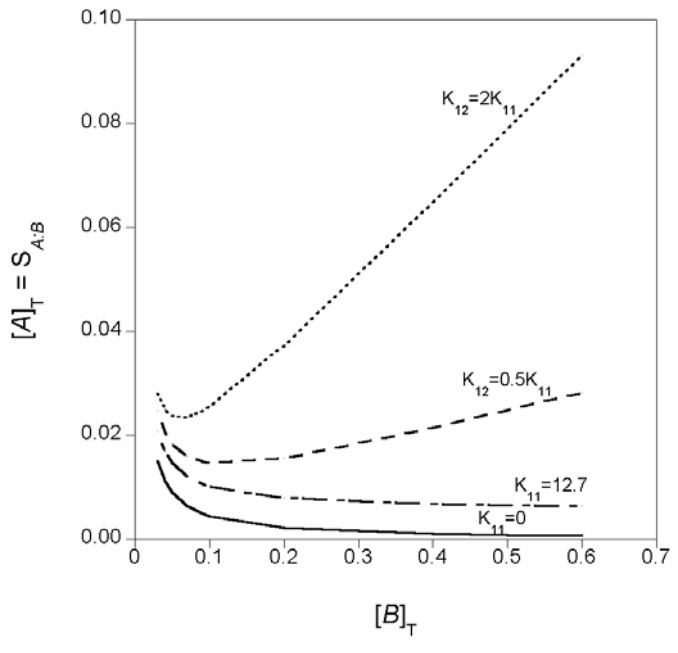

(a)

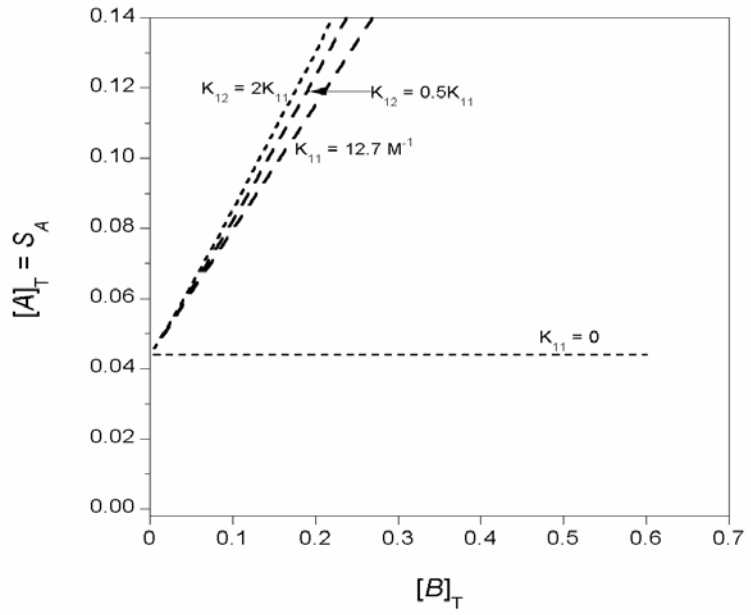

(b)

Figure 2.3: Effect of solution complexation on the solubility of (a) cocrystal *AB* and (b) single component crystal *A* as a function of total ligand concentration. The cocrystal solubility was calculated from equation (22) or (32) depending on the solution complex stoichioimetries as discussed in the text: no complex, 1:1 complex, and 1:1 + 1:2 complexes. Cocrystal $K_{sp} = 4.5 \times 10^{-4}\ M^2$ and the complexation constant values used are indicated in the graph. A minimum cocrystal solubility is predicted when a 1:2 complex is formed and this concentration can be calculated from equation (35). Single component crystal solubility was calculated from equation (25) or (36) considering the same solution complex stoichiometries.

The K_{11} determined from the binary cocrystal solubility as a function of ligand concentration can also be used to predict the solubility increase of single component crystal (*A*) in solutions of ligand, according to

$$A_{solid} \overset{K_s}{\rightleftharpoons} A_{soln} \tag{23}$$

$$A_{soln} + B_{soln} \overset{K_{11}}{\rightleftharpoons} AB_{soln} \tag{24}$$

where K_s is the equilibrium constant for the solubility of crystal *A*, and K_{11} is the binding constant for the formation of the complex *AB* in solution. The equilibrium reaction for complex formation in solution, equation (24), is the same as that in the case of binary cocrystals presented above, equation (13). Using the mass balance for total *A* and total *B*, the solubility of the single component *A* is given by

$$[A]_T = [A]_0 + \frac{K_{11}[A]_0[B]_T}{1 + K_{11}[A]_0} \tag{25}$$

where $[A]_0$ is the intrinsic solubility of crystal *A* in the absence of ligand. When the solubility of cocrystal in solutions of ligand is lower than that of the single component crystal, direct measurement of the solubility of *A* may not be possible due to crystallization of cocrystal. Therefore, this method provides a means of predicting the solubility of *A* in the presence of ligand.

1:1 and 1:2 Solution Complexation

The dependence of cocrystal *AB* solubility on ligand concentration will reveal the presence of 1:1 and 1:2 solution complexes as described below. Consider a 1:2 complex of *A* and *B* formed by bimolecular collisions where *B* binds to *AB* to form the soluble complex AB_2. The equilibrium expression for the formation of the AB_2 complex is

$$AB_{soln} + B_{soln} \overset{K_{12}}{\rightleftharpoons} AB_{2,soln} \tag{26}$$

The equilibria described by equations (12) and (13) lead to formation of the 1:2 complex in a stepwise fashion, and by taking into account the equilibrium constants for these reactions, K_{12} can be expressed in terms of K_{11} and K_{sp} by

$$K_{12} = \frac{[AB_2]}{[AB][B]} = \frac{[AB_2]}{K_{11}K_{sp}[B]} \tag{27}$$

The mass balance of A now becomes

$$[A]_T = [A] + [AB] + [AB_2] \tag{28}$$

Substituting expressions developed for K_{sp}, K_{11}, and K_{12} into this equation leads to an expression for $[A]_T$ in terms of the free ligand concentrations and equilibrium constants by

$$[A]_T = \frac{K_{sp}}{[B]} + K_{11}K_{sp} + K_{11}K_{12}K_{sp}[B] \tag{29}$$

If $[B]$ is not known, the expression for total ligand concentration in solution

$$[B]_T = [B] + K_{11}K_{sp} + 2K_{11}K_{12}K_{sp}[B] \tag{30}$$

can be rearranged and substituted into the mass balance equation for $[A]_T$, equation (29) obtaining

$$[A]_T = \frac{K_{sp}(1 + 2K_{11}K_{12}K_{sp})}{[B]_T - K_{11}K_{sp}} + K_{11}K_{sp} + \frac{K_{11}K_{12}K_{sp}([B]_T - K_{11}K_{sp})}{1 + 2K_{11}K_{12}K_{sp}} \tag{31}$$

This equation can be simplified for the case where $K_{11}K_{sp} << [B]_T$, and $2\ K_{12}K_{11}K_{sp} << 1$ to give

$$[A]_T = \frac{K_{sp}}{[B]_T} + K_{11}K_{sp} + K_{11}K_{12}K_{sp}[B]_T \tag{32}$$

To gain information about the shape of this curve, the first derivative $d[A]_T / d[B]_T$ is examined and reveals that that a plot of $[A]_T$ vs. $[B]_T$ would be concave upward according to the change in slope from negative to positive, corresponding to low values of $[B]_T$ and high values of $[B]_T$, respectively.

The total ligand concentration at which the cocrystal has the minimum solubility ($[A]_T$ has the minimum value) is calculated from

$$\frac{d[A]_T}{d[B]_T} = 0 \quad \text{when} \quad K_{11}K_{12}K_{sp} = \frac{K_{sp}}{[B]_T^{\,2}} \tag{33}$$

and solving for $[B]_T$ gives

$$[B]_T = \sqrt{\frac{1}{K_{11}K_{12}}} \tag{34}$$

The minimum solubility of cocrystal is then obtained by substituting equation (34) in equation (32) and solving for $[B]_T$ to give

$$[A]_{T,\min} = K_{sp}(K_{11} + 2\sqrt{K_{11}K_{12}}) \tag{35}$$

Thus the concentration of ligand at which the minimum cocrystal solubility occurs is inversely proportional to the binding constants and independent of the solubility product, whereas the minimum cocrystal solubility is directly proportional to the solubility product and the binding constants. This behavior is shown in the plot of $[A]_T$ vs. $[B]_T$ for a hypothetical system using equations (30) and (31) and assuming that $K_{sp}= 4.5\text{x}10^{-4}$ M^2, $K_{11}= 12.7$ M^{-1}, and $K_{12}= 0.5\ K_{11}$ or $K_{12}= 2\ K_{11}$, Figure 2.3a.

The solubility of single component crystal of *A* is also dependent on the complexation behavior in solution. For 1:1 and 1:2 complex formation in solution and based on the equilibrium reactions (equations 24 and 26), the solubility of *A* is given by

$$[A]_T = [A]_o + [B]_T \left(\frac{K_{11}[A]_o + K_{12}K_{11}[A]_o[B]}{1 + K_{11}[A]_o + 2K_{12}K_{11}[A]_o[B]} \right) \quad (36)$$

This equation predicts that the solubility of *A* increases in a nonlinear fashion as $[B]_T$ increases, since the slope is a function of $[B]$. A plot of $[A]_T$ vs. $[B]_T$ according to this equation is shown in Figure 2.3b by calculating $[B]$ from the mass balance equation and binding constants according to

$$[B]_T = [B] + K_{11}[A]_o[B] + 2K_{11}K_{12}[A]_o[B]^2 \quad (37)$$

and solving for $[B]$ from the quadratic equation. Values for the binding constants are the same as those used for the prediction of cocrystal solubilities and are K_{11}= 12.7 M^{-1}, K_{12}= 0.5 K_{11} or K_{12} = 2 K_{11}. Theoretical models for evaluating binding constants from the solubility analysis of single component crystals were developed by Higuchi and Zuck (Higuchi and Zuck 1953) for 1:1 complexes and Higuchi and Bolton (Higuchi and Bolton 1959) for higher order complexes and reviewed by Connors and Higuchi (Higuchi and Connors 1965; Connors 1987).

Materials and Methods

Materials

Anhydrous monoclinic carbamazepine (CBZ(III); lot #093K1544 USP grade and 99.8% purity) was purchased from Sigma Chemical Company (St. Louis, MO), stored at 5 °C over anhydrous calcium sulfate and used as received. Nicotinamide (NCT(I); lot #122K0077) was purchased from Sigma Chemical Company (St. Louis, MO) and used as received. Solid state forms were identified by x-ray powder diffraction or differential scanning calorimetry.

Ethyl acetate and 2-propanol were of HPLC grade and were purchased from Fisher Scientific (Fair Lawn, NJ). Anhydrous ethanol (200 proof) was USP grade and was purchased from Pharmco (Brookfield, CT).

Preparation of Cocrystals

Carbamazepine-Nicotinamide (CBZ-NCT)

CBZ-NCT cocrystals (1:1 molar ratio) were prepared by either a solvo-thermal method or by methods based on the phase diagrams presented here, where supersaturation with respect to cocrystal is created by the effect of cocrystal components on reducing the solubility of the molecular complex to be crystallized. In the latter method, the cocrystal was prepared from solutions of non-stoichiometric composition of CBZ and NCT, or by suspending solid CBZ(III) in NCT aqueous or organic solutions, or by suspending CBZ(III) and NCT(I) in pure solvents. No cooling or evaporation was necessary for co-crystallization. In the solvo-thermal method, however, supersaturation was created by cooling a solution of NCT (0.35 g; 2.83 mmol) and CBZ (0.67g; 2.83 mmol) in ethyl acetate (50 g) from 40 °C to 25 °C. The solid phases by any of the above methods were harvested by vacuum filtration and dried at room temperature (22-23 °C) under reduced pressure (25 mmHg) on Whatman #50 filter paper (Maidstone, England) for 30 minutes to remove loosely bound solvent. The solid phases were confirmed to be CBZ:NCT cocrystal by x-ray powder diffraction, FT-IR spectroscopy, and differential scanning calorimetry. Cocrystals were stored at 5 °C over anhydrous calcium sulfate.

Solubility of Cocrystals in Organic Solvents

The equilibrium solubility of CBZ-NCT cocrystal in pure organic solvents (ethanol, 2-propanol, or ethyl acetate) was determined from undersaturation by adding excess cocrystal solid phase in each solvent. The suspensions were stirred with magnetic stirrers in 20 mL glass vials at constant temperature (25 ± 0.5 °C) maintained with a circulating temperature bath (Neslab RTE-110, Portsmouth, NH). Samples were drawn at various time intervals over 72 h and filtered using a 0.22 μm nylon filter (Osmonics, Minnetonka, MN), allowing at least 2 mL to saturate the filter prior to sample collection. Samples were diluted with the same solvent in which the solubility analysis was performed. The solutions equilibrated within 48 h and average sample concentration differed by < 2% at 24 and 48 h. CBZ concentrations were calculated by measuring the absorbance of CBZ (λ_{max} = 284 nm) by UV/Vis spectroscopy (Beckman DU-650, Fullerton, CA). The CBZ concentration corresponds to the CBZ-NCT solubility based on the 1:1 molar ratio cocrystal.

Because of the cocrystal to CBZ dihydrate transformation in water(Rodríguez-Spong 2005), the solubility in aqueous systems is not reported here. The solubility of CBZ-NCT in NCT solutions of ethanol, 2-propanol, or ethyl acetate was determined by the same methods as described above. A large dilution factor (~1000x) was necessary to maintain linearity according to Beer's Law. Under these conditions the complexation reported in the results section is not detectable. NCT solutions were prepared by diluting stock solutions of NCT with the respective solvents. The NCT concentrations studied varied from 30 to 50% of the NCT(I) solubility in the solvents (Table 2.1).

Solubility of Cocrystal Components in Organic Solvents

Equilibrium solubility of CBZ and NCT in ethanol, 2-propanol, or ethyl acetate was determined from undersaturation by adding excess solid CBZ(III) or NCT(I) to each solvent, respectively. Experiments were carried out in a similar manner as described for the cocrystal, and samples were analyzed by UV/Vis spectroscopy for CBZ and HPLC for NCT. The HPLC instrument (Agilent 1100 series, Palo Alto, CA) was equipped with a UV diode array detector (Agilent Technologies G1315B, Palo Alto, CA) and contained a Zorbax SB-Phenyl 2.1 x 150 mm column packed with 5 μm media (Agilent Technologies, Palo Alto, CA). The maximum wavelength for absorbance for NCT was set at 260 nm. NCT concentrations were analyzed following a 15 minute isocratic method using a 60/40 water/methanol mobile phase containing 0.1% trifluoroacetic acid.

X-ray Powder Diffraction (XRPD)

Powder diffraction patterns of solid phases were recorded with a Scintag X-ray diffractometer (Franklin, MA) using CuKα radiation (λ = 1.54Å), tube voltage of 40kV, and tube current of 20mA. The intensities were measured at 2-theta values from 2° to 50° at a continuous scan rate of 5 °/min. When steady state concentrations were obtained during the solubility experiments, the solid phase was analyzed by x-ray powder diffraction and results were compared to the diffraction patterns of each pure phase.

Infrared (IR) Spectroscopy

FTIR spectra of solid phases were collected on a Bruker Vertex 70 FT-IR (Billerica, MA) unit equipped with a DTGS detector. Samples were placed on a zinc

selenide (ZnSe) Attenuated Total Reflectance (ATR) crystal accessory and 64 scans were collected for each sample at a resolution of 4 cm^{-1} over a wavenumber region of 4000-600 cm^{-1}.

Differential Scanning Calorimetry (DSC)

The thermal behavior of solid phases was studied using a TA Instruments 2920 modulated DSC (TA Instruments, New Castle, DE) with refrigerated cooling system (RCS) in standard mode. Approximately 5-10 mg samples were weighed into aluminum DSC pans, crimped, and heated at 10 °C/min. A dry nitrogen purge was used at a flow rate of 50 cc/min through the DSC cell and 110 cc/min through the RCS. The DSC was calibrated for temperature using n-dodecane (T_m = -9.65°C, Aldrich, Milwaukee, WI) and indium (T_m = 156.60°C, TA Instruments, New Castle, DE) at 10ºC/min. Indium was used to calibrate the cell constant.

Results

The solubilities of cocrystal CBZ-NCT (1:1) and the single component crystals of CBZ and NCT in three organic solvents are presented in Table 2.1.

Table 2.1: Solubilities of cocrystal CBZ-NCT and single component crystals, CBZ(III) and NCT(I), in organic solvents at T = 25 °C. Solubility values are the mean ± standard deviation of n=3.

Compound	Ethanol (M)	2-Propanol (M)	Ethyl acetate (M)
CBZ-NCT (1:1)	$0.116^{a} \pm 0.003$	$0.044^{b} \pm 0.003$	$0.024^{c} \pm 0.001$
CBZ(III)	$0.1080^{a} \pm 0.0001$	$0.039^{b,d} \pm 0.003$	$0.0440^{c,d} \pm 0.0001$
NCT(I)	0.841 ± 0.008	0.496 ± 0.004	0.098 ± 0.002

[a]Statistically significant difference in solubilties, $P < 0.05$
[b]Statistically insignificant difference in solubilities, $P > 0.10$
[c]Statistically significant difference in solubilities, $P < 0.001$
[d]Statistically insignificant difference in solubilities, $P > 0.05$

The cocrystal solubility depends on the solvent as follows: ethanol > 2-propanol > ethyl acetate. CBZ is the least soluble of the two cocrystal components in these solvents and the solubility of the most thermodynamically stable polymorph, monoclinic form (III) ranks as follows: ethanol > 2-propanol = ethyl acetate. NCT solubility follows the same order as the cocrystal solubility.

The solubility ratio of cocrystal to single component crystal is important when considering solvents and conditions for the crystallization and isolation of cocrystals by solvent evaporation or cooling methods. Results show that the largest difference in the solubility of cocrystal and CBZ(III) is observed in ethyl acetate, with a solubility ratio (cocrystal/CBZ(III)) of 0.55. The solubilities of cocrystal and CBZ(III) are very similar in ethanol (ratio = 1.07 and significant at $P < 0.05$) while in 2-propanol the solubilities are not significantly different ($P > 0.10$).

The cocrystal solubility decreases nonlinearly as the total nicotinamide concentration increases in the solvents studied, as shown in Figure 2.4.

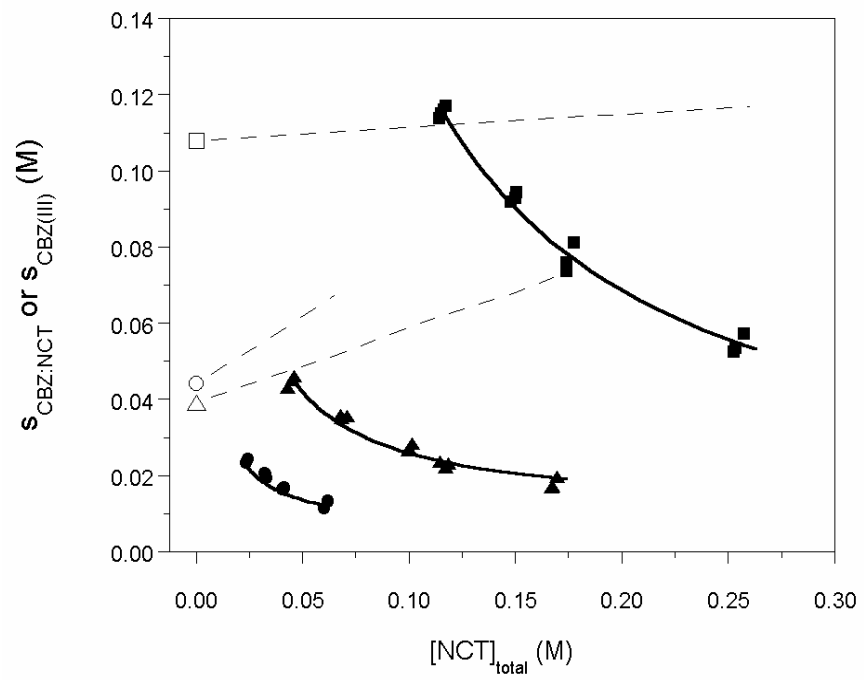

Figure 2.4: Solubility of CBZ-NCT cocrystal (1:1) and single component crystal of CBZ(III) at 25 °C as a function of total NCT concentration in ethanol, 2-propanol, and ethyl acetate. The solid lines represent the predicted solubility, according to equation (43) with values for K_{sp} and K_{11} in Table 3. Filled symbols are experimental cocrystal solubility values in (■) ethanol, (▲) 2-propanol, and (●) ethyl acetate. The dashed lines represent the predicted solubility of CBZ(III) according to equation (25) and the K_{11} values calculated from the cocrystal solubility analysis, Table 3. Open symbols are experimental CBZ(III) polymorph solubility values in pure solvent.

This behavior is anticipated from the solubility product according to the equilibrium reaction, equation (1), in the absence of solution complexation and the solubility of cocrystal given by equation (9). When applied to this cocrystal the equilibrium reaction is

$$\text{CBZ-NCT}_{solid} \overset{K_{sp}}{\rightleftharpoons} \text{CBZ}_{soln} + \text{NCT}_{soln} \tag{38}$$

and the solubility product becomes

$$K_{sp} = [\text{CBZ}][\text{NCT}] \tag{39}$$

Solubility products were calculated from the slopes of plots of the total CBZ concentration in solution versus the inverse of the total NCT concentration according to

$$[\text{CBZ}] = \frac{K_{sp}}{[\text{NCT}]}. \tag{40}$$

The results follow this linear dependence as shown in Figure 2.5.

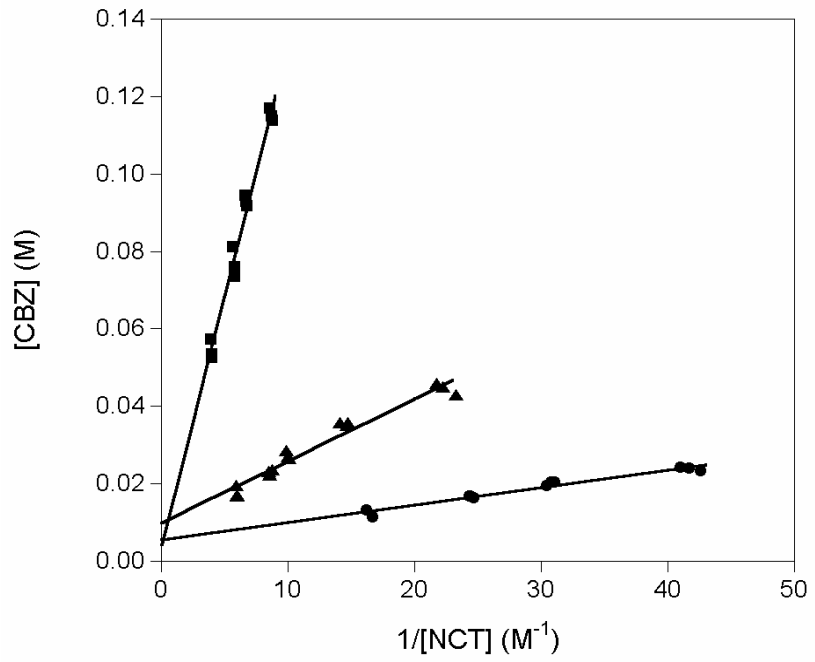

Figure 2.5: Total CBZ concentration in equilibrium with cocrystal, CBZ-NCT, at 25 °C as a function of the inverse total NCT concentration in (■) ethanol, (▲) 2-propanol, and (●) ethyl acetate, showing the linear dependence predicted by equation (43).

Examination of the linear regression analysis in Table 2.2 reveals that in 2-propanol and ethyl acetate the y-intercepts are statistically different from zero, suggesting that a 1:1 solution complex is in equilibrium with the dissolved single components and the cocrystal according to the equilibrium reactions given by equations (12) and (13), that when applied to this system become

$$\text{CBZ-NCT}_{\text{solid}} \overset{K_{sp}}{\rightleftharpoons} \text{CBZ}_{\text{soln}} + \text{NCT}_{\text{soln}} \tag{41}$$

$$CBZ_{soln} + NCT_{soln} \overset{K_{11}}{\rightleftharpoons} CBZ{:}NCT_{soln} \quad (42)$$

Table 2.2: Linear regression analysis according to equation (43).

Solvent	**Equation of line** (± standard error of slope and y-intercept)	**R^2 value**
Ethanol	y = 0.0129 (± 0.0006) x + 0.0042 (± 0.0037)	0.98
2-Propanol	y = 0.0016 (± 0.0001) x + 0.010 (± 0.001)	0.96
Ethyl acetate	y = 0.00045 (± 0.00003) x + 0.0057 (± 0.0008)	0.97

The solubility products and complexation constants were calculated from equation (22) when $K_{11}K_{sp} << [B]_T$ in the form of

$$[CBZ]_T = \frac{K_{sp}}{[NCT]_T} + K_{11}K_{sp}. \quad (43)$$

Table 2.3 presents the K_{sp} values calculated from the slopes and the K_{11} values calculated from the y-intercepts according to equation (43).

Table 2.3: CBZ-NCT cocrystal solubility product, K_{sp}, and solution complexation constant, K_{11}, in organic solvents.

Solvent	**K_{sp} (M^2)**	**K_{11} (M^{-1})**
Ethanol	0.0129 ± 0.0006^a	0.3 ± 0.3^a
2-Propanol	0.0016 ± 0.0001	6.3 ± 0.7
Ethyl acetate	0.00045 ± 0.00003	12.7 ± 1.8

[a]standard error in each solvent system.

The cocrystal solubility curves predicted from this equation and shown in Figure 2.4 are in very good agreement with the experimental solubility values. K_{sp} values follow the same relative order as the cocrystal solubilities: ethanol > 2-propanol > ethyl acetate, whereas K_{11} values follow a trend inverse to the solubility of cocrystal. Although in ethanol the y-intercept was not statistically different from zero, the K_{11} was still calculated; however, the small K_{11} value obtained and the large standard error associated with it suggests that 1:1 complexation is negligible in this solvent.

Figure 2.6 compares the experimental and predicted cocrystal solubilities had solution complexation been neglected, according to equation (40).

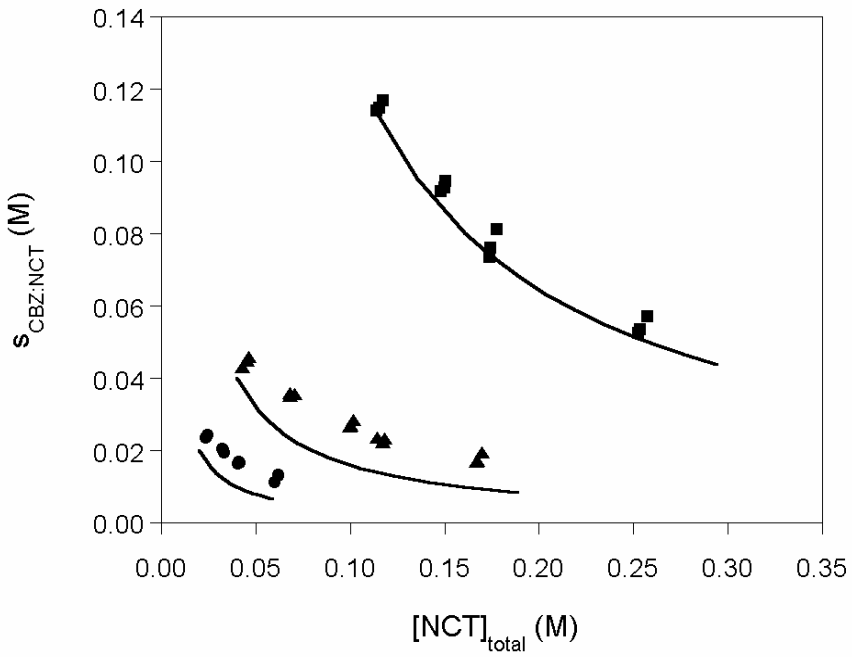

Figure 2.6: Comparison of experimental and calculated cocrystal solubilities as a function of ligand concentration, when solution complexation is neglected, according to equation (40), and using the K_{sp} values calculated from the slopes of the lines in Figure 5, Table 3. Symbols represent experimental solubility values in (■) ethanol, (▲) 2-propanol, and (●) ethyl acetate.

This shows that 1:1 solution complexation of cocrystal components increases the solubility of a 1:1 cocrystal by a constant, which is the product of K_{sp} and K_{11}. Thus, if only the K_{sp} calculated from the solubility of cocrystal in pure solvents was considered to predict the cocrystal solubility dependence on nicotinamide concentration, the cocrystal solubility would have been underestimated.

Preliminary experiments to measure the solubility of the single component crystal, CBZ(III), in nicotinamide solutions at concentrations above the solubility of the cocrystal, *S*, showed transformation of CBZ(III) to cocrystal. Figure 2.4 shows the measured solubility of CBZ(III) in pure solvent (Kelly 2003) and the predicted dependence on NCT solution concentration as a result of solution complexation. K_{11} values in Table III were used in equation (25) to predict the solubility of CBZ(III) in nicotinamide solutions. The solubility of CBZ(III) and transformation to cocrystal in solutions of cocrystal components is currently under investigation in our laboratory.

Discussion

Theoretical analysis and experimental results presented here show that the solubility of cocrystal depends on the concentration of cocrystal components in solution, and that this dependence can be explained by a cocrystal solubility product and by the binding constants of complexes formed in solution. The solubility product behavior is analogous to that described for sparingly soluble salts (Butler 1964; Sohnel and Garside 1979; Nielsen and Toft 1984; Rodríguez-Clemente 1989) however, with the main difference that cocrystals dissociate into molecules that can crystallize as single component phases. Thus, in addition to explaining the solubility behavior of binary

cocrystals, the analysis presented here can reveal complexation in solution and identify well-defined regions in the parameter space from which to crystallize the desired components, and where solid phase transformations may occur.

Our results show that the CBZ-NCT cocrystal solubility decreases as the ligand concentration, NCT, increases in organic solutions. This behavior is expected based on the cocrystal K_{sp} alone when solution complexation is negligible, as well as by K_{sp} and K_{11} when there are complexes in solution with the same stoichiometry as the cocrystal. Similar observations have been reported for the descending segment of type B phase solubility diagrams (Higuchi and Connors 1965).

In contrast to the phase solubility analysis that studies the solubility of substrate or API starting with the single component crystal, here we consider the solubility of cocrystals when the cocrystal under study is the only solid phase at equilibrium. The theoretical analysis presented in this report shows that (1) the solubility of a 1:1 cocrystal *AB* is described by a solubility product, (2) the cocrystal solubility is increased by a constant value when there is 1:1 solution complexation, because the concentration of this complex is a constant (the product of $K_{11}K_{sp}$), and (3) the cocrystal solubility goes through a minimum value when there are 1:1 and 1:2 solution complexes. Thus a graphical representation of the cocrystal solubility dependence on ligand concentration will serve as a diagnostic tool for the stoichiometry of solution complexes.

This analysis was applied to the solubility of the CBZ-NCT (1:1) cocrystal and allowed for measurement of the solubility product and the 1:1 equilibrium constant for solution complex formation. The K_{sp} values were dependent on solvent and were proportional to the solubility of cocrystal in pure solvent. The K_{11} values were inversely

related to cocrystal solubility and to cocrystal component solubilities. This indicates that complex formation is favored in solvents where these components have lower solubilities. Similar trends have been reported for solution complexation of various drugs with ligands as reviewed by Higuchi and Connors (Higuchi and Connors 1965), and have been explained by considering that solubility of a solute reflects the affinity of the solute with the solvent, thus higher solubilities favor solute-solvent interactions whereas lower solubilities favor solute-solute interactions.

Given these observations it is of interest to consider what drives the molecular complexes of CBZ and NCT in solution and how these might relate to the supramolecular complex in the cocrystal. The structure of the cocrystal (Fleischman, Kuduva et al. 2003) shows that nicotinamide links with the carbamazepine homodimer (carboxamide dimer) by forming a hydrogen-bonded tape where donors and acceptors of both amide groups are fulfilled. The nitrogen atom within the ring structure of nicotinamide does not form strong hydrogen bonds. There are also π-π interactions between the carbamazepine and nicotinamide rings. Studies of solution complexation of nicotinamide and other aliphatic amides with various APIs (diazepam, steroids, griseofulvin) concluded that the aromaticity of the pyridine ring, promotes plane-to plane stacking of molecules in solution and favors complex formation (Rasool, Hussain et al. 1991). Amides have also been shown to participate in hydrogen-bonding with carboxylic acids in solution (Kostenbauder and Higuchi 1956). While we only studied three solvents, ethanol, 2-propanol and ethyl acetate, the hydrogen bonding properties differ and the ability of the solvent to interact as hydrogen bond donor and acceptor appears to weaken the complex formation.

K_{11} values calculated for CBZ and NCT in this study are similar to those reported for drug nicotinamide complexes in water at 25 ^{o}C in the range of 4 to 20 M^{-1}. The strongest binding is exhibited by moricizine (17 M^{-1} in pH 6 and 8 M^{-1} in pH 7, both parabolic fits) (Hussain, DiLuccio et al. 1993), halofantrine (5 to 9 and 18 to 20 M^{-1}, depending on linear or parabolic fits) (Lim and Go 2000) and nifedipine (9 M^{-1}) (Suzuki and Sunada 1998) followed by diazepam, griseofulvin, progesterone, 17 –α estradiol, testosterone (Rasool, Hussain et al. 1991), and oxytetracycline (Higuchi and Bolton 1959), all between 4 and 5 M^{-1}.

Although CBZ-NCT did not form a 1:2 complex in the solvents studied, NCT has been reported to form a 1:2 complex with other compounds, and the K_{12} values span a much larger range than the K_{11} values. For example, the highest K_{12} value observed is of the halofantrine and NCT complex (82 to 150 and 30 to 38 M^{-1}, depending on linear or parabolic fits) (Lim and Go 2000), followed by the steroids (progesterone, 17 –α estradiol, and testosterone) between 25 and 45 M^{-2} (Rasool, Hussain et al. 1991), and moricizine exhibits the smallest K_{12} value of 1 M^{-1} in pH 6 and 5 M^{-1} in pH 7 (both parabolic fits) (Hussain, DiLuccio et al. 1993).

Phase solubility methods have been applied to pharmaceutical compounds since the 1950s to identify the solution complexation behavior of poorly-water-soluble drugs or substrates with a soluble ligand (Higuchi and Zuck 1953; Higuchi and Zuck 1953; Kostenbauder and Higuchi 1956; Higuchi and Bolton 1959). In these reports, the solubility of the single component crystal of a drug or substrate is studied and the solid phase is examined for the formation of solid-state complexes that are less soluble than the single component crystal of substrate.

The focus of these earlier reports was to enhance the solubility of drugs in water and address the behavior of soluble solution complexes, or type A phase solubility diagrams. Formation of solid-state complexes received less attention, although work was done to identify the stoichiometry of complexes from the solubility behavior. Models were developed that describe the solubility behavior in terms of solution complexation and the transformation of a single component crystal of substrate to an insoluble complex that resulted in type B solubility diagrams (Higuchi and Zuck 1953; Kostenbauder and Higuchi 1956; Higuchi and Pitman 1973).

While cocrystal solubility is a useful operational variable its value depends on the solution composition of cocrystal constituents, whereas under these conditions the solubility product is a constant. Solubility products are dependent on temperature, solvent, and conditions that affect the activity coefficients of cocrystal components in solution (Tomazic and Nancollas 1979; Rodríguez-Clemente 1989). In view of the fact that the concentration of cocrystal components in solution can be varied independently, the solubility product is a meaningful parameter to consider when developing methods for cocrystal screening or designing liquid solution formulations where crystallization of cocrystal is to be avoided. Thus, an evaluation of K_{sp} from only the cocrystal solubility in pure solvents can be used to estimate the cocrystal solubility dependence on ligand concentration. Although this may underestimate the cocrystal solubility (due to neglecting solution complexation), it is a useful and conservative prediction when developing solution formulations with components that form cocrystals.

Conclusions

In this chapter mathematical models are presented that explain the solubility behavior of cocrystals as a function of cocrystal component concentration in solution by considering the solution complexation of cocrystal components. The immediate implication of the results is that cocrystal solubility products and solution complexation constants can be evaluated from solubility studies. This is shown for the carbamazepine-nicotinamide cocrystal in organic solvents. The broader implications are that these concepts can be applied to calculate crystallization diagrams for cocrystal preparation, to develop cocrystal screening methods, and to formulate solutions with cocrystal components where crystallization is to be avoided.

References

Aakeroy, C. B., A. M. Beatty, et al. (2003). "Do polymorphic compounds make good cocrystallizing agents? A structural case study that demonstrates the importance of synthon flexibility." *Crystal Growth & Design* **3**: 159-165.

Amai, M., T. Endo, et al. (1998). "1:1 Complex of Octadecanoic Acid and 3-Pyridinecarboxamide." *Acta Crystallographica Section C* **54**: 1367-1369.

Bettinetti, G., M. R. Caira, et al. (2000). "Structure and Solid-State Chemistry of Anhydrous and Hydrated Crystal Forms of the Trimethoprim-Sulfamethoxypyridazine 1:1 Molecular Complex." *Journal of Pharmaceutical Sciences* **89**: 478-489.

Brader, M. L., M. Sukumar, et al. (2002). "Hybrid insulin cocyrstals for controlled release delivery." *Nature Biotechnology* **20**: 800-804.

Butler, J. N. (1964). *Ionic Equilibrium: A Mathematical Approach* Massachusetts, Addison-Wesley.

Childs, S. L., L. J. Chyall, et al. (2004). "Crystal Engineering Approach to Forming Cocrystals of Amine Hydrochlorides with Organic Acids. Molecular Complexes of Fluoxetine Hydrochloride with Benzoic, Succinic, and Fumaric Acids." *Journal of the American Chemical Society* **126**: 13335-13342.

Connors, K. A. (1987). *Binding Constants: The Measurement of Molecular Complex Stability*. New York, John Wiley & Sons.

Desiraju, G. R. (1995). "Supramolecular Synthons in Crystal Engineering--A New Organic Synthesis." *Angewandte Chemie International Edition in English* **34**: 2311-2327.

Etter, M. C. (1990). "Encoding and Decoding Hydrogen-Bond Patterns of Organic Compounds." *Accounts of Chemical Research* **23**: 120-126.

Fleischman, S. G., S. S. Kuduva, et al. (2003). "Crystal Engineering of the Composition of Pharmaceutical Phases: Multiple-Component Crystalline Solids Involving Carbamazepine." *Crystal Growth & Design* **3**: 909-919.

Grant, D. J. W. and T. Higuchi (1990). *Solubility Behavior of Organic Compounds*. New York, Wiley.

Higuchi, T. and S. Bolton (1959). "The Solubility and Complexing Properties of Oxytetracycline and Tetracycline III." *Journal of the American Pharmaceutical Association* **48**: 557-564.

Higuchi, T. and K. A. Connors (1965). Phase-Solubility Techniques. *Advances in Analytical Chemistry and Instrumentation*. H. W. Nurnberg. New York, Wiley-Interscience**:** 117-212.

Higuchi, T. and I. H. Pitman (1973). "Caffeine Complexes with Low Water Solubility: Synthesis and Dissolution Rates of 1:1 and 1:2 Caffeine-Gentisic Acid Complexes." *Journal of Pharmaceutical Sciences* **62**: 55-58.

Higuchi, T. and D. A. Zuck (1953). "Investigation of Some Complexes Formed in Solution by Caffeine. II. Benzoic Acid and Benzoate Ion." *Journal of the American Pharmaceutical Association* **42**: 132-138.

Higuchi, T. and D. A. Zuck (1953). "Investigation of Some Complexes Formed in Solution. III. Interactions Between Caffeine and Aspirin, p-Hydroxybenzoic Acid, m-Hydroxybenzoic Acid, Salicylic Acid, Salicylate Ion, and Butyl Paraben." *Journal of the American Pharmaceutical Association* **42**: 138-145.

Hussain, M. A., R. C. DiLuccio, et al. (1993). "Complexation of Moricizine with Nicotinamide and Evaluation of the Complexation Constants by Various Methods." *Journal of Pharmaceutical Sciences* **82**: 77-79.

Kelly, R. C. (2003). A Molecular Approach to Understanding the Directed Nucleation and Phase Transformation of Carbamazepine and Nitrofurantoin in Aqueous and Organic Solutions, Ph.D. Thesis, University of Michigan.

Khankari, R. K. and D. J. W. Grant (1995). "Pharmaceutical Hydrates." *Thermochemica Acta* **248**: 61-79.

Kostenbauder, H. B. and T. Higuchi (1956). "Formation of Molecular Complexes by Some Water-Soluble Amides I." *Journal of the American Pharmaceutical Association* **45**: 518-522.

Leiserowitz, L. and G. M. J. Schmidt (1969). "Molecular Packing Modes. Part III. Primary Amides." *Journal of the Chemical Society (A): Inorganic, Physical, Theoretical*: 2372-2382.

Lim, L.-Y. and M.-L. Go (2000). "Caffeine and nicotinamde enhances the aqueous solubility of the antimalarial agent halofantrine." *European Journal of Pharmaceutical Sciences* **10**: 17-28.

Nielsen, A. E. and J. M. Toft (1984). "Electrolyte Crystal Growth Kinetics." *Journal of Crystal Growth* **67**: 278-288.

Rasool, A. A., A. A. Hussain, et al. (1991). "Solubility Enhancement of Some Water-Insoluble Drugs in the Presence of Nicotinamide and Related-Compounds." *Journal of Pharmaceutical Sciences* **80**: 387-393.

Remenar, J. F., S. L. Morissette, et al. (2003). "Crystal Engineering of Novel Cocrystals of a Triazole Drug with 1,4-Dicarboxylic Acids." *Journal of the American Chemical Society* **125**: 8456-8457.

Rodríguez-Clemente, R. (1989). "Complexing and Growth Units in Crystal Growth from Solutions of Electrolytes." *Journal of Crystal Growth* **98**: 617-629.

Rodríguez-Spong, B. (2005). Enhancing the Pharmaceutical Behavior of Poorly Soluble Drugs Through the Formation of Cocrystals and Mesophases, Ph.D. Thesis, University of Michigan.

Rodríguez-Spong, B., P. Zocharski, et al. (2003). "Enhancing the Pharmaceutical Behavior of Carbamazepine Through the Formation of Cocrystals " *The AAPS Journal* **5**: Abstract M1298.

Shefter, E. and T. Higuchi (1963). "Dissolution Behavior of Crystalline Solvated and Nonsolvated Forms of Some Pharmaceuticals." *Journal of Pharmaceutical Sciences* **52**: 781-791.

Sohnel, O. and J. Garside (1979). "The Thermodynamic Driving Force for Crystallization from Solution." *Journal of Crystal Growth* **46**: 238-240.

Suzuki, H. and H. Sunada (1998). "Mechanistic Studies on Hydrotropic Solubilization of Nifedipine in Nicotinamide Solution." *Chemical and Pharmaceutical Bulletin* **46**: 125-130.

Tomazic, B. and G. H. Nancollas (1979). "The Kinetics of Dissolution of Calcium Oxalate Hydrates." *Journal of Crystal Growth* **46**: 355-361.

Trask, A. V., W. D. S. Motherwell, et al. (2005). "Pharmaceutical Cocrystallization: Engineering a Remedy for Caffeine Hydration." *Crystal Growth & Design* **5**: 1013-1021.

Walsh, R. D. B., M. W. Bradner, et al. (2003). "Crystal Engineering of the Composition of Pharmaceutical Phases." *Chemical Communications*: 186-187.

Zocharski, P., S. Nehm, et al. (2004). "Can Solubility Products Explain Cocrystal Solubility and Predict Crystallization Conditions?" *The AAPS Journal* **6**: Abstract R6192.

CHAPTER THREE

APPLYING SOLUBILITY PRODUCT BEHAVIOR AND SOLUTION COMPLEXATION TO CARBAMAZEPINE-SACCHARIN COCRYSTAL

Introduction

Pharmaceutical cocrystals, crystalline complexes, are multi-component compounds connected primarily through hydrogen bonds. Cocrystals increase the diversity of solid-state forms of an API, even for non-ionizable APIs, and can enhance pharmaceutical properties by modification of chemical stability, moisture uptake, mechanical behavior, solubility, dissolution rate, and bioavailability (Remenar, Morissette et al. 2003; Childs, Chyall et al. 2004; Rodríguez-Spong 2005; McNamara, Childs et al. 2006; Jayasankar, Good et al. 2007; Remenar, Peterson et al. 2007; Bak, Gore et al. 2008; Childs, Rodríguez-Hornedo et al. 2008). Research from our group has shown that cocrystal solubility can be explained by heterogeneous and homogeneous equilibria, including cocrystal dissociation, solution complexation, and ionization (Nehm, Rodríguez-Spong et al. 2006; Nehm, Jayasankar et al. 2006; Rodríguez-Hornedo, Nehm et al. 2006; Jayasankar, Reddy et al. 2008).

The dependence of cocrystal solubility on solubility product and complexation constants provides a powerful approach to design cocrystal screening methods and to formulate solutions with cocrystal components where crystallization does not occur (Nehm, Seefeldt et al. 2005; Nehm, Rodríguez-Spong et al. 2006; Childs, Rodríguez-

Hornedo et al. 2008; Jayasankar, Reddy et al. 2008). This chapter applies cocrystal and solution chemistry to the carbamazepine-saccharin (CBZ-SAC) cocrystal solubility dependence on saccharin concentration in ethanol and 2-propanol.

Materials and Methods

Materials

Anhydrous monoclinic carbamazepine (CBZ(III); lot #093K1544 USP grade and 99.8% purity) was purchased from Sigma Chemical Company (St. Louis, MO), stored at 5 °C over anhydrous calcium sulfate and used as received. Saccharin (SAC; lot #07028EU) was purchased from Sigma Chemical Company (St. Louis, MO) and used as received. Solid state forms were identified by x-ray powder diffraction or differential scanning calorimetry.

Anhydrous ethanol (200 proof) was USP grade and was purchased from Pharmco (Brookfield, CT). 2-propanol was of HPLC grade and was purchased from Fisher Scientific (Fair Lawn, NJ). Solvents were stored over molecular sieves prior to use.

Preparation of Cocrystals

Carbamazepine-Saccharin (CBZ-SAC)

CBZ-SAC cocrystals (1:1 molar ratio) were prepared by either a solvo-thermal method or by methods based on the phase diagrams presented here, where supersaturation with respect to cocrystal is created by the effect of cocrystal components on reducing the solubility of the molecular complex to be crystallized. In the latter method, the cocrystal was prepared from solutions of non-stoichiometric composition of

CBZ and SAC, or by suspending solid CBZ(III) in SAC ethanolic solutions, or by suspending CBZ(III) and SAC in pure solvents. No cooling or evaporation was necessary for co-crystallization. In the solvo-thermal method, however, supersaturation was created by cooling a solution of SAC (2.3g; 12.7mmol) and CBZ (3g; 12.7mmol) in ethanol (91g) from 40 °C to 25 °C. The solid phases by any of the above methods were harvested by vacuum filtration and dried at room temperature (22-23 °C) under reduced pressure (25 mmHg) on Whatman #50 filter paper (Maidstone, England) for 30 minutes to remove loosely bound solvent. The solid phases were confirmed to be CBZ-SAC cocrystal by x-ray powder diffraction.

Solubility of Cocrystals in Organic Solvents

The equilibrium solubility of CBZ-SAC cocrystal in pure organic solvents (ethanol or 2-propanol) was determined from undersaturation by adding excess cocrystal solid phase in each solvent. The suspensions were stirred with magnetic stirrers in 20 mL glass vials at constant temperature (25 ± 0.5 °C) maintained with a circulating temperature bath (Neslab RTE-110, Portsmouth, NH). Samples were drawn at various time intervals over 72 h and filtered using a 0.45 μm PTFE filter (Fisherbrand, Pittsburgh, PA). Samples were diluted with the same solvent in which the solubility analysis was performed. The solutions equilibrated within 48 h and average sample concentration differed by < 2% at 24 and 48 h. CBZ and SAC concentrations were analyzed by HPLC on a Waters system (Milford, MA) equipped with a UV/Vis photodiode array detector. Mobile phase was 70% water/30% acetonitrile with 0.5% perchloric acid and was set at 1mL/min. The CBZ concentration corresponds to the

CBZ-SAC solubility based on the 1:1 molar ratio cocrystal. CBZ was analyzed at 284nm and SAC was analyzed at 260nm.

Solubility of Cocrystal Components in Organic Solvents

Equilibrium solubility of CBZ and SAC in ethanol or 2-propanol was determined from undersaturation by adding excess solid CBZ(III) or SAC to each solvent, respectively. Experiments were carried out in a similar manner as described for the cocrystal, and samples were analyzed on the same HPLC system with the same method as described above.

X-ray Powder Diffraction (XRPD)

Powder diffraction patterns of solid phases were recorded with a Scintag X-ray diffractometer (Franklin, MA) using CuKα radiation (λ = 1.54Å), tube voltage of 40kV, and tube current of 20mA. The intensities were measured at 2-theta values from 2° to 50° at a continuous scan rate of 5 °/min. When steady state concentrations were obtained during the solubility experiments, the solid phase was analyzed by x-ray powder diffraction and results were compared to the diffraction patterns of each pure phase.

Results

The solubilities of cocrystal CBZ-SAC (1:1) and the single component crystals of CBZ and SAC in two organic solvents are presented in Table 3.1. Cocrystal solubility, CBZ concentration, and SAC concentration are all higher in ethanol than in 2-propanol. CBZ(III) is also more soluble than the cocrystal in either solvent. Therefore CBZ(III)

added to any SAC concentration at or above the 1:1 stoichiometric ratio has the propensity transform to cocrystal.

Table 3.1: Solubilities of cocrystal CBZ-SAC and single component crystals, CBZ(III) and SAC, in organic solvents at T = 25 °C. Solubility values are the mean ± standard deviation of n = 3.

Compound	Ethanol (M)	2-Propanol (M)
CBZ-SAC (1:1)	0.0495 ± 0.0004	0.0230 ± 0.0002
CBZ(III)	0.1080 ± 0.0001	0.039 ± 0.003
SAC[a]	0.187	0.25

[a]average and standard deviation for SAC solubilities were not calculated.

Cocrystal solubility decreases nonlinearly as the total saccharin concentration increases in the solvents studied, as shown in Figure 3.1. This behavior is anticipated from the solubility product according to the equilibrium reaction in the absence of solution complexation as shown below:

$$\text{CBZ-SAC} \overset{K_{sp}}{\rightleftharpoons} \text{CBZ} + \text{SAC} \qquad (1)$$

and the solubility product, assuming activity coefficients to be equal to one, becomes

$$K_{sp} = [\text{CBZ}][\text{SAC}] \qquad (2)$$

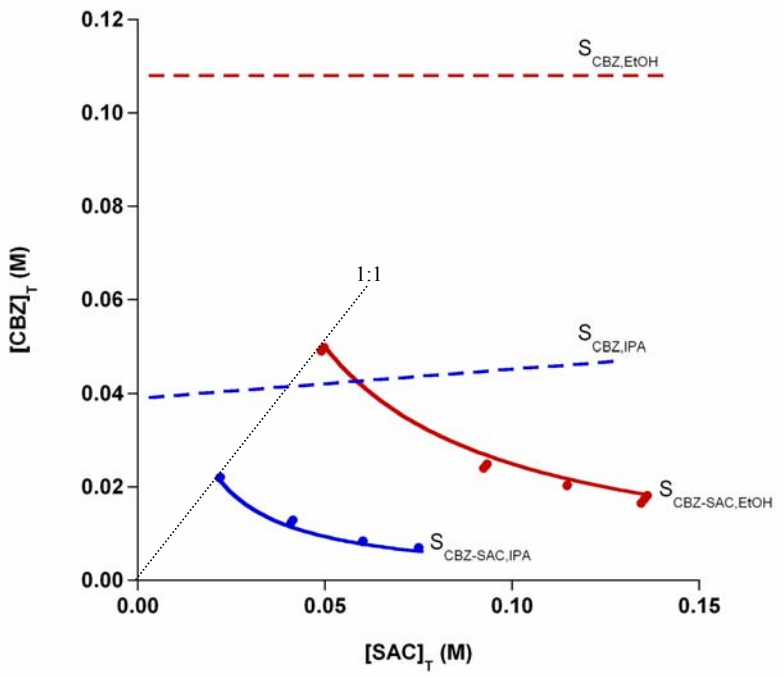

Figure 3.1. Solubility of CBZ-SAC cocrystal (1:1) and single component crystal of CBZ(III) at 25 °C as a function of total SAC concentration in ethanol and 2-propanol. The solid lines represent the predicted solubility, according to equation (6) with values for K_{sp} and K_{11} in Table 3. Filled symbols are experimental cocrystal solubility values in (●) ethanol and (■) 2-propanol. The dashed lines represent CBZ(III) solubility dependence on SAC concentration. The dotted line represents the solution reactant stoichiometry equal to the 1:1 cocrystal.

Solubility products were calculated from the slopes of plots of the total CBZ concentration in solution versus the inverse of the total SAC concentration according to

$$[\mathrm{CBZ}] = \frac{K_{sp}}{[\mathrm{SAC}]}. \qquad (3)$$

The results follow this linear dependence as shown in Figure 3.2.

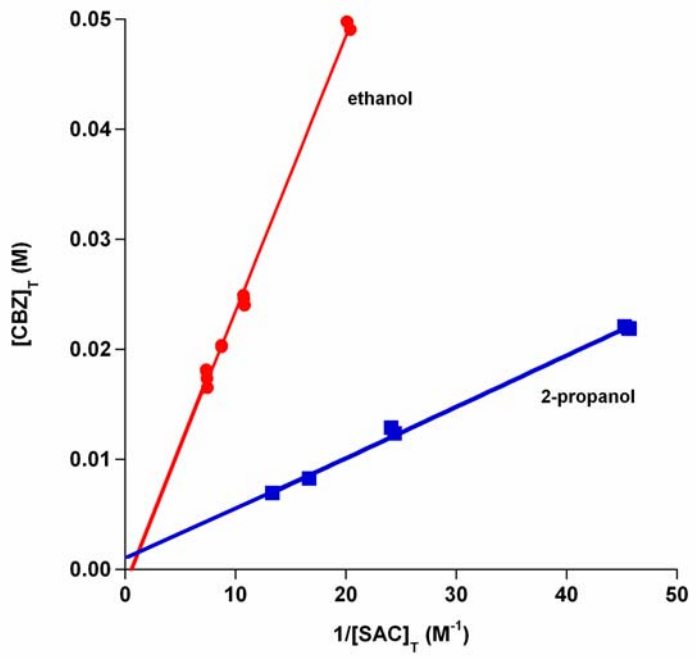

Figure 3.2. Total CBZ concentration in equilibrium with cocrystal, CBZ-SAC, at 25 °C as a function of the inverse total SAC concentration in (●) ethanol and (■) 2-propanol, showing linear dependence predicted by equation (3) or (6).

Examination of the linear regression analysis in Table 3.2 reveals that in 2-propanol the y-intercept is statistically different from zero, suggesting that a 1:1 solution complex is in equilibrium with the dissolved single components and the cocrystal according to the equilibrium reactions given by the following equations

$$\text{CBZ-SAC}_{\text{solid}} \overset{K_{sp}}{\rightleftharpoons} \text{CBZ}_{\text{soln}} + \text{SAC}_{\text{soln}} \qquad (4)$$

$$\text{CBZ}_{\text{soln}} + \text{SAC}_{\text{soln}} \overset{K_{11}}{\rightleftharpoons} \text{CBZ-SAC}_{\text{soln}} \qquad (5)$$

Chapter 2 presents the full derivation for calculating the solubility product and complexation constant. The final equation is shown below:

$$[CBZ]_T = \frac{K_{sp}}{[SAC]_T} + K_{11}K_{sp} \quad (6)$$

Therefore, a plot such as Figure 3.2 can be used to evaluate the solubility product but also the 1:1 solution complexation constant from the y-intercept.

Table 3.3 presents the K_{sp} values calculated from the slopes and the K_{11} value calculated from the y-intercepts according to equation (6). The cocrystal solubility curves predicted from this equation and shown in Figure 3.2 are in very good agreement with the experimental solubility values. K_{sp} values follow the same relative order as the cocrystal solubilities: ethanol > 2-propanol. Solution complexation is only observed in 2-propanol. Because the y-intercept for the linear regression of CBZ-SAC in ethanol was negative and not statistically significant from zero, solution complexation was assumed to be negligible.

Table 3.2. Linear regression analysis according to equation (6).

Solvent	**Equation of line** (± standard error of slope and y-intercept)	**R^2 value**
Ethanol	y = 0.00250 (± 0.00004) x – 0.0015 (± 0.0005)	0.99
2-propanol	y = 0.000467 (± 0.000008) x + 0.00081 (± 0.00022)	0.99

Table 3.3: CBZ-SAC cocrystal solubility product, K_{sp}, and solution complexation constant, K_{11}, in organic solvents.

Solvent	K_{sp} (M^2)	K_{11} (M^{-1})
Ethanol	0.00250 ± 0.00004[a]	--
2-propanol	0.000467 ± 0.000008	1.7 ± 0.5

[a]standard error in each solvent system.

Although complexation constants in 2-propanol are not as large as CBZ-NCT in 2-propanol or ethyl acetate, solution complexation increases the overall solubility of the CBZ-SAC cocrystal. Just as was seen in CBZ-NCT solubility in 2-propanol and ethyl acetate (Nehm, Rodríguez-Spong et al. 2006), 1:1 solution complexation of cocrystal components increases the solubility of a 1:1 cocrystal by a constant, which is the product of K_{sp} and K_{11}. If only K_{sp} was used to describe cocrystal solubility, this solubility would have been underpredicted in 2-propanol.

As described in chapter 2, attempts to measure CBZ(III) solubility in saccharin solutions at concentrations above the transition concentration would have resulted in precipitation of CBZ-SAC. Therefore, the K_{11} value was used to estimate the predicted CBZ(III) solubility dependence on saccharin in 2-propanol (Figure 3.1). Because no solution complexation was observed in ethanol, CBZ(III) solubility was shown to be independent of saccharin concentration.

Conclusions

This chapter is a continuation of chapter 2 in which cocrystal and solution chemistry is used to describe cocrystal solubility. Carbamazepine-saccharin follows

solubility product behavior. In 2-propanol, solution complexation was found to contribute to the overall cocrystal solubility. The K_{11} constant was evaluated graphically from solubility experimental results. The phase solubility diagram which resulted from these studies can be used to design cocrystal synthesis and screening methods.

References

Bak, A., A. Gore, et al. (2008). "The co-crystal approach to improve the exposure of a water insoluble compound: AMG 517 sorbic acid cocrystal characterization and pharmacokinetics." *Journal of Pharmaceutical Sciences* **97**: 3942-3956.

Childs, S. L., L. J. Chyall, et al. (2004). "Crystal Engineering Approach to Forming Cocrystals of Amine Hydrochlorides with Organic Acids. Molecular Complexes of Fluoxetine Hydrochloride with Benzoic, Succinic, and Fumaric Acids." *Journal of the American Chemical Society* **126**: 13335-13342.

Childs, S. L., N. Rodríguez-Hornedo, et al. (2008). "Screening strategies based on solubility and solution composition generate pharmaceutically acceptable cocrystals of carbamazepine." *Crystal Engineering Communications* **10**: 856-864.

Jayasankar, A., D. J. Good, et al. (2007). "Mechanisms by which moisture generates cocrystals." *Molecular Pharmaceutics* **4**: 360-372.

Jayasankar, A., L. S. Reddy, et al. (2008). "The Role of Cocrystal and Solution Chemistry on the Formation and Stability of Cocrystals with Different Stoichiometry." *Crystal Growth & Design* (in press).

McNamara, D. P., S. L. Childs, et al. (2006). "Use of a glutaric acid cocrystal to improve oral bioavailability of a low solubility API." *Pharmaceutical Research* **23**: 1888-1897.

Nehm, S., B. Rodríguez-Spong, et al. (2006). "Phase Solubility Diagrams of Cocrystals Are Explained by Solubility Product and Solution Complexation." *Crystal Growth & Design* **6**: 592-600.

Nehm, S., K. F. Seefeldt, et al. (2005). "Phase Diagrams to Predict Solubility and Crystallization of Cocrystals." *The AAPS Journal* **7**: Abstract W4235.

Nehm, S. J., A. Jayasankar, et al. (2006). "Cocrystals Impart pH-Dependent Solubility to Non-ionizable APIs." *The AAPS Journal* **8**: Abstract W5205.

Remenar, J. F., S. L. Morissette, et al. (2003). "Crystal Engineering of Novel Cocrystals of a Triazole Drug with 1,4-Dicarboxylic Acids." *Journal of the American Chemical Society* **125**: 8456-8457.

Remenar, J. F., M. L. Peterson, et al. (2007). "Celecoxib:Nicotinamide Dissociation: Using excipients to capture the cocrystal's potential." *Molecular Pharmaceutics* **4**: 386-400.

Rodríguez-Hornedo, N., S. J. Nehm, et al. (2006). Cocrystals: Design, Properties and Formation Mechanisms. *Encyclopedia of Pharmaceutical Technology*. J. Swarbrick. London, Taylor & Francis Group.

Rodríguez-Spong, B. (2005). Enhancing the Pharmaceutical Behavior of Poorly Soluble Drugs Through the Formation of Cocrystals and Mesophases, Ph.D. Thesis, University of Michigan.

CHAPTER FOUR

REACTION CRYSTALLIZATION OF PHARMACEUTICAL MOLECULAR COMPLEXES

Introduction

Understanding how molecules assemble by non-covalent bonds to form multiple component crystalline complexes or cocrystals is important for the design and discovery of pharmaceutical solids (Etter 1991; Etter and Reutzel 1991; Desiraju 1995; Nangia and Desiraju 1998; Rodríguez-Spong, Price et al. 2004; Nehm, Rodríguez-Spong et al. 2006). The improved physicochemical and pharmaceutical properties of cocrystals compared to the single component crystal of a drug have been reported, such as dissolution rate, solubility, chemical stability, and moisture uptake (Remenar, Morissette et al. 2003; Rodríguez-Spong, Zocharski et al. 2003; Childs, Chyall et al. 2004; Zocharski, Nehm et al. 2004; Rodríguez-Spong 2005; Trask, Motherwell et al. 2005; McNamara, Childs et al. 2006; Jayasankar, Good et al. 2007; Remenar, Peterson et al. 2007; Bak, Gore et al. 2008).

The key to designing these extended architectures lies in identifying intermolecular interactions that direct molecular assembly (Leiserowitz and Schmidt 1969; Etter 1990; Pedireddi, Jones et al. 1996; Desiraju 1997; Desiraju 2002). Hydrogen bonds, because of their strength and directionality, have been one of the most useful interactions in building these molecular networks. Many pharmaceutical molecules are

known to form hydrogen bonded assemblies in solution and in the solid-state and are therefore good reactants for supramolecular synthesis with other components. In fact, hydrogen bonds have been employed in the formation of crystalline supramolecular assemblies of binary and ternary composition where at least one of the components is a drug (Caira 1991; Caira 1992; Madarasz, Bombicz et al. 2002; Fleischman, Kuduva et al. 2003; Remenar, Morissette et al. 2003; Walsh, Bradner et al. 2003; Childs, Chyall et al. 2004; Trask, Motherwell et al. 2005; Vishweshwar, McMahon et al. 2005; Rodríguez-Hornedo 2007).

Cocrystallization is an essential step in the successful synthesis of cocrystals. The most generally used solution-based method to synthesize these materials is slow evaporation from solutions of cocrystal components with stoichiometric composition (Caira 1991; Etter and Reutzel 1991; Ghosh, Basak et al. 1991; Caira 1992; Fleischman, Kuduva et al. 2003; Walsh, Bradner et al. 2003; Childs, Chyall et al. 2004). Solvo-thermal methods are also reported in the literature, although less frequently (Bettinetti, Caira et al. 2000; Rodríguez-Spong 2005). These techniques, however, suffer from the risk of crystallizing the single component phases, thereby reducing the possibility of cocrystal formation. As a result of the empirical basis of the approaches used in search of cocrystals, a very large number of experimental conditions are often tested (Morissette, Almarsson et al. 2004) and transferability to larger scale crystallization processes is limited.

In this chapter, a method is reported for the rapid generation of cocrystals by reaction cocrystallization in microscopic and macroscopic scales under ambient conditions, where nucleation and cocrystallization are initiated by the effect of the

cocrystal components on reducing the solubility of the molecular complex to be crystallized (Nehm, Rodríguez-Spong et al. 2006). We also discuss the importance of the cocrystal solubility product in explaining the phase solubility diagram of cocrystals and in identifying conditions to prepare cocrystals in solutions, suspensions, slurries, or wet solid phases of cocrystal components. This method offers significant improvements over traditional cocrystallization methods in that it is: (1) applicable to develop rational *in situ* techniques for high-throughput screening of cocrystals, (2) transferable to larger scale cocrystallization processes, and (3) more environmentally friendly.

The carbamazepine-nicotinamide cocrystal (CBZ-NCT) was chosen as a model system to study the reaction cocrystallization pathways and kinetics in aqueous and organic solvents. The crystal structure of CBZ-NCT has been reported (Fleischman, Kuduva et al. 2003) (refcode in the Cambridge Structural Database is UNEZES (Allen 2002)) and is characterized by N–H···O=C hydrogen bonds between nicotinamide and carbamazepine molecules as shown in Figure 4.1. Nicotimanide in this structure hydrogen bonds with the carbamazepine carboxamide dimers forming a hydrogen bonded tape down the *a* crystallographic axis.

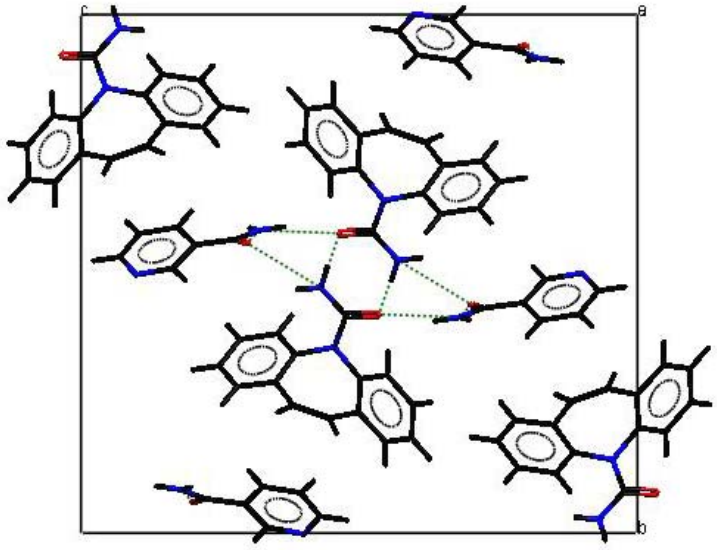

Figure 4.1. Crystal structure of CBZ-NCT viewed down the *a* crystallographic axis showing the molecular assembly.

Theoretical

The cocrystal phase solubility diagram (Figure 4.2), for which this new method of cocrystal synthesis is based on, reveal conditions of undersaturation, saturation, and supersaturation with respect to cocrystal and/or single component crystalline phases. While crystallization will occur in supersaturated conditions, dissolution will occur in undersaturated conditions. Therefore supersaturation with respect to only cocrystal can be generated by preparing a solution of reactants A and B such that the solution concentrations are in region IV. These conditions can be achieved by mixing solutions of dissolved reactants or by dissolving solid reactant(s) A and/or B in a pure solvent or in a solution of reactants. Solid phases A and B can therefore transform to cocrystalline phase AB by a solution mediated transformation. As cocrystal AB forms, it consumes A

and B from solution and more A and B dissolve until the process reaches an equilibrium state determined by the cocrystal solubility curve.

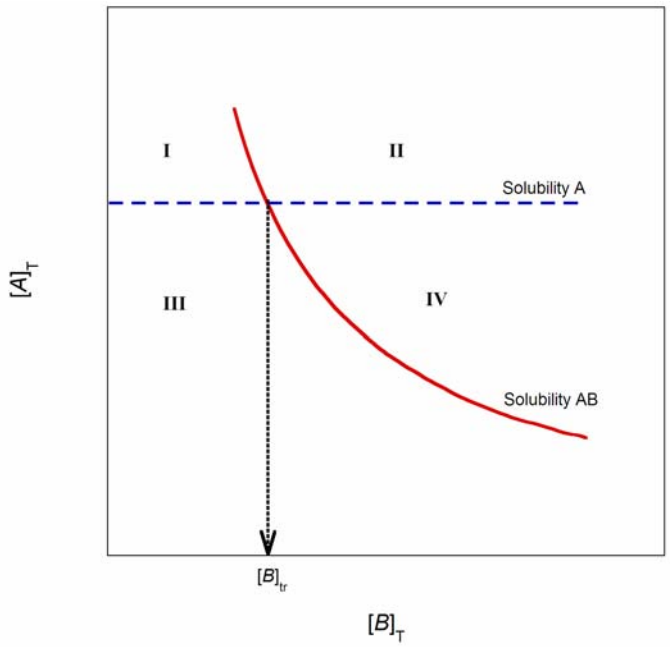

Figure 4.2 Solubility phase diagram for crystal A and cocrystal AB, showing the transition concentration, $[B]_{tr}$.

Understanding the solubility behavior of cocrystals as a function of cocrystal components in solution is valuable not only for the design of reliable cocrystallization processes but for the anticipation of process conditions where transformations between single component crystal A and cocrystal AB can occur. A reversal in the phase transformation of AB to A or A to AB can occur depending on the cocrystal component concentrations in solution. As indicated in Figure 4.2, the transition concentration is essential for the control of a process since:

(1) at the transition concentration the solubility of crystal A = solubility of cocrystal AB for a 1:1 cocrystal. This means that transformations will not occur even when there is a mixed phase of both crystalline phases A and AB.

(2) below the transition concentration solubility of A < solubility of AB. Therefore in region I crystalline form AB will transform to crystalline form A.

(3) above the transition concentration solubility of A > solubility of AB. Therefore in region IV crystalline form A will transform to cocrystalline form AB.

Experimental Section

Materials

Anhydrous monoclinic carbamazepine (CBZ(III), 5H-Dibenz[b,f]azepine-5-carboxamide; lot #093K1544 USP grade) was purchased from Sigma Chemical Company (St. Louis, MO), stored at 5 °C over anhydrous calcium sulfate and used as received. Nicotinamide (NCT(I), Pyridine-3-carboxylic acid amide; lot #122K0077) was purchased from Sigma Chemical Company (St. Louis, MO) and used as received. Solid state forms were identified by x-ray powder diffraction.

Ethyl acetate and 2-propanol were of HPLC grade and were purchased from Fisher Scientific (Fair Lawn, NJ). Anhydrous ethanol (200 proof) was USP grade and was purchased from Pharmco (Brookfield, CT).

Solubility of CBZ-NCT

The equilibrium solubility of CBZ-NCT cocrystal was determined from undersaturation by adding excess cocrystal solid phase to pure ethanol and ethanol

solutions of NCT ranging between 0.2 M and 0.05 M. The suspensions were stirred with magnetic stirrers in 20 mL glass vials at constant temperature (25 ± 0.5 °C) maintained with a circulating temperature bath (Neslab RTE-110, Portsmouth, NH). Samples were drawn at 48 h using a 0.45 μm PTFE filter (Fisherbrand, Pittsburg, PA) and were diluted with ethanol. CBZ concentrations were calculated by measuring the absorbance of CBZ (λ_{max} = 284 nm) by UV/Vis spectroscopy (Beckman DU-650, Fullerton, CA). The CBZ concentration corresponds to the CBZ-NCT solubility based on the 1:1 molar ratio cocrystal.

Screening Experiments

Solid drug or drug solutions were added to ligand solutions such that an excess molar ratio of ligand to drug was attained. Ligand concentrations used were close to saturation. Screening experiments were carried out in 8 mL vials, on 96-well plates, and on microscope slides. All screening experiments were carried out at room temperature.

Raman Spectroscopy

For the macroscopic experiments, Raman spectra were collected with a Kaiser Optical Systems, Inc. (Ann Arbor, MI) RXN1 Raman Spectrometer equipped with a 785nm laser and a ¼" fiber optic immersion probe. Crystallization and dissolution were monitored *in situ* in macrophases with the probe and in microphases using a Leica DMLP (Wetzlar, Germany) Raman microscope. Acquisition conditions were optimized so that the spectra collected had maximum intensity above 8×10^6 counts. The spectra collected

had a spectral resolution of 4 cm^{-1} and were collected between 100 and 3200 cm^{-1}. Solid phases were characterized by Raman spectroscopy.[‡ appendix (Figure 1)]

High-throughput screening experiments were carried out in 96 well plates, the Raman spectra were collected using a PhAT-enabled WorkstationTM (Kaiser Optical Systems, Ann Arbor, MI). The unit was equipped with a Leica DMLP microscope (Wetzlar, Germany) and a Prior Motorized Stage (Cambridge, UK). The Raman spectrometer was equipped with a 785-nm laser, and a 1-millimeter spot lens was used. Spectra were collected using 15-second exposures and an automated wellplate protocol.

Polarized Optical Microscopy

Crystallization in microphases was visually monitored with a Leica DMPL polarizing optical microscope (Wetzlar, Germany). Images were collected with a Spot Insight FireWire 4 Megasample Color Mosaic camera controlled with Spot software (Diagnostics Inc, Sterling Heights, MI). Solid phases crystallized were identified by Raman microscopy.

X-ray Powder Diffraction (XRPD)

X-ray powder diffraction patterns of solid phases were recorded with a Rigaku MiniFlex X-ray diffractometer (Danvers, MA) using CuKα radiation (λ = 1.54Å), tube voltage of 30kV, and tube current of 15mA. The intensities were measured at 2-theta values from 2° to 50° at a continuous scan rate of 2.5°/min. Solid phases at equilibrium during solubility experiments were analyzed by x-ray powder diffraction and results were

compared to the diffraction patterns calculated from the crystal structure reported in the Cambridge Structural Database (Allen 2002). ‡ appendix (Figures 2-5)

Infrared (IR) Spectroscopy

FTIR spectra of solid phases were collected on a Bruker Vertex 70 FT-IR (Billerica, MA) unit equipped with a DTGS detector. Samples were placed on a zinc selenide (ZnSe) Attenuated Total Reflectance (ATR) crystal accessory and 64 scans were collected for each sample at a resolution of 4 cm^{-1} over a wavenumber region of 4000-600 cm^{-1}.

Results and Discussion

The phase solubility diagram for the carbamazepine-nicotinamide cocrystal (CBZ-NCT) as a function of the ligand or cocrystal component concentration (NCT) in ethanol solutions is shown in Figure 4.3.

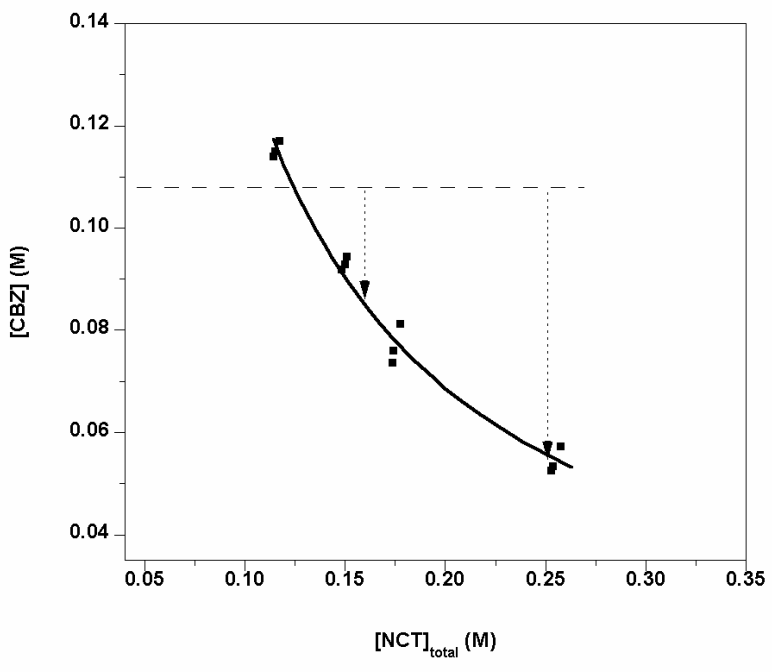

Figure 4.3. Phase solubility diagram of carbamazepine-nicotinamide (1:1) cocrystal as a function of cocrystal component concentration in ethanol at 25 ˚C. The solid line represents the predicted solubility according to Equation (3) with a solubility product K_{sp} = 0.0129 M^2. The dashed line represents the solubility of CBZ(III) in ethanol, 0.108 M. The dotted arrows represent the cocrystallization conditions studied.

This solubility study reveals that addition of cocrystal component to solutions in excess of the stoichiometric composition reduces the cocrystal solubility and is explained by considering the equilibrium reaction for a binary cocrystal *AB* dissociating in solution to *A* and *B* according to

$$A_aB_{b\ solid} \rightleftharpoons aA_{solution} + bB_{solution} \quad (1)$$

where *A* represents API or CBZ and *B* represents ligand or cocrystal component or NCT. Subscripts refer to the stoichiometric number of molecules of *A* or *B* in the cocrystal. The equilibrium constant for this reaction is given

$$K_{eq} = \frac{a_A^a a_B^b}{a_{AB}} \quad (2)$$

and is proportional to the thermodynamic activity product of the cocrystal components. If the activity of the solid is equal to 1 or is constant, the cocrystal solubility can be described by a solubility product

$$K_{sp} = a_A^a a_B^b \approx [A]^a [B]^b \tag{3}$$

where $[A]$ and $[B]$ are the molar concentrations of each cocrystal component at equilibrium, as long as the activity coefficients are unity. This equation predicts that addition of either cocrystal component in excess of its stoichiometric composition will decrease the cocrystal solubility, in agreement with the observed trend in Figure 4.3. Mathematical models that consider solution complexation equilibria and solubility of solid-state complex or cocrystal have been derived and are presented elsewhere (Nehm, Rodríguez-Spong et al. 2006). It is important to note that the solubility predicted by the solubility product alone is smaller than the solubility in the presence of solution complexes, as shown by the equations that follow.

In the case of 1:1 solution complexes the cocrystal solubility is given by

$$[A]_T = \frac{K_{sp}}{[B]_T - K_{11}K_{sp}} + K_{11}K_{sp} \tag{4}$$

If $K_{11}K_{sp} << [B]_T$, then

$$[A]_T = \frac{K_{sp}}{[B]_T} + K_{11}K_{sp} \tag{5}$$

This equation predicts that cocrystal solubility is higher than the value calculated in the absence of solution complexation by a constant value, the product of the complexation constant and the solubility product, $K_{11}K_{sp}$. In the absence of solution complexation, $K_{11} = 0$, the cocrystal solubility is predicted by the solubility product alone. In the case of 1:1

and 1:2 solution complexes the cocrystal solubility initially decreases, passes through a minimum at $[B]_T = \sqrt{\frac{1}{K_{11}K_{12}}}$, and then increases.

The solubility product of CBZ-NCT cocrystal in ethanol solutions was determined to be $K_{sp} = 0.0129\ M^2$ by plotting $[A]_T$ versus $1/[B]_T$ according to Equation (5), using the measured cocrystal solubilities shown in Figure 4.3. Linear regression results showed that the intercept is not significantly different from zero and suggests that solution complexation is negligible in this solvent (Nehm, Rodríguez-Spong et al. 2006). The cocrystal solubility predicted by the solubility product alone is shown in Figure 4.3 and is in excellent agreement with the experimentally measured solubility. These results demonstrate that there is a common cocrystal component effect on cocrystal solubility, similar to that of the common ion effect in the case of sparingly soluble salts (Tomazic and Nancollas 1979; Nielsen and Toft 1984; Rodríguez-Clemente 1989; Khankari and Grant 1995).

Based on this solubility behavior, we developed reaction cocrystallization methods under ambient conditions, where nucleation and crystallization of the molecular complex are directed by decreasing the solubility of the molecular complex to be crystallized. Supersaturation is the driving force for crystallization and can be generated by adding excess cocrystal component to a solution so that non-stoichiometric concentrations are achieved. As nicotinamide is added to solutions of ethanol, the solubility of CBZ-NCT cocrystal decreases below the solubility of the pure anhydrous CBZ(III) as shown in Figure 4.3. In pure ethanol the solubilities of CBZ-NCT cocrystal and CBZ(III) single component crystal are very similar, 0.116 ± 0.003 M and 0.1080 ±

0.0001 M. However, the solubility ratio (cocrystal/CBZ(III)) is decreased from 1.07 in pure ethanol to 0.48 in 0.25 M NCT.

With the purpose of investigating the rates of cocrystallization under the conditions described by the solubility product behavior, we studied the cocrystallization of CBZ-NCT in organic solutions (ethanol, 2-propanol, or ethyl acetate) and in aqueous solutions in micro and macrophases. Reaction cocrystallizations were studied in suspensions of reactant or reactants and in solutions of reactants as described below.

The cocrystallization of CBZ-NCT by dissolving anhydrous CBZ(III) (385 mg) in ethanol solutions of NCT 0.16 M (10 mL) was monitored by Raman spectroscopy as shown in Figure 4.4. This amount of CBZ is higher than the solubility of CBZ(III) in ethanol by 50.8%. The shift in the Raman peak with respect to time, from 722 to 718 cm^{-1}, indicates that pure CBZ(III) transformed to CBZ-NCT cocrystal within 3 hours. These results suggest a solution-mediated transformation where dissolution of pure CBZ creates supersaturated conditions with respect to cocrystal and leads to cocrystallization of CBZ-NCT. When one of the reactants is in the solid state and in an amount greater than its solubility value, it is consumed by the cocrystallization reaction, as shown in this case, and the final product is the cocrystalline phase.

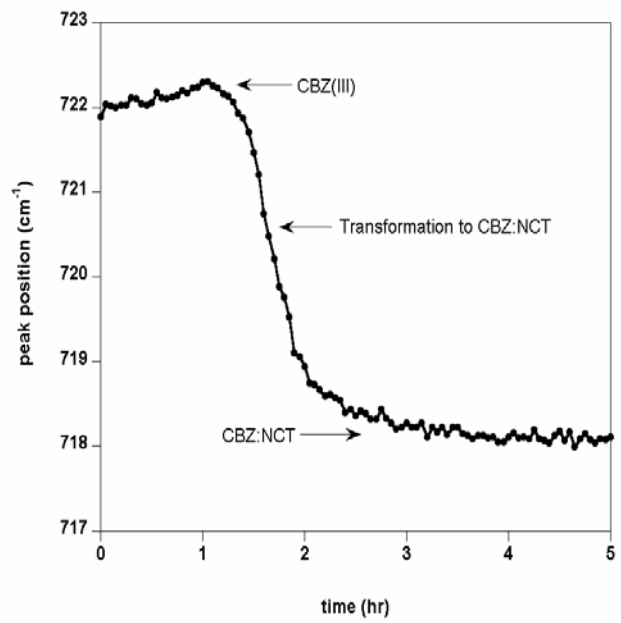

Figure 4.4. Raman peak position with respect to time showing the slurry conversion or transformation of solid phase CBZ(III) to cocrystal CBZ-NCT at 25˚C after adding 0.16 M solution of nicotinamide in ethanol to CBZ(III). (It is noted that transition states do not exist during the transformation from CBZ(III) to CBZ-NCT between 722 and 718cm^{-1}.)

Increasing the NCT concentration in the experiment above to 0.25 M resulted in faster conversion of pure anhydrous CBZ(III) to cocrystal, within 2 to 3 minutes. This time was shorter than that required to collect the Raman spectra and the time course for this transformation is not shown. Increasing NCT concentration in the dissolution/cocrystallization medium, increased the initial supersaturation with respect to cocrystal and significantly increased the cocrystallization rate as shown by the shorter times for transformation to cocrystal from 3 hours to 3 minutes. The supersaturation, σ, for a cocrystal is derived from the difference in chemical potential between the supersaturated solution state and the saturated solution state (Rodríguez-Spong 2005) and is given by

$$\sigma = \left(\frac{\Pi c_i^{\nu_i}}{K_{sp}} \right)^{1/\nu} \tag{6}$$

where $\Pi c_i^{\nu_i}$ is the product of the concentration of cocrystal components in the supersaturated solution when the activity coefficients are unity, ν is the stoichiometric coefficient in the chemical equation or stoichiometric number of cocrystal components, *i,* in the cocrystal chemical formula $\nu = \Sigma \nu_i$, and K_{sp} is the solubility product. The supersaturation with respect to a (1:1) cocrystal, such as CBZ-NCT, is expressed by

$$\sigma = \left(\frac{[CBZ][NCT]}{K_{sp}} \right)^{1/2} \tag{7}$$

Equation 7 shows that supersaturation and crystallization rate can be increased by increasing the concentration of individual components. The success of crystallizing the molecular complex is significantly improved by varying reactant concentrations such that the supersaturation with respect to cocrystal is selectively increased.

A priori knowledge of the solubility of cocrystal in pure solvent is useful to predict the cocrystal phase solubility diagram as a function of ligand concentration and to determine conditions under which cocrystals dissolve or precipitate (Nehm, Rodríguez-Spong et al. 2006). Figure 4.5 shows that CBZ-NCT cocrystal can be prepared in water by suspending anhydrous CBZ(III) or CBZ(D) in saturated solutions of nicotinamide at room temperature. It is interesting to note that anhydrous CBZ(III) transforms to dihydrate CBZ, CBZ(D), (Figure 4.5a) and then to cocrystal in this aqueous solution, and suggests that the order of the solubility is CBZ(III)>CBZ(D)>CBZ-NCT. This is an important finding since in pure water at room temperature the solubility of CBZ-NCT is

greater than that of CBZ(D), and cocrystal transforms to CBZ(D) (Figure 4.6). (Rodríguez-Spong, Zocharski et al. 2003; Rodríguez-Spong 2005) The reason for this reversal in transformations is the reduced solubility of cocrystal by addition of cocrystal component, nicotinamide, to solution in excess of the cocrystal stoichiometry.

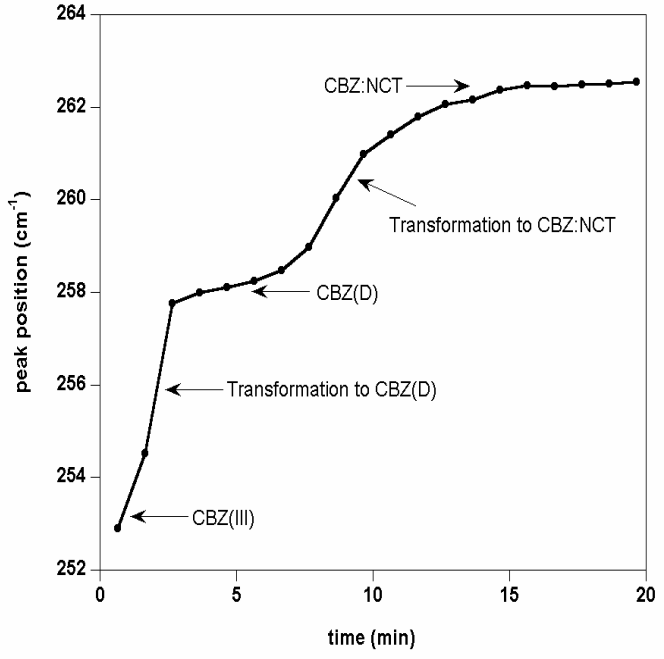

(a)

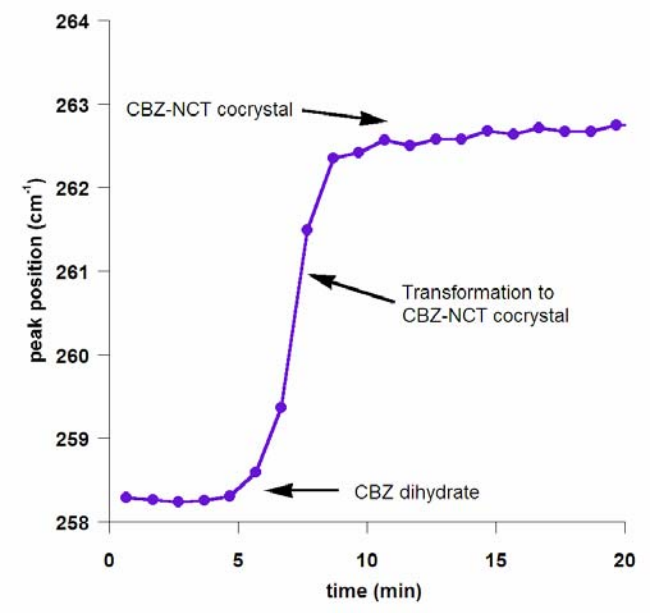

(b)

Figure 4.5. Raman peak position with respect to time showing the slurry conversion or solution-mediated transformation (a) from anhydrous CBZ(III) to cocrystal CBZ-NCT according to the following pathway: CBZ(III) → CBZ(D) → CBZ-NCT and (b) from CBZ(D) to cocrystal at 23°C.

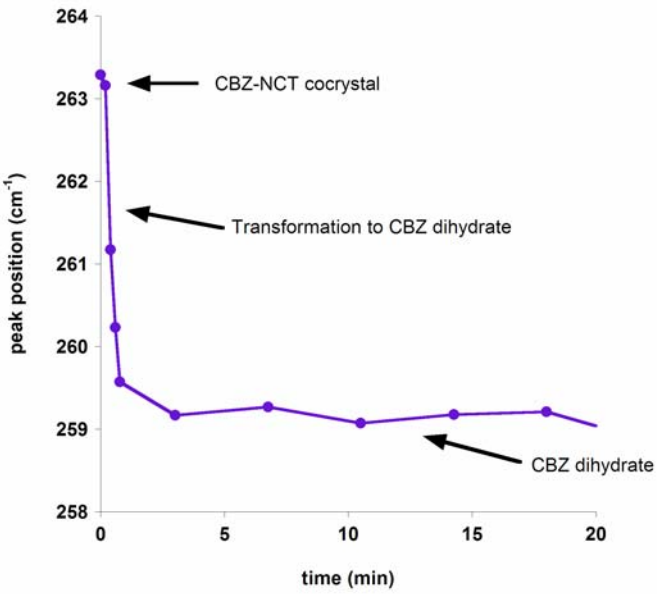

Figure 4.6. Raman peak position versus time indicating the solution-mediated transformation at room temperature from CBZ-NCT cocrystal to CBZ dihydrate in pure water.

CBZ-NCT cocrystal was also prepared *in-situ* in covered depression slides on the polarizing optical light and Raman microscopes by adding a small drop of solvent to the solid reactants, CBZ(III) and NCT(I). Photographs from the ethyl acetate experiment obtained through the polarized light microscope are shown in Figure 4.7. These images show cocrystal formation in less than 3 minutes after ethyl acetate addition. Solid phase of the product was confirmed to be CBZ-NCT cocrystal by Raman microscopy. Similar behavior was observed by using microphases of water (Figure 4.8), suggesting that more environmentally friendly solvents can be used to synthesize cocrystals.

In these cases the cocrystallization reaction proceeds by a similar pathway to those of macrophase suspensions described above. In microphases the solvent added must allow for dissolution of both reactants so that concentrations in solution reach non-stoichiometric concentrations (Figure 4.9). For instance, Figure 4.7b shows unreacted CBZ(III) in an isolated drop where cocrystallization had not occurred in the time course of the experiment due to lower concentrations of NCT than in other regions of the sample.

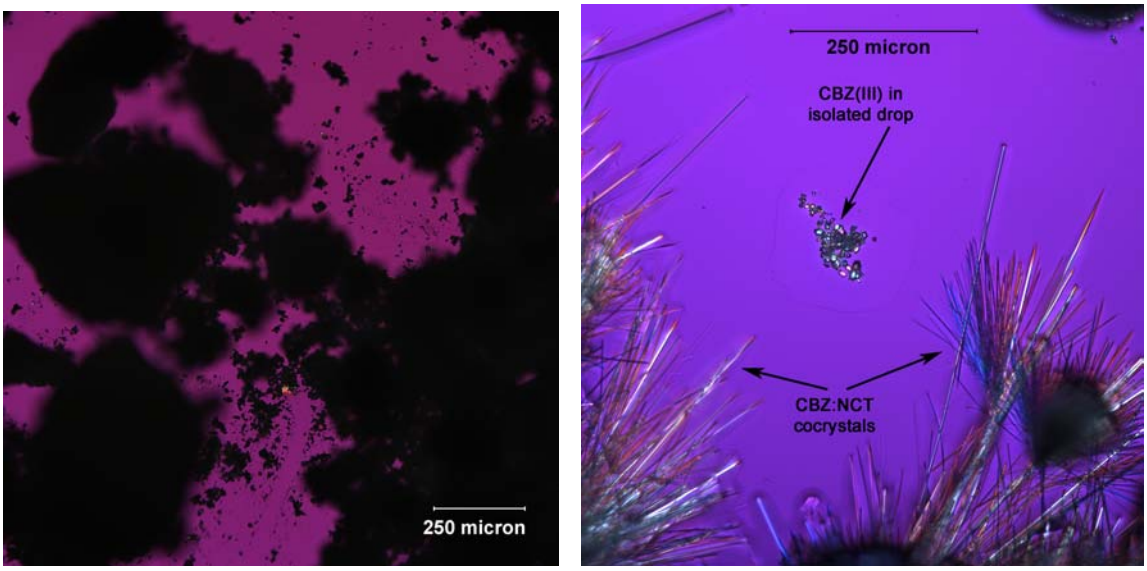

(a) (b)

Figure 4.7. Photomicrographs of CBZ (III) and NCT(I) (a) before addition of ethyl acetate and (b) 3 minutes after addition of small drop of ethyl acetate. Needles were confirmed to be cocrystal CBZ-NCT by Raman microscopy.

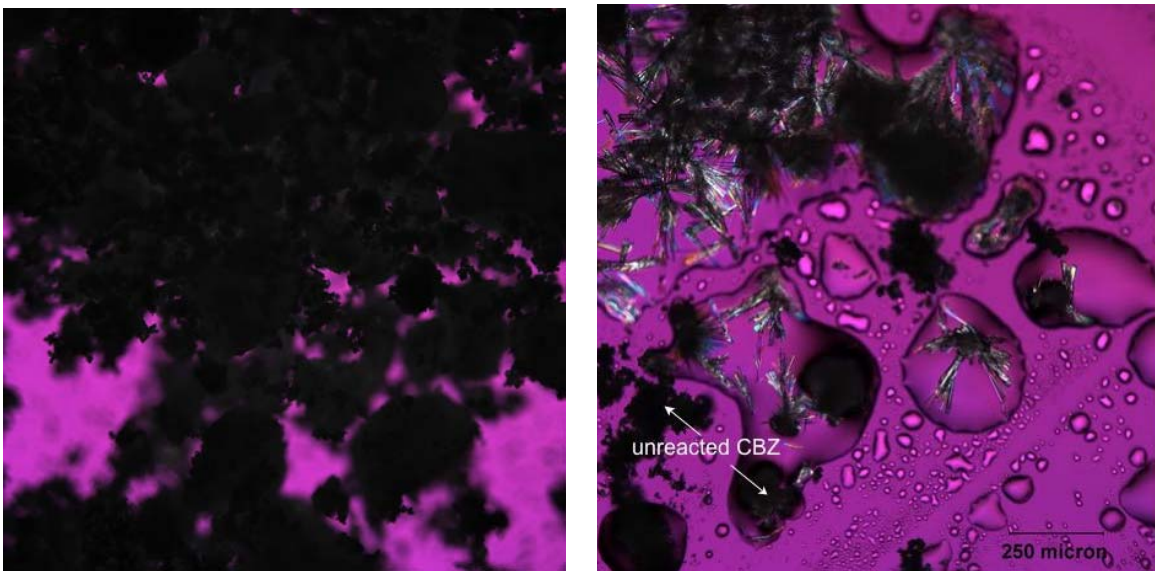

(a) (b)

Figure 4.8. Photomicrographs showing (a) mixture of solid reactants, carbamazepine and nicotinamide, and (b) dissolution-mediated transformation of carbamazepine to dihydrate and to cocrystal after addition of a small volume of water to solid reactants. Carbamazepine transforms to dihydrate and to cocrystal as discussed in the text. Nicotinamide dissolves at a faster rate than carbamazepine due to its higher water solubility, and generates supersaturation with respect to cocrystal.

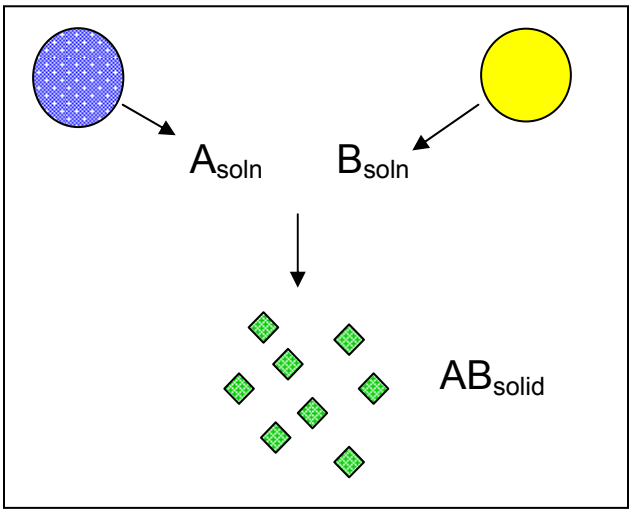

Figure 4.9. Cocrystallization of molecular complex *AB* from the supersaturation generated by the dissolution of solid reactants, *A* and *B*, in a microphase of solvent.

Precipitation or reaction cocrystallization was also achieved by mixing solutions of reactants or cocrystal components in non-stoichiometric concentrations according to the solubility product behavior. CBZ-NCT cocrystal was prepared by mixing solutions of CBZ and NCT in the same solvent. Solvents studied included: ethanol, 2-propanol, and ethyl acetate. Cocrystals were observed within 10 to 25 minutes (n=4) after initial gentle mixing of an ethanol solution of NCT (2.25 mL of 0.8 M)) and an ethanol solution of CBZ (3.75 mL of 0.1 M). Similar behavior was observed in 2-propanol and ethyl acetate.

Transformation to cocrystal from single-component solid reactants has also been observed for sulfadimidine-anthranilic acid and sulfadimidine-salicylic acid from acetonitrile, ethanol, and water and carbamazepine-saccharin from water and 0.1N HCl.[‡appendix (Figures 6-9)]

The reaction crystallization method was extended to high-throughput screening of cocrystals using environmentally friendly solvents (Jayasankar, Nehm et al. 2007; Childs, Rodríguez-Hornedo et al. 2008). Several ligands, based on published literature

(Fleischman, Kuduva et al. 2003; Trask, Motherwell et al. 2005; Trask, Motherwell et al. 2006; Childs, Stahly et al. 2007; Childs, Rodríguez-Hornedo et al. 2008), were chosen to screen for cocrystals of carbamazepine, caffeine, and theophylline. Cocrystal screening was carried out by adding 50-75 mL of pre-saturated aqueous or ethanolic ligand solutions to solid drug in 96-well plates. Raman spectroscopy was successful in monitoring cocrystal formation within minutes to a few hours. Table 4.1 indicates systems that were successful in cocrystal formation by the reaction crystallization method.

Table 4.1. Results of cocrystal high-throughput screening by reaction crystallization. (NT = not tested)

Carbamazepine (CBZ) + Ligand

Ligand	Solvent	
	Water	Ethanol
Nicotinamide (NCT)	+	+
4-aminobenzoic acid (4ABA)	+	+
4-hydroxybenzoic acid (4HBA)	+	+
Glutaric acid (GTA)	+	+
Maleic acid (MLE)	+	+
Malonic acid (MLO)	+	+
Oxalic acid (OXA)	+	+
1-hydroxy-2-naphthoic acid (1HNA)	+	+
Glycolic acid (GCL)	+	NT
Ketoglutaric acid (KTG)	+	+
(+) camphoric acid (CMP)	+	+
D-malic acid (D-MLI)	+	+
DL-malic acid (DL-MLI)	+	+
DL-tartaric acid (DL-TRT)	+	+
Fumaric acid (FMR)	+	+
L-tartaric acid (L-TRT)	+	+
Salicylic acid (SLC)	+	+
Benzoic acid (BNZ)	+	+
Trimesic acid (TMS)	+	+
Adipic acid (ADP)	-	+
Saccharin (SAC)	-	+

Theophylline (THP) + Ligand

Ligand	Solvent	
	Water	Ethanol
4-hydroxybenzoic acid (4HBA)	+	+
Glutaric acid (GTA)	+	-
Maleic acid (MLE)	+	+
Malonic acid (MLO)	+	+
Oxalic acid (OXA)	-	+
1-hydroxy-2-naphthoic acid (1HNA)	+	+
DL-tartaric acid (DL-TRT)	+	-
L-tartaric acid (L-TRT)	-	-
Salicylic acid (SLC)	+	+
Benzoic acid (BNZ)	+	+
Glycolic acid (GCL)	+	NT
Citric acid (CTR)	+	+

Caffeine (CFN) + Ligand

Ligand	Solvent	
	Water	Ethanol
Glutaric acid (GTA)	+	+
Maleic acid (MLE)*	-	-
Malonic acid (MLO)	+	-
Oxalic acid (OXA)	+	+
1-hydroxy-2-naphthoic acid (1HNA)	+	+
DL-tartaric acid (DL-TRT)	-	+
Citric acid (CTR)	-	+

*Cocrystallization in acetonitrile and ethyl acetate has been shown in studies from our lab.

Raman spectroscopy was used to analyze all solid phases and in some cases further confirmed by XRPD or FTIR. Raman spectra and XRPD patterns of the solid phases resulting from the high-throughput screen were compared to the respective drug spectra and patterns (Figures 4.10 – 4.12). As can be seen from Figures 4.10 – 4.12, which show examples of CBZ, THP, and CFN cocrystals tested from Table 1, Raman spectroscopy and XRPD can be used to distinguish between crystalline and cocrystalline phases.

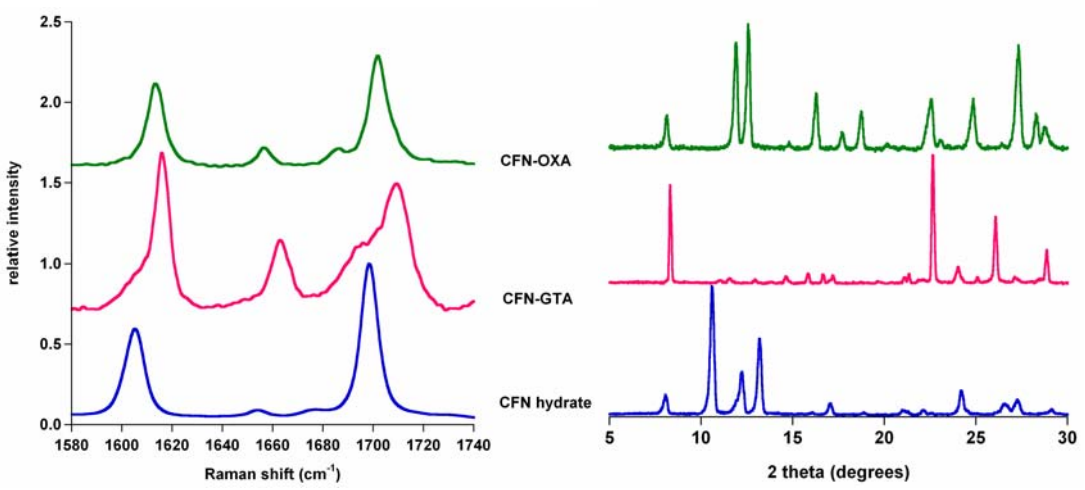

(a) (b)

Figure 4.10. (a) Raman spectra and (b) XRPD patterns of caffeine hydrate and two cocrystal examples (caffeine-oxalic acid and caffeine-glutaric acid) prepared in aqueous solutions. Pure cocrystalline phases were detected by XRPD.

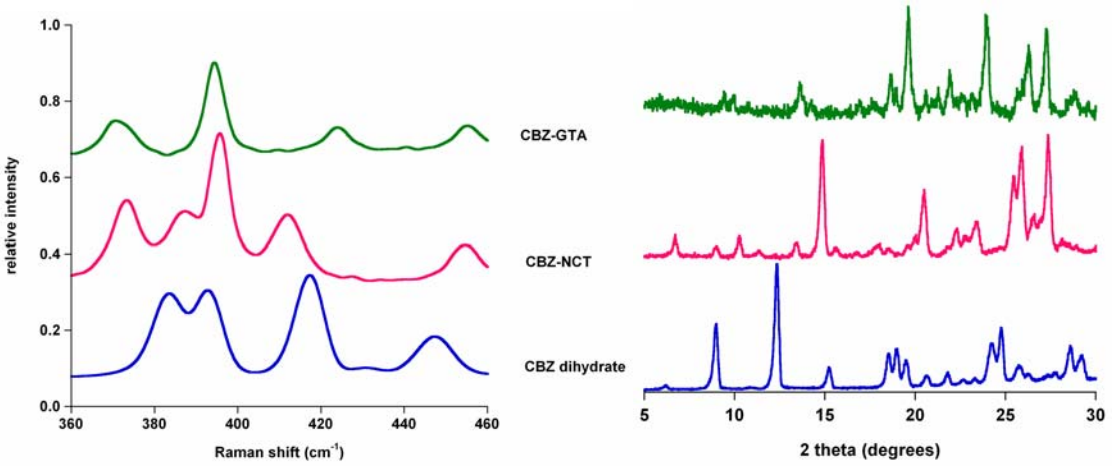

(a) (b)

Figure 4.11. (a) Raman spectra and (b) XRPD patterns of carbamazepine dihydrate and two cocrystal examples (carbamazepine-nicotinamide and carbamazepine-glutaric acid) prepared in aqueous solutions. Pure cocrystalline phases were detected by XRPD.

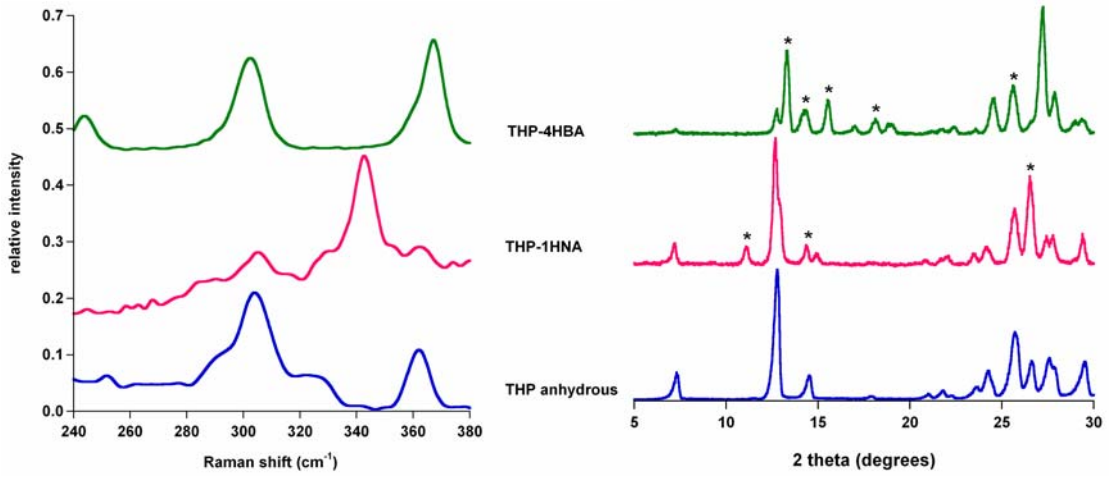

(a) (b)

Figure 4.12. (a) Raman spectra and (b) XRPD patterns of anhydrous theophylline and two cocrystal examples (theophylline-1-hydroxy-2-naphthoic acid and theophylline-4-hydroxybenzoic acid) prepared in aqueous solutions. Mixed phases were detected by XRPD. Peaks associated with cocrystal are indicated by (*).

Reaction crystallization proved to be an effective and efficient method to screen for cocrystals. This high-throughput method was material sparing and indicated that water could be used as a solvent to screen for cocrystals. This is unexpected since carbamazepine, theophylline, and caffeine form hydrates when slurried in water. Increasing the ligand solution concentration causes the thermodynamically stability to shift from the hydrated drug to the cocrystal.

Conclusions

The results presented here demonstrate that reaction cocrystallization allows for the effective and rapid formation of cocrystals under ambient conditions, in micro and macrophases of aqueous and organic solvents or solutions. This research also identifies the mechanism for cocrystal formation from solutions or solid-liquid systems (slurries or

wet solid phases), where cocrystallization is initiated by the effect of non-stoichiometric concentrations of cocrystal components on reducing the solubility of the molecular complex to be crystallized. These findings provide a powerful approach to develop rational screening methods for cocrystal discovery, and *in situ* cocrystallization techniques, as well as to develop batch and continuous cocrystallization processes. The solubility product behavior indicates that a wider range of solvents can be used for cocrystallization, with the advantage over traditional methods that cocrystallization is no longer limited by the different solubilities of the components, and will lead to environmentally friendly methods for cocrystal synthesis.

Appendix

Spectroscopic and x-ray powder diffraction diagrams of reactants (cocrystal components) and cocrystals are displayed in the following figures.

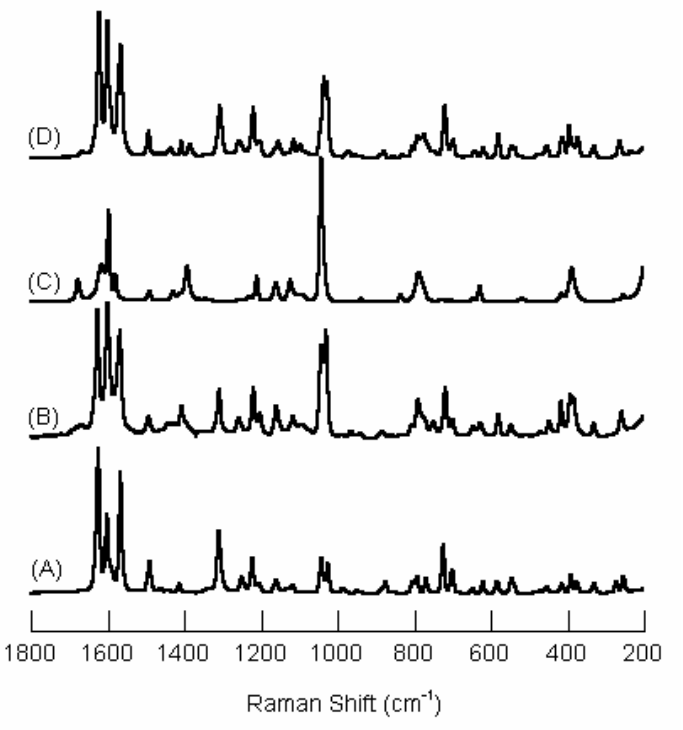

Figure 4.1A. Raman spectra of single components and CBZ-NCT cocrystal. (A) CBZ(III), (B) CBZ(D), (C) NCT(I), (D) CBZ-NCT.

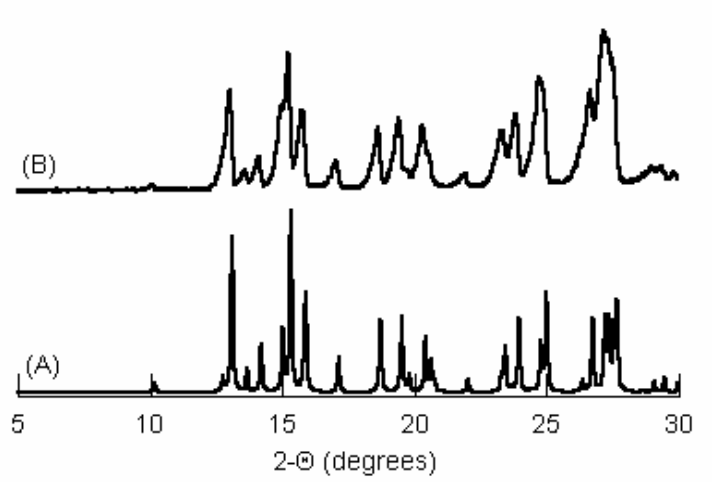

Figure 4.2A. XRPD of CBZ(III), (A) calculated from the crystal structure found in the Cambridge Structural Database (Allen 2002) (Refcode: CBMZPN) using Mercury 1.3 (Bruno, Cole et al. 2002) (B) as received.

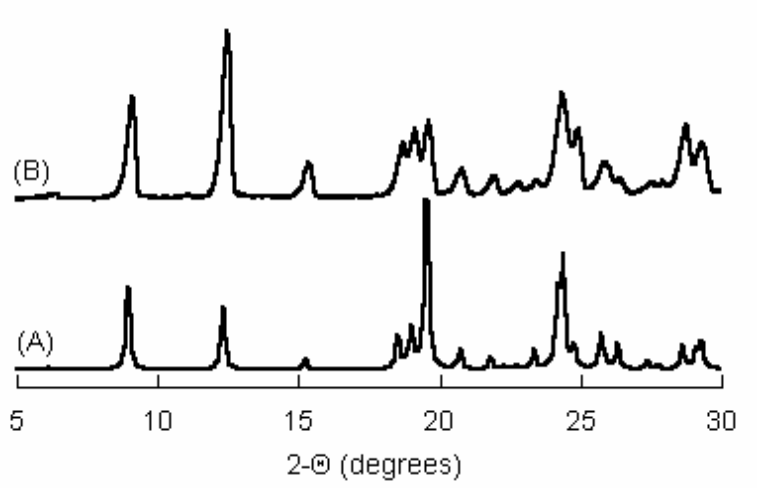

Figure 4.3A. XRPD of CBZ(D), (A) computed from the single crystal XRD (Morris, Griesser et al.) (B) prepared by aqueous slurry method.

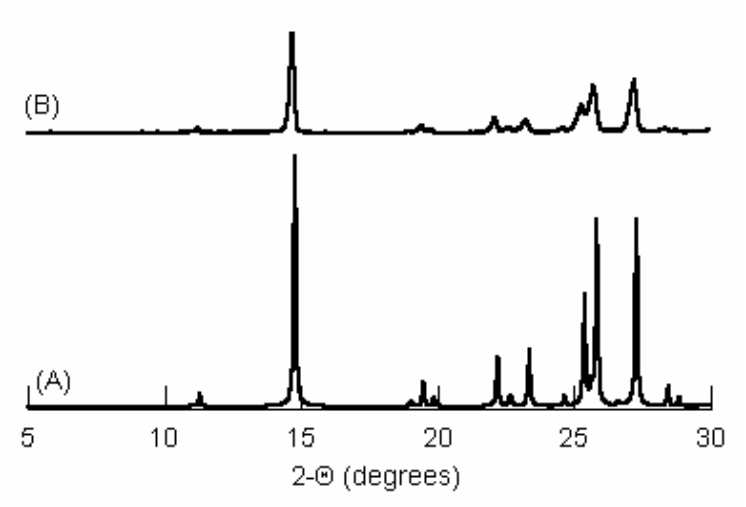

Figure 4.4A. XRPD of NCT(I), (A) calculated from the crystal structure found in the Cambridge Structural Database (Allen 2002) (Refcode: NICOAM) using Mercury 1.3 (Bruno, Cole et al. 2002) (B) as received

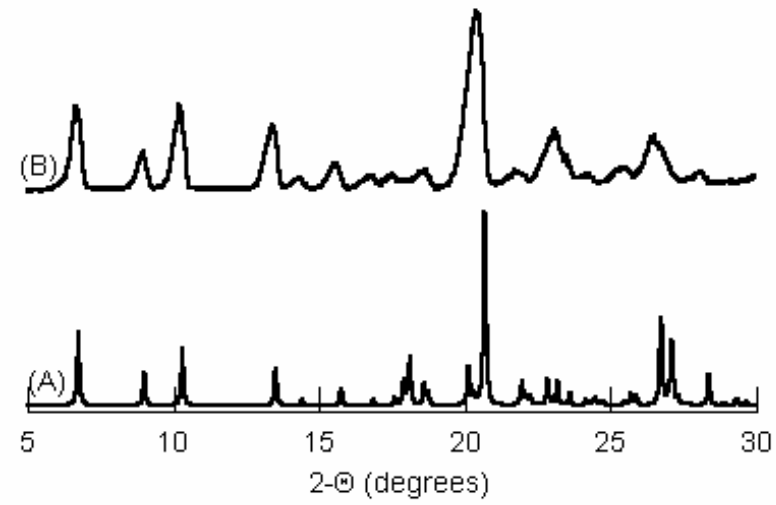

Figure 4.5A. XRPD of CBZ-NCT, (A) calculated from the crystal structure found in the Cambridge Structural Database (Allen 2002) (Refcode: UNEZES) using Mercury 1.3 (Bruno, Cole et al. 2002) (B) prepared from ethyl acetate.

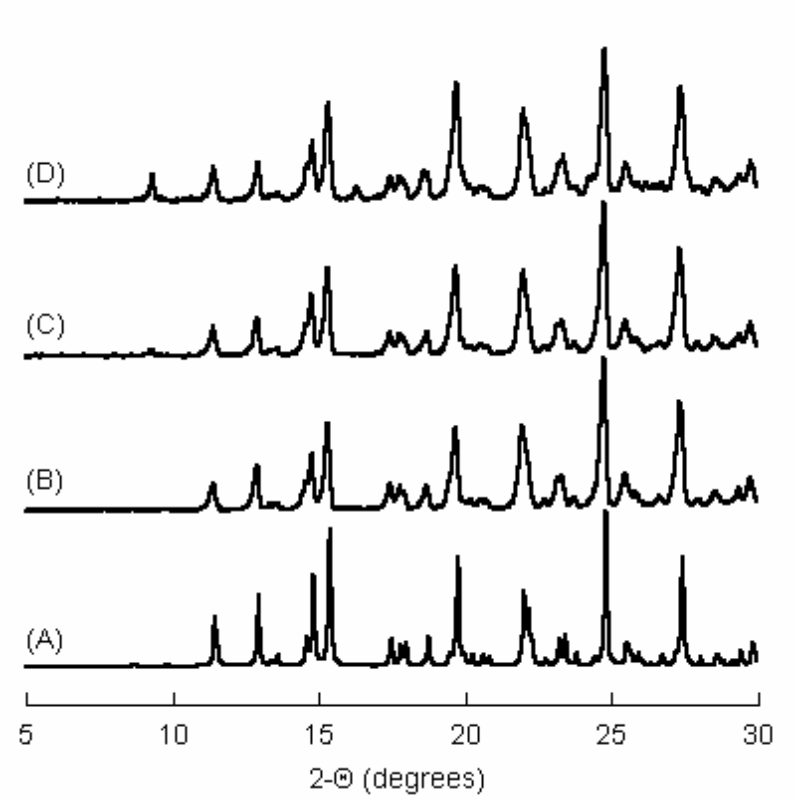

Figure 4.6A. XRPD of sulfadimidine-anthranilic acid cocrystal, (A) calculated from the crystal structure found in the Cambridge Structural Database (Allen 2002) (Refcode: SORWEB) using Mercury 1.3 (Bruno, Cole et al. 2002) and prepared from (B) acetonitrile, (C) ethanol, and (D) water.

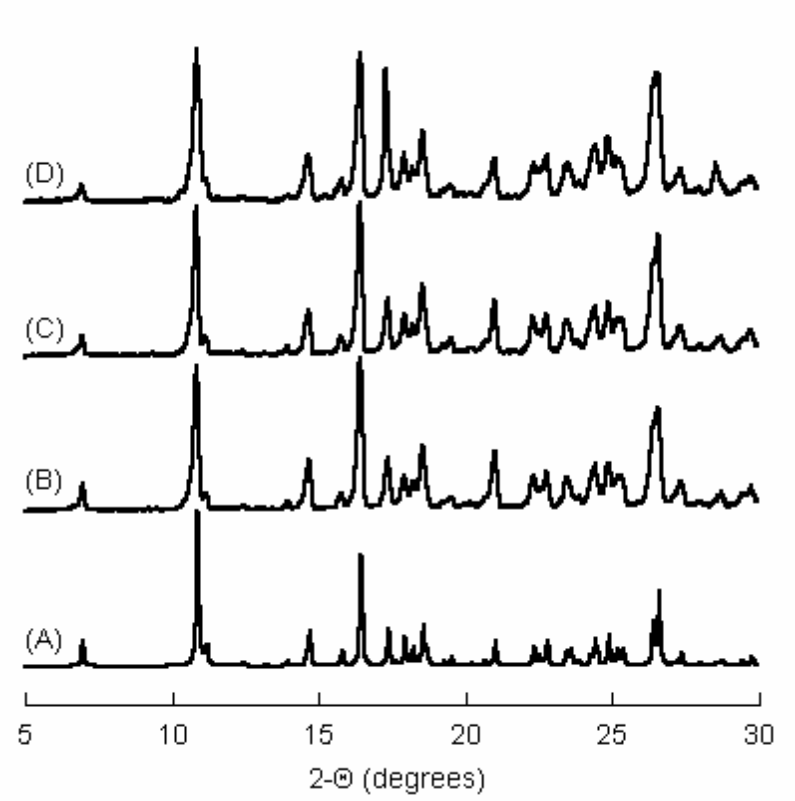

Figure 4.7A. XRPD of sulfadimidine-salicylic acid cocrystal, (A) calculated from the crystal structure found in the Cambridge Structural Database (Allen 2002) (Refcode: GEYSAE) using Mercury 1.3 (Bruno, Cole et al. 2002) and prepared from (B) acetonitrile, (C) ethanol, and (D) water.

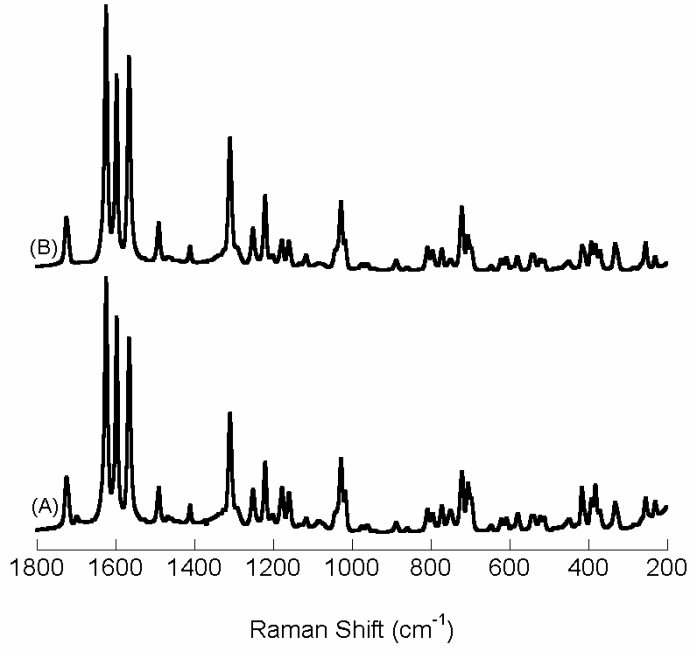

Figure 4.8A. Raman spectra of the CBZ-SAC cocrystal prepared from (A) water and (B) by the solvo-thermal method (Rodríguez-Spong 2005).

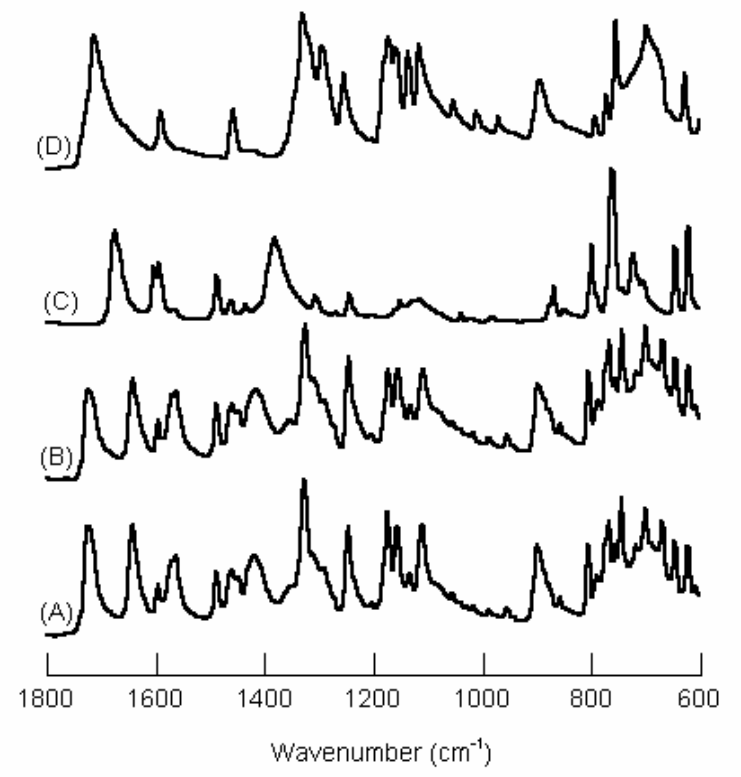

Figure 4.9A. FTIR spectra of CBZ-SAC cocrystal prepared from (A) 0.1N HCl, and (B) prepared by solvo-thermal method (Rodríguez-Spong 2005), (C) CBZ(III) as received, and (D) SAC as received.

References

Allen, F. H. (2002). "The Cambridge Structural Database: a quarter of a million crystal structures and rising." *Acta Crystallographica* **B58**: 380-388.

Bak, A., A. Gore, et al. (2008). "The co-crystal approach to improve the exposure of a water insoluble compound: AMG 517 sorbic acid cocrystal characterization and pharmacokinetics." *Journal of Pharmaceutical Sciences* **97**: 3942-3956.

Bettinetti, G., M. R. Caira, et al. (2000). "Structure and Solid-State Chemistry of Anhydrous and Hydrated Crystal Forms of the Trimethoprim-Sulfamethoxypyridazine 1:1 Molecular Complex." *Journal of Pharmaceutical Sciences* **89**: 478-489.

Bruno, I. J., J. C. Cole, et al. (2002). "New software for searching the Cambridge Structural Database and visualising crystal structures " *Acta Crystallographica* **B58**: 389-397.

Caira, M. R. (1991). "Molecular complexes of sulfonamides. Part 1. 1:1 complexes between sulfadimidine [4-amino-N-(4,6-dimethyl-2-pyrimidinyl)benzenesulfonamide] and 2- and 4-aminobenzoic acids." *Journal of Crystallographic and Spectroscopic Research* **21**: 641-648.

Caira, M. R. (1992). "Molecular complexes of sulfonamides. 2. 1:1 complexes between drug molecules: sulfadimidine-acetylsalicylic acid and sulfadimidine-4-aminosalicylic acid." *Journal of Crystallographic and Spectroscopic Research* **22**: 193-200.

Childs, S. L., L. J. Chyall, et al. (2004). "Crystal Engineering Approach to Forming Cocrystals of Amine Hydrochlorides with Organic Acids. Molecular Complexes of Fluoxetine Hydrochloride with Benzoic, Succinic, and Fumaric Acids." *Journal of the American Chemical Society* **126**: 13335-13342.

Childs, S. L., N. Rodríguez-Hornedo, et al. (2008). "Screening strategies based on solubility and solution composition generate pharmaceutically acceptable cocrystals of carbamazepine." *Crystal Engineering Communications* **10**: 856-864.

Childs, S. L., G. P. Stahly, et al. (2007). "The salt-cocrystal continuum: the influence of crystal structure on ionization state." *Molecular Pharmaceutics* **4**: 323-338.

Desiraju, G. R. (1995). "Supramolecular Synthons in Crystal Engineering--A New Organic Synthesis." *Angewandte Chemie International Edition in English* **34**: 2311-2327.

Desiraju, G. R. (1997). "Designer crystals: intermolecular interactions, network structures and supramolecular synthons." *Chemical Communications*: 1475-1482.

Desiraju, G. R. (2002). "Hydrogen Bridges in Crystal Engineering: Interactions without Borders." *Accounts of Chemical Research* **35**: 565-573.

Etter, M. C. (1990). "Encoding and Decoding Hydrogen-Bond Patterns of Organic Compounds." *Accounts of Chemical Research* **23**: 120-126.

Etter, M. C. (1991). "Hydrogen Bonds as Design Elements in Organic Chemistry." *Journal of Physical Chemistry* **95**: 4601-4610.

Etter, M. C. and S. M. Reutzel (1991). "Hydrogen Bond Directed Cocrystallization and Molecular Recognition Properties of Acyclic Imides." *Journal of the American Chemical Society* **113**: 2586-2598.

Fleischman, S. G., S. S. Kuduva, et al. (2003). "Crystal Engineering of the Composition of Pharmaceutical Phases: Multiple-Component Crystalline Solids Involving Carbamazepine." *Crystal Growth & Design* **3**: 909-919.

Ghosh, M., A. K. Basak, et al. (1991). "Structure and Conformation of the 1:1 Molecular Complex of Sulfaproxyline-Caffeine." *Acta Crystallographica* **C47**: 577-580.

Jayasankar, A., D. J. Good, et al. (2007). "Mechanisms by which moisture generates cocrystals." *Molecular Pharmaceutics* **4**: 360-372.

Jayasankar, A., S. J. Nehm, et al. (2007). "Solution-mediated high-throughput cocrystal screening using Raman spectroscopy." *The AAPS Journal* **9**.

Khankari, R. K. and D. J. W. Grant (1995). "Pharmaceutical Hydrates." *Thermochemica Acta* **248**: 61-79.

Leiserowitz, L. and G. M. J. Schmidt (1969). "Molecular Packing Modes. Part III. Primary Amides." *Journal of the Chemical Society (A): Inorganic, Physical, Theoretical*: 2372-2382.

Madarasz, J., P. Bombicz, et al. (2002). "Thermal, FTIR and XRD Study on Some 1:1 Molecular Compounds of Theophylline." *Journal of Thermal Analysis and Calorimetry* **69**: 281-290.

McNamara, D. P., S. L. Childs, et al. (2006). "Use of a glutaric acid cocrystal to improve oral bioavailability of a low solubility API." *Pharmaceutical Research* **23**: 1888-1897.

Morissette, S. L., O. Almarsson, et al. (2004). "High-throughput crystallization: polymorphs, salts, co-crystals and solvates of pharmaceutical solids." *Advanced Drug Delivery Reviews* **56**: 275-300.

Morris, K. R., U. J. Griesser, et al. personal communication.

Nangia, A. and G. R. Desiraju (1998). "Supramolecular Synthons and Pattern Recognition." *Topics in Current Chemistry* **198**: 57-95.

Nehm, S., B. Rodríguez-Spong, et al. (2006). "Phase Solubility Diagrams of Cocrystals Are Explained by Solubility Product and Solution Complexation." *Crystal Growth & Design* **6**: 592-600.

Nielsen, A. E. and J. M. Toft (1984). "Electrolyte Crystal Growth Kinetics." *Journal of Crystal Growth* **67**: 278-288.

Pedireddi, V. R., W. Jones, et al. (1996). "Creation of crystalline supramolecular arrays: a comparison of co-crystal formation from solution and by solid-state grinding." *Chemical Communications*: 987-988.

Remenar, J. F., S. L. Morissette, et al. (2003). "Crystal Engineering of Novel Cocrystals of a Triazole Drug with 1,4-Dicarboxylic Acids." *Journal of the American Chemical Society* **125**: 8456-8457.

Remenar, J. F., M. L. Peterson, et al. (2007). "Celecoxib:Nicotinamide Dissociation: Using excipients to capture the cocrystal's potential." *Molecular Pharmaceutics* **4**: 386-400.

Rodríguez-Clemente, R. (1989). "Complexing and Growth Units in Crystal Growth from Solutions of Electrolytes." *Journal of Crystal Growth* **98**: 617-629.

Rodríguez-Hornedo, guest editor. (2007). "Special Issue: Pharmaceutical Cocrystals." *Molecular Pharmaceutics* **4**: 299-486.

Rodríguez-Spong, B. (2005). Enhancing the Pharmaceutical Behavior of Poorly Soluble Drugs Through the Formation of Cocrystals and Mesophases, Ph.D. Thesis, University of Michigan.

Rodríguez-Spong, B., C. P. Price, et al. (2004). "General principles of pharmaceutical solid polymorphism: A supramolecular perspective." *Advanced Drug Delivery Reviews* **56**: 241-274.

Rodríguez-Spong, B., P. Zocharski, et al. (2003). "Enhancing the Pharmaceutical Behavior of Carbamazepine Through the Formation of Cocrystals " *The AAPS Journal* **5**: Abstract M1298.

Tomazic, B. and G. H. Nancollas (1979). "The Kinetics of Dissolution of Calcium Oxalate Hydrates." *Journal of Crystal Growth* **46**: 355-361.

Trask, A., W. D. S. Motherwell, et al. (2006). "Physical Stability Enhancement of Theophylline Via Cocrystallization." *International Journal of Pharmaceutics* **320**: 114-123.

Trask, A. V., W. D. S. Motherwell, et al. (2005). "Pharmaceutical Cocrystallization: Engineering a Remedy for Caffeine Hydration." *Crystal Growth & Design* **5**: 1013-1021.

Vishweshwar, P., J. McMahon, et al. (2005). "Crystal engineering of pharmaceutical co-crystals from polymorphic active pharmaceutical ingredients." *Chemical Communications*: 4601-4603.

Walsh, R. D. B., M. W. Bradner, et al. (2003). "Crystal Engineering of the Composition of Pharmaceutical Phases." *Chemical Communications*: 186-187.

Zocharski, P., S. Nehm, et al. (2004). "Can Solubility Products Explain Cocrystal Solubility and Predict Crystallization Conditions?" *The AAPS Journal* **6**: Abstract R6192.

CHAPTER FIVE

PH-DEPENDENT SOLUBILITY, DISSOLUTION, AND STABILITY OF COCRYSTALS WITH NON-IONIZABLE DRUGS

Introduction

The solubility of a drug is important because it affects its dissolution and for many drugs its bioavailability. Serajuddin estimates that one third of all medicinal compounds synthesized have solubilities less than 10 μg/mL, and that another third have solubilities between 10 and 100 μg/mL (Serajuddin 2007). Salt formation is a common approach, but is limited to improving the aqueous solubility of ionizable drugs. The challenge to improve the solubility and dissolution of non-ionizable drugs, however, can be overcome by making cocrystals. This has been shown for cocrystals of carbamazepine-nicotinamide, carbamazepine-saccharin, exemestane-maleic acid, and megestrol acetate-saccharin for example (Nehm, Seefeldt et al. 2005; Hickey, Peterson et al. 2006; Shiraki, Takata et al. 2008). The objective of the research presented here is to demonstrate that cocrystals of non-ionizable drugs with ionizable coformers can achieve a pH-dependent solubility.

The solution equilibria involved in the solubility of a 1:1 cocrystal RHA where R is a non-ionizable drug and HA is a monoprotic acidic coformer is shown in Scheme 1. It is assumed that other equilibria, such as solution complexation or crystallization of either component, do not occur.

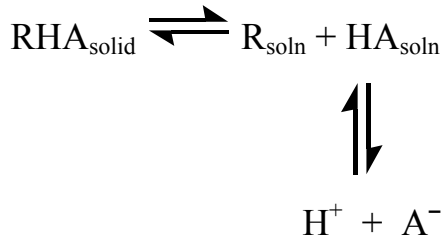

Scheme 5.1. Cocrystal dissociation and acid ionization.

As [HA] ionizes according to its pK_a and solution pH, more cocrystal dissolves to maintain its dissociation equilibrium, thereby increasing the drug concentration in solution.

Pharmaceutical cocrystals with one or more ionizable components have been reported. Drug and/or coformer are ionizable and include acidic, amphoteric and zwiterionic molecules such as carbamazepine cocrystals with benzoic acid, glycolic acid, saccharin, 1-hydroxy-2-naphthoic acid, etc (Fleischman, Kuduva et al. 2003; Childs, Rodríguez-Hornedo et al. 2008); caffeine with maleic acid, glutaric acid, oxalic acid, etc (Trask, Motherwell et al. 2005); piroxicam with malonic acid, caprylic acid, fumaric acid, etc (Childs and Hardcastle 2007); and gabapentin with 3-hydroxybenzoic acid (Reddy, Bethune et al. 2008). Cocrystal solubility can be higher or lower than the pure drug or its hydrate, depending on the coformer (Remenar, Morissette et al. 2003; Childs, Chyall et al. 2004; McNamara, Childs et al. 2006; Bak, Gore et al. 2008). These studies suggest that dissolution and therefore solubility of a cocrystal can be tailored based on the choice of coformer. This ability to control solubility and dissolution profiles enable cocrystals to be considered as a viable alternative to solid state drug forms.

The purpose of the study presented here is to understand how the ionization properties of cocrystal components modify the solubility pH dependence of cocrystals. The pH behavior of cocrystals with ionizable coformers was investigated for three carbamazepine cocrystals: carbamazepine-saccharin (CBZ-SAC), carbamazepine-salicylic acid (CBZ-SLC) and carbamazepine-4-aminobenzoic acid hydrate (CBZ-4ABA-HYD). Saccharin and salicylic acid are monoprotic acids with pK_a of 1.8 and 3.0, 4-aminobenzoic acid is amphoteric with pK_a values of 2.4 and 4.9 (Howard and Gould 1987; Williamson, Nagel et al. 1987; Lukacs, Barcsa et al. 1998). Mathematical models for the solubility of cocrystals with different stoichiometries and components of different ionization properties (monoprotic and diprotic acids, amphoteric, basic, and zwitterionic) are also derived. A method based on transition concentration or eutectic composition measurements is proposed to estimate the thermodynamic cocrystal solubility, when transformation to a more thermodynamically stable form prevents it from being experimentally accessible.

Theoretical

Solubility of a Cocrystal with an Acidic Coformer

We have previously shown that when a cocrystal follows solubility product behavior, the solubility decreases with increasing coformer concentration (Nehm, Seefeldt et al. 2005; Nehm, Rodríguez-Spong et al. 2006; Jayasankar, Reddy et al. 2008). If one or both cocrystal components are ionizable, acid or base equilibria will also exist. Consider a 1:1 (drug : coformer) cocrystal RHA where the drug is R and the coformer is

HA, a monoprotic acid. The equilibrium reactions for cocrystal dissociation and coformer ionization are given below:

$$RHA_{solid} \rightleftharpoons R_{soln} + HA_{soln}$$

$$K_{sp} = [R][HA] \quad (1)$$

$$HA \rightleftharpoons A^- + H^+$$

$$K_a = \frac{[H^+][A^-]}{[HA]} \quad (2)$$

where K_{sp} is the solubility product of the cocrystal, and K_a is the acid ionization constant. Species without subscripts indicate solution phase. The analysis presented here assumes ideal behavior with concentrations replacing activities in the equilibrium constants. This is an approximation with the purpose of establishing general trends, and nonidealities due to complexation, ionic interactions, and solvent-solute interactions will need to be considered for a more rigorous analysis, particularly at high concentrations and ionic strengths.

The analytical or total acid concentration, the sum of the ionized and non-ionized species, is given by:

$$[A]_T = [HA] + [A^-], \quad (3)$$

while total drug, which is non-ionizable, is given by:

$$[R]_T = [R] \quad (4)$$

By substituting for [HA] and $[A^-]$ from equations (1) and (2), respectively, equation (3) is rearranged as:

$$[A]_T = \frac{K_{sp}}{[R]_T}\left(1 + \frac{K_a}{[H^+]}\right) \quad (5)$$

For a 1:1 molar ratio binary cocrystal, the solubility is equal to the total concentration of either drug or coformer in solution,

$$S_{cocrystal} = [R]_T = [A]_T, \quad (6)$$

and equation (5) is rewritten as:

$$S_{cocrystal} = \sqrt{K_{sp}\left(1 + \frac{K_a}{[H^+]}\right)} \quad (7)$$

Equation (7) predicts that cocrystal solubility will increase with increasing pH (decreasing $[H^+]$). Cocrystal solubility is also dependent on cocrystal K_{sp} and coformer pK_a. Figure 5.1a shows the predicted solubility-pH dependence for two cocrystals with different K_{sp} values but the same coformer pK_a. At pH values below the coformer pK_a, or $[H^+] >> K_a$, cocrystal solubility approaches its intrinsic solubility, given by $(K_{sp})^{1/2}$. At pH = pK_a, or $[H^+] = K_a$, the cocrystal solubility is $\sqrt{2K_{sp}}$ or 1.4 times the intrinsic cocrystal solubility. At pH values above the coformer pK_a, or $[H^+] << K_a$, cocrystal solubility increases exponentially. The effect of coformer pK_a on predicted cocrystal solubility is shown in figure 5.1b. Cocrystal solubility is predicted to increase at lower pH values as the coformer pK_a decreases. Thus, the pH at which the solubility will increase is directly related to coformer pK_a.

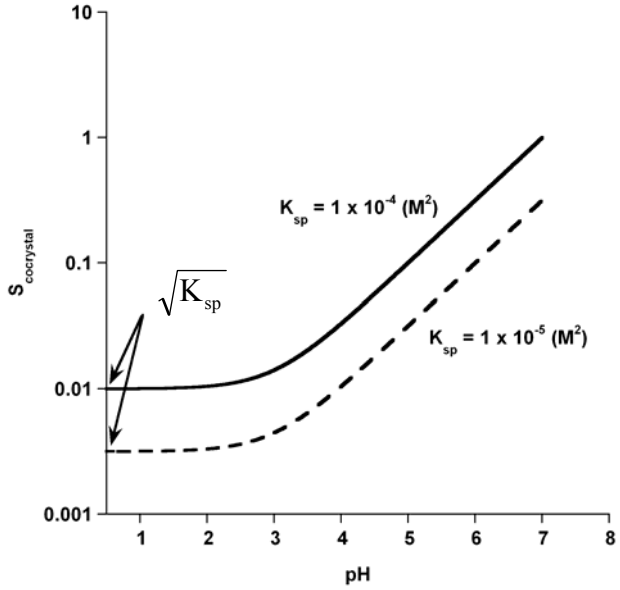

(a)

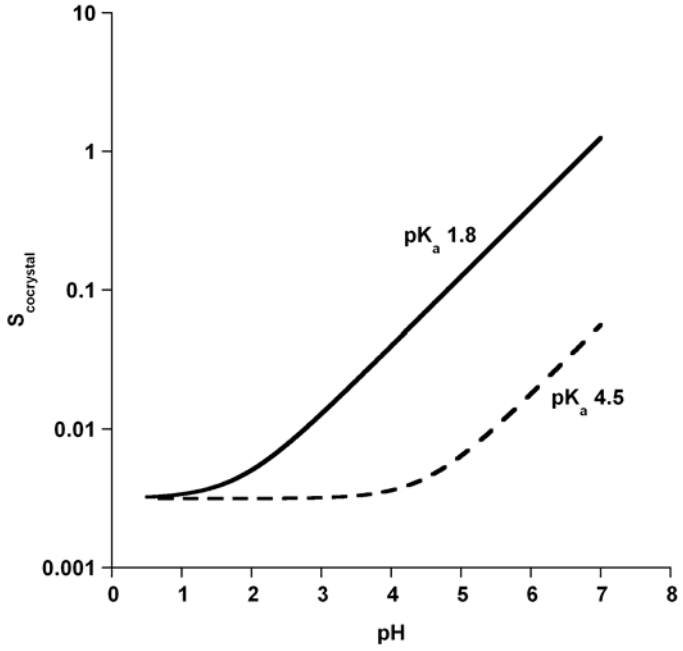

(b)

Figure 5.1. Predicted solubility pH profile for 1:1 RHA cocrystal using equation (7) with (a) K_{sp} values of 1x10^{-4} M^2 and 1x10^{-5} M^2 and pK_a of 3.0; (b) K_{sp} = 1x10^{-5} M^2 and pK_a values of 1.8 and 4.5.

The preceding analysis predicts that cocrystals with acidic coformers impart pH-dependent solubility to non-ionizable drugs. High cocrystal solubility, and therefore high drug concentration, can be achieved by increasing pH. With reports of drugs forming cocrystals with many different coformers and the resulting variety of K_{sp} and pK_a values, one may now have the ability to design and select cocrystals with the desired pH-dependent solubility.

Solubility of Cocrystals with Different Ionization Properties and Stoichiometries

Equations that describe the solubility dependence on K_{sp}, pH, and pK_a as well as total drug concentration dependence on coformer concentration for several types of cocrystals are presented in Table 5.1. The interested reader is directed to the appendix for the full derivations. The four graphs in Figure 5.2 show the theoretical solubility-pH profile for selected cocrystals with components that differ in their ionization properties, from Table 5.1. Figures 5.2a and 5.2b show that cocrystals of a non-ionizable drug can exhibit very different solubility-pH behavior, depending on the coformer ionization properties. A diprotic acid will lead to increases in solubility with pH, similar to a monoprotic acid. An amphoteric coformer will result in a U shape curve with a solubility minimun in a pH range between the two pK_a values. Similar behavior is predicted for a cocrystal of a basic drug and an acidic coformer where the ionizable groups reside in different molecules (Fig. 5.2c). The pH range over which this minimum occurs is dependent on the difference between the two pK_a values; the greater the difference, the wider this minimum range will be, as has been shown for zwitterionic solutes

(Yalkowsky 1999). This same U shape curve is predicted for solubility of a cocrystal with a zwitterionic drug, but in this specific case, the solubility of the drug also has a predicted U shape solubility-pH profile (Fig. 5.2d).

Table 5.1. Cocrystals of different stoichiometry and ionization properties and their respective solubility and drug concentration dependence on coformer concentration. Detailed derivations are included in the appendix.

Cocrystal	Dependence of drug concentration on coformer concentration	Eq.	Dependence of solubility on pH, K_{sp}, and pK_a	Eq.
RH_2A (1:1, neutral:diprotic) carbamazepine-glutaric acid	$[R]_T = \frac{K_{sp}}{[A]_T}\left(1+\frac{K_{a1,H_2A}}{[H^+]}+\frac{K_{a1,H_2A}K_{a2,H_2A}}{[H^+]^2}\right)$	8	$S = \sqrt{K_{sp}\left(1+\frac{K_{a1,H\ A}}{[H^+]}+\frac{K_{a1,H_2A}K_{a2,H_2A}}{[H^+]^2}\right)}$	9
R_2H_2A (2:1, neutral:diprotic) carbamazepine-succinic acid	$[R]_T = \sqrt{\frac{K_{sp}}{[A]_T}\left(1+\frac{K_{a1,H_2A}}{[H^+]}+\frac{K_{a1,H_2A}K_{a2,H_2A}}{[H^+]^2}\right)}$	10	$S = \sqrt[3]{\frac{K_{sp}}{4}\left(1+\frac{K_{a1,H_2A}}{[H^+]}+\frac{K_{a1,H_2A}K_{a2,H_2A}}{[H^+]^2}\right)}$	11
R_2HAB (2:1, neutral:amphoteric) carbamazepine-4-aminobenzoic acid	$[R]_T = \sqrt{\frac{K_{sp}}{[AB]_T}\left(1+\frac{K_{a1,HAB}}{[H^+]}+\frac{[H^+]}{K_{a2,HAB}}\right)}$	12	$S = \sqrt[3]{\frac{K_{sp}}{4}\left(1+\frac{K_{a1,HAB}}{[H^+]}+\frac{[H^+]}{K_{a2,HAB}}\right)}$	13
BHA (1:1, basic:acidic) theophylline-salicylic acid	$[B]_T = \frac{K_{sp}}{[A]_T}\left(1+\frac{K_{a,HA}}{[H^+]}\right)\left(1+\frac{[H^+]}{K_{a,B}}\right)$	14	$S = \sqrt{K_{sp}\left(1+\frac{K_{a,HA}}{[H^+]}\right)\left(1+\frac{[H^+]}{K_{a,B}}\right)}$	15
B_2H_2A (2:1, basic:diprotic) itraconazole-L-tartaric acid	$[B]_T = \sqrt{\frac{K_{sp}}{[A]_T}\left(1+\frac{[H^+]}{K_{a,B}}\right)^2\left(1+\frac{K_{a1,H_2A}}{[H^+]}+\frac{K_{a1,H_2A}K_{a2,H_2A}}{[H^+]^2}\right)}$	16	$S = \sqrt[3]{\frac{K_{sp}}{4}\left(1+\frac{[H^+]}{K_{a,B}}\right)^2\left(1+\frac{K_{a1,H_2A}}{[H^+]}+\frac{K_{a1,H_2A}K_{a2,H_2A}}{[H^+]^2}\right)}$	17
HABHX (1:1, amphoteric:acidic) piroxicam-caprylic acid	$[AB]_T = \frac{K_{sp}}{[X]_T}\left(1+\frac{K_{a,HX}}{[H^+]}\right)\left(1+\frac{K_{a1,HAB}}{[H^+]}+\frac{[H^+]}{K_{a2,HAB}}\right)$	18	$S = \sqrt{K_{sp}\left(1+\frac{K_{a,HX}}{[H^+]}\right)\left(1+\frac{K_{a1,HAB}}{[H^+]}+\frac{[H^+]}{K_{a2,HAB}}\right)}$	19
$^-ABH^+H_2X$ (1:1, zwitterionic:diprotic) gabapentin-3-hydroxybenzoic acid	$[AB]_T = \frac{K_{sp}}{[X]_T}\left(1+\frac{K_{a1,H_2X}}{[H^+]}+\frac{K_{a1,H_2X}K_{a2,H_2X}}{[H^+]^2}\right)\times \left(1+\frac{[H^+]}{K_{a1,^-ABH^+}}+\frac{K_{a2,^-ABH^+}}{[H^+]}\right)$	20	$S = \sqrt{K_{sp}\left(1+\frac{K_{a1,H_2X}}{[H^+]}+\frac{K_{a1,H_2X}K_{a2,H_2X}}{[H^+]^2}\right)\times \sqrt{\left(1+\frac{[H^+]}{K_{a1,^-ABH^+}}+\frac{K_{a2,^-ABH^+}}{[H^+]}\right)}}$	21

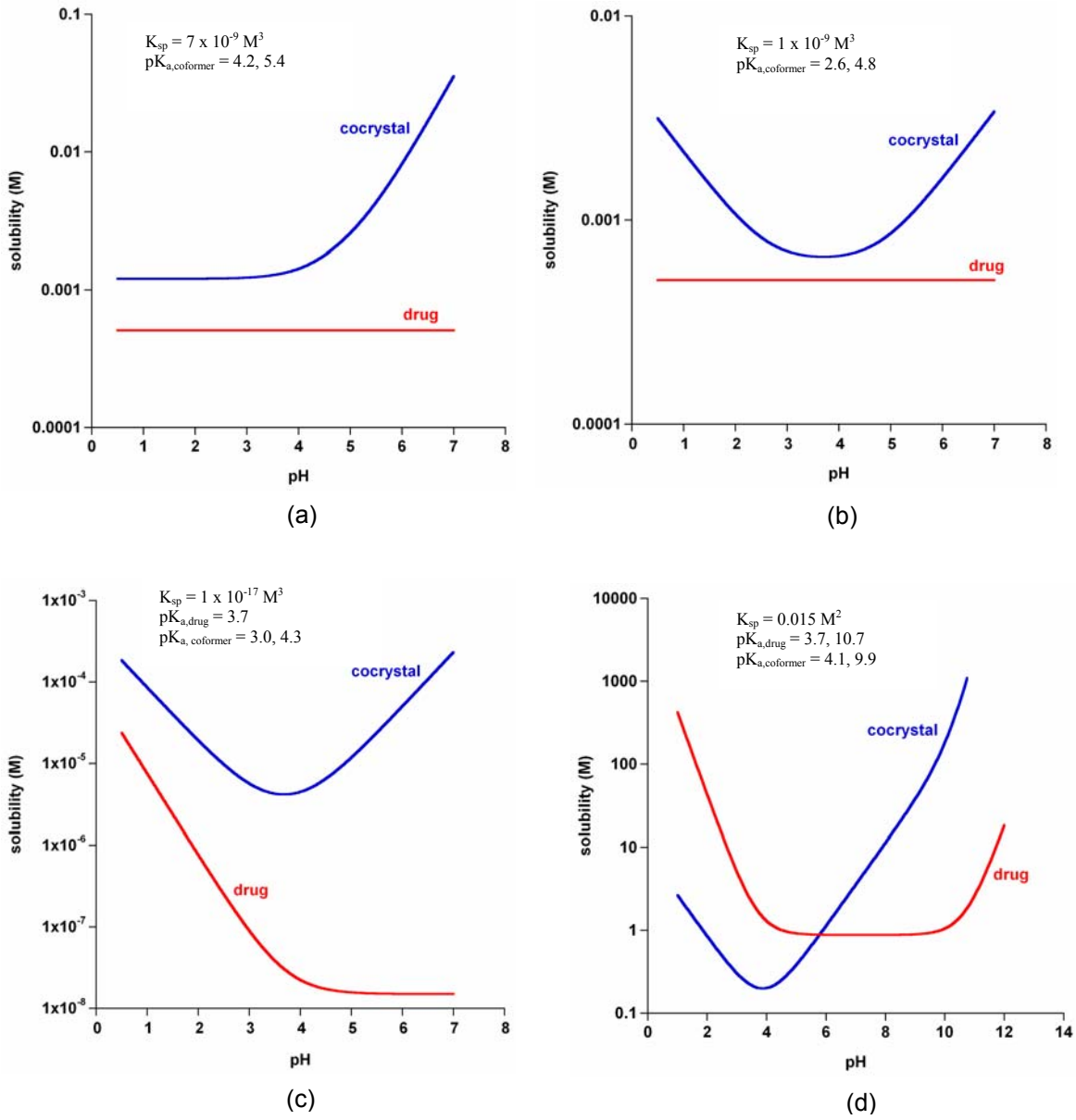

Figure 5.2. Theoretical solubility-pH profile for (a) 2:1 R_2H_2A cocrystal calculated using equation (11), (b) 2:1 R_2HAB cocrystal calculated using equation (13), (c) 2:1 B_2H_2A calculated using equation (17), and (d) 1:1 $^{-}ABH^{+}H_2X$ cocrystal calculated using equation (21). pK_a values for drug and coformer and cocrystal K_{sp} are included in each graph. K_{sp} values used are experimental values or reasonable estimations of published cocrystals for the selected type in each graph (Remenar, Morissette et al. 2003; Childs, Rodríguez-Hornedo et al. 2008; Reddy, Bethune et al. 2008).

Cocrystal Stability Dependence on pH

Cocrystal stability is dependent on the drug and coformer concentration in solution. For a 1:1 cocrystal the molar drug concentration in solution is equal to the cocrystal solubility. Figure 5.3 shows the predicted cocrystal solubility or drug concentration, $[R]_T$, dependence on coformer concentration, $[A]_T$, and pH for a 1:1 RHA cocrystal, generated from equation 5. The cocrystal solubility is predicted to increase with pH and to decrease as the coformer solution concentration increases.

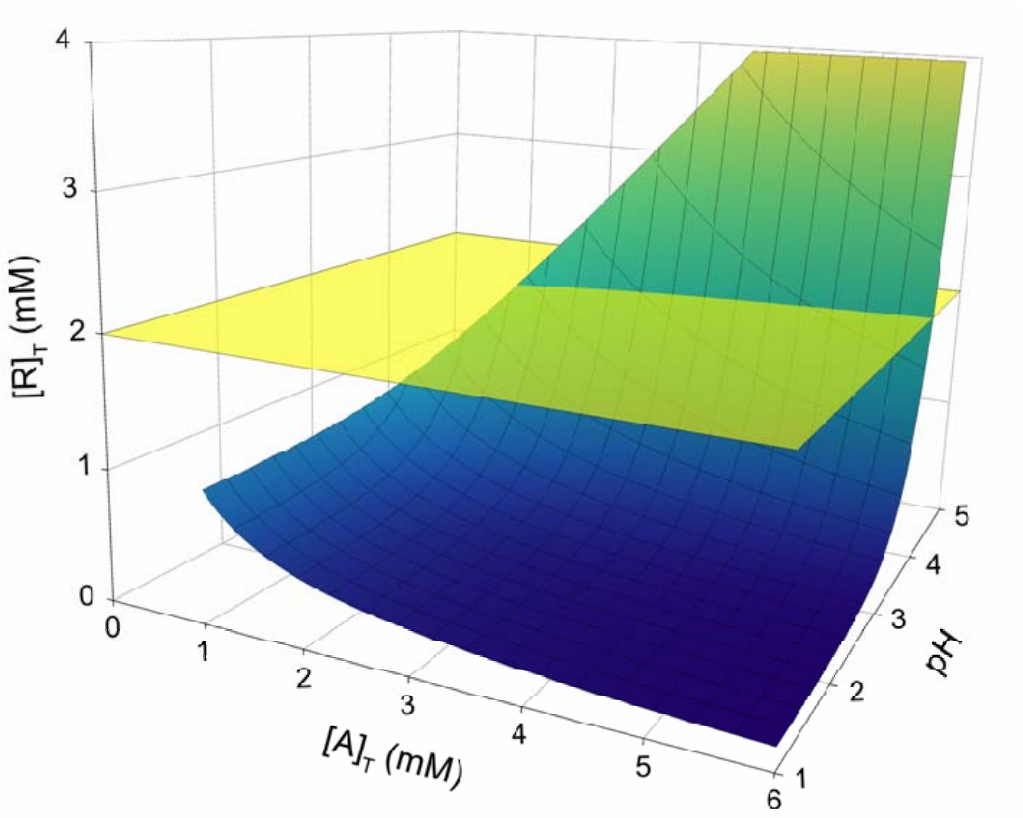

Figure 5.3. Theoretical dependence of cocrystal solubility or drug concentration, $[R]_T$, on coformer concentration and pH for a 1:1 RHA cocrystal. Calculated from equation 5 with K_{sp} = 1 x 10^{-6} M^2 and coformer pK_a = 3. Solubility of drug, S_R, in neat solvent is represented by the yellow plane (S_R = 2 x 10^{-3} M). Transition concentrations are located at the intersection of the drug solubility with cocrystal solubility.

The transition concentration or eutectic composition (C_{tr}) is where the cocrystal solubility curve intersects the drug solubility curve. At this point, two solid phases (cocrystal and drug) coexist in equilibrium with the solution. At coformer concentrations below the A_{tr}, the drug is thermodynamically stable and cocrystal can transform to drug. At coformer concentrations above the A_{tr}, the cocrystal is thermodynamically stable and drug can transform to cocrystal (Nehm, Rodríguez-Spong et al. 2006; Childs, Rodríguez-Hornedo et al. 2008; Good and Rodríguez-Hornedo 2008; Jayasankar, Reddy et al. 2008).

Figure 5.3 also shows that A_{tr} is pH dependent, and thus cocrystal stability is pH dependent. At low pH values (pH < 3.5), the cocrystal is thermodynamically stable compared to crystalline drug. As pH increases above 3.5, cocrystal solubility increases above the solubility of the single component drug which predisposes the cocrystal to transform to the drug. For this theoretical example, cocrystal could be synthesized under stoichiometric conditions at pH values less than 3.5, but non-stoichiometric conditions would be necessary to synthesize the same cocrystal at pH > 3.5.

The terms $[A]_{tr}$ and $[R]_{tr}$ represent the coformer and drug concentrations at the transition concentration. The case considered here assumes that drug solubility is independent of pH and coformer concentration; hence $[R]_{tr}$ is constant. The coformer concentration, $[A]_{tr}$, can also be expressed by using equation (5) with the appropriate substitutions as:

$$[A]_{tr} = \frac{K_{sp}}{[R]_{tr}}\left(1 + \frac{K_a}{[H^+]}\right) \tag{22}$$

This equation predicts that coformer transition concentration, $[A]_{tr}$, increases with pH as shown in Figure 5.4, implying that higher coformer concentrations are necessary to maintain cocrystal stability. Under ideal conditions, it may be assumed that $[R]_{tr} = S_R$

where S_R is the solubility of the drug in pure solvent. This assumption, however, is a first approximation and further analysis may be necessary to determine if nonidealities such as activity coefficients or solution complexation may cause $[R]_{tr} \neq S_R$. Therefore, measuring both the drug and coformer concentrations at the transition concentration could lead to a more accurate calculation of K_{sp} using equation 22.

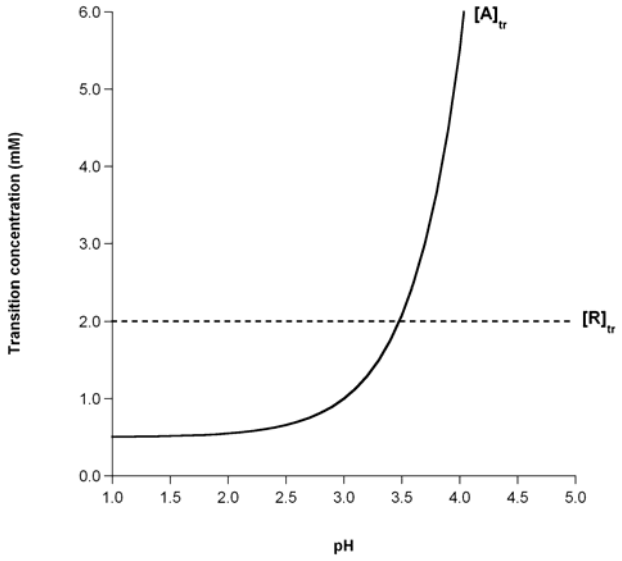

Figure 5.4. Drug and coformer transition concentrations, $[R]_{tr}$ and $[A]_{tr}$, as a function of pH for 1:1 cocrystal RHA, calculated from equation (22) with $K_{sp} = 1 \times 10^{-6}$ M^2, $pK_a = 3$, and $[R]_{tr} = 2 \times 10^{-3}$ M.

When cocrystal equilibrium solubility is not experimentally accessible due to phase transformation, the transition concentration represents a measurable equilibrium value from which the true cocrystal solubility dependence on pH can be predicted, as has been demonstrated for cocrystals without the effect of pH in aqueous and organic solvents (Good and Rodríguez-Hornedo 2008). Therefore, the above analysis shows that a minimum number of experiments can be performed to gain information about cocrystal solubility and stability domains. This can become critical if time or sample quantity is limited.

Other transition concentrations exist where other solid phases are in equilibrium with solution, such as cocrystal/coformer or two cocrystals of different stoichiometries and have been presented elsewhere (Childs, Rodríguez-Hornedo et al. 2008; Jayasankar, Reddy et al. 2008). These will not be discussed here because the transition concentration between drug and cocrystal is more relevant to phase stability in aqueous solutions during dissolution and solubility studies, as presented in the results section.

Table 5.2 includes the equations that predict the transition concentration (coformer and drug components) in equilibrium with drug and cocrystal for the same type of cocrystals as in Table 5.1. The transition concentrations (drug and coformer components) dependence on pH for four different types of cocrystals is shown in Figure 5.5. These predictions parallel those of cocrystal solubility dependence on component pK_a and solution pH described for Figure 5.2. The models predict that for a cocrystal with a non-ionizable drug and diprotic acidic coformer, the coformer transition concentration will increase with pH while the drug transition concentration is independent of pH (Fig. 5.5a). An amphoteric coformer will result in a U shape curve with an $[AB]_{tr}$ minimum in a pH range between the two pK_a values (Fig. 5.5b). For cocrystals of a basic drug and an acidic coformer where the ionizable groups reside in different molecules the drug transition concentration decreases with pH while the coformer transition concentration increases with pH (Fig. 5.5c). For a cocrystal with an amphoteric drug and diprotic acidic ligand, the drug transition concentration will result in a U shape curve with a minimum concentration in a pH range between the two pK_a values and the coformer transition concentration increases with pH (Fig. 5.5d). $[B]_o$,

$[AB]_o$, and $[^-ABH^+]_o$ are the intrinsic solubility of the basic, amphoteric, and zwitterionic components, respectively.

Table 5.2. Transition concentration (coformer and drug component) dependence on pH for cocrystals of different stoichiometry and with different ionization property.

Cocrystal	Coformer transition concentration	Eq	Drug transition concentration	Eq
RH_2A (1:1, neutral:diprotic) carbamazepine-glutaric acid	$[A]_{tr} = \frac{K_{sp}}{[R]_{tr}}\left(1+\frac{K_{a1,H_2A}}{[H^+]}+\frac{K_{a1,H_2A}K_{a2,H_2A}}{[H^+]^2}\right)$	23	$[R]_{tr}$	24
R_2H_2A (2:1, neutral:diprotic) carbamazepine-succinic acid	$[A]_{tr} = \frac{K_{sp}}{[R]_{tr}^2}\left(1+\frac{K_{a1,H_2A}}{[H^+]}+\frac{K_{a1,H_2A}K_{a2,H_2A}}{[H^+]^2}\right)$	25	$[R]_{tr}$	26
R_2HAB (2:1, neutral:amphoteric) carbamazepine-4-aminobenzoic acid	$[AB]_{tr} = \frac{K_{sp}}{[R]_{tr}^2}\left(1+\frac{K_{a1,HAB}}{[H^+]}+\frac{[H^+]}{K_{a2,HAB}}\right)$	27	$[R]_{tr}$	28
BHA (1:1, basic:acidic) theophylline-salicylic acid	$[A]_{tr} = \frac{K_{sp}}{[B]_o}\left(1+\frac{K_{a,HA}}{[H^+]}\right)$	29	$[B]_{tr} = [B]_o\left(1+\frac{[H^+]}{K_{a,B}}\right)$	30
B_2H_2A (2:1, basic:diprotic) itraconazole-L-tartaric acid	$[A]_{tr} = \frac{K_{sp}}{[B]_o^2}\left(1+\frac{K_{a1,H_2A}}{[H^+]}+\frac{K_{a1,H_2A}K_{a2,H_2A}}{[H^+]^2}\right)$	31	$[B]_{tr} = [B]_o\left(1+\frac{[H^+]}{K_{a,B}}\right)$	32
HABHX (1:1, amphoteric:acidic) piroxicam-malonic acid	$[X]_{tr} = \frac{K_{sp}}{[AB]_o}\left(1+\frac{K_{a,HX}}{[H^+]}\right)$	33	$[AB]_{tr} = [AB]_o\left(1+\frac{K_{a1,HAB}}{[H^+]}\frac{[H^+]}{K_{a2,HAB}}\right)$	34
$^-ABH^+HX$ (1:1, zwitterionic:acidic) gabapentin-3-hydroxybenzoic acid	$[X]_{tr} = \frac{K_{sp}}{[^-ABH^+]_o}\left(1+\frac{K_{a1,H_2X}}{[H^+]}+\frac{K_{a1,H_2X}K_{a2,H_2X}}{[H^+]^2}\right)$	35	$[AB]_{tr} = [^-ABH^+]_o\left(1+\frac{[H^+]}{K_{a1,^-ABH^+}}+\frac{K_{a2,^-ABH^+}}{[H^+]}\right)$	36

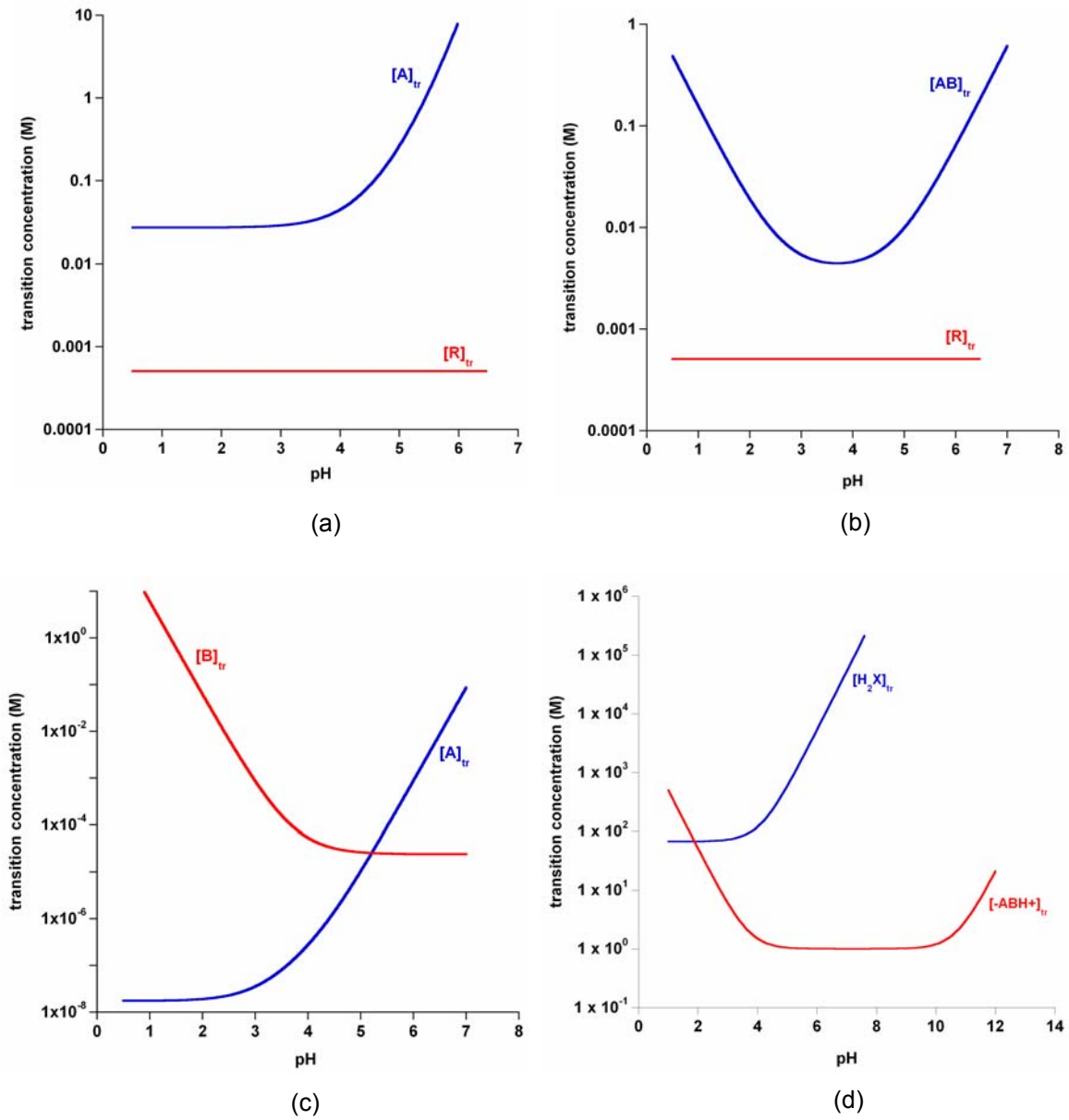

Figure 5.5. Transition concentrations for (a) R_2 H_2A 2:1 cocrystal calculated using equations (25) and (26), (b) R_2 HAB 2:1 cocrystal calculated using equations (27) and (28), (c) B_2 H_2A 2:1 cocrystal calculated using equations (31) and (32), and (d) $^{-}ABH^{+}H_2A$ 1:1 cocrystal calculated using equations (35) and (36). The same cocrystal K_{sp} and component pK_a values were used as in Figure 5.2.

Materials and Methods

Materials

Anhydrous monoclinic carbamazepine (CBZ(III); lot #013K1381 USP grade) was purchased from Sigma Chemical Company (St. Louis, MO), stored at 5 °C over anhydrous calcium sulfate and used as received. Saccharin (SAC; lot # 03111DD) (pK_a = 1.8), salicylic acid (SLC; lot #11111KC) (pK_a = 3.0), and 4-aminobenzoic acid (4ABA; lot #05102HD) (pK_a = 2.6, 4.8) were purchased from Sigma Chemical Company (St. Louis, MO) and used as received. Water used in this study was filtered through a double deionized purification system (Milli Q Plus Water System from Millipore Co., Bedford, MA).

Cocrystal synthesis

Cocrystals were prepared by the reaction crystallization method at room temperature by adding carbamazepine to solutions at close to saturation with coformer (Nehm, Seefeldt et al. 2005; Nehm, Rodríguez-Spong et al. 2006). CBZ-SAC and CBZ-SLC were prepared in ethanol while CBZ-4ABA-HYD was prepared in water. Non-stoichiometric concentrations of coformer created supersaturated conditions with respect to the cocrystal. Slurries were dried by vacuum filtration and confirmed by XRPD.

Measurement of transition concentration, C_{tr}

The transition concentrations, drug and coformer, were measured by HPLC after equilibrating carbamazepine dihydrate and cocrystal in solution at various pH values and at ambient temperature (~22-23°C). The pH of the solution was varied by the addition

of small volumes of concentrated HCl or NaOH and the pH at equilibrium was measured. The solid phases at equilibrium were characterized by XRPD. The system was determined to have reached equilibrium when two solid phases, drug and cocrystal, were confirmed by XRPD and the solution concentration remained constant over consecutive days.

Dissolution studies

Initial dissolution rates were calculated from the initial concentration vs. time profile of CBZ-SAC and CBZ-4ABA-HYD cocrystals using a rotating disk apparatus. Solid cocrystal was compressed in a USP standard Wood's die of 8 mm diameter. Samples were compressed in the die using a Carver hydraulic press (Wabash, IN) by applying 1000 psi for 15 min. Compressed samples were analyzed by XRPD before and after dissolution to determine whether a phase transformation occurred during compression or dissolution. The die containing the compressed sample was rotated at 200 rpm, in 150 mL of 0.1N HCl (pH ~ 1), 0.1M acetate buffer (pH ~ 4), or 0.1M phosphate buffer (pH ~ 7). Solution concentrations were measured by HPLC. Sink conditions were maintained throughout the experiment. Initial dissolution rates were determined from the initial linear portion of the dissolution profile.

Powder dissolution studies of CBZ-SAC were performed in aqueous solutions of 1% hydroxypropylcellulose (HPC, grade EF, Hercules, Hopewell, Virginia) in pH 1 (0.1N HCl) and pH 7 (0.1M phosphate buffer). CBZ-SAC was sieved to a particle size fraction between 63 and 125μm. HPC was added to slow the transformation of cocrystal to dihydrate.

High performance liquid chromatography

The solution concentration of CBZ and coformer was analyzed by Waters HPLC (Milford, MA) equipped with a UV/Vis spectrometer detector. Waters' operation software, Empower, was used to collect and process the data. A C18 Atlantis column (5μm, 4.6 x 250mm; Waters, Milford, MA) at ambient temperature was used to separate the drug and the coformer. The mobile phase was composed of 55% methanol and 45% water with 0.1% trifluoroacetic acid and the flow rate was 1mL/min using an isocratic method. Injection sample volume was 20μL or 50μL. Absorbance of CBZ, SAC, 4ABA, and SLC was monitored at 284, 260, 284, and 303nm, respectively.

X-ray powder diffraction

XRPD patterns of solid phases were collected with a bench top Rigaku Miniflex X-ray Diffractometer (Danvers, MA) using Cu Kα radiation (λ = 1.54Å), a tube voltage of 30 kV, and a tube current of 15 mA. Data was collected from 2 to 40° at a continuous scan rate of 2.5° min^{-1}.

FTIR spectroscopy

IR absorbance spectra of CBZ-SAC and CBZ-4ABA-HYD after disk dissolution studies were collected on a Bruker Vertex 70 FT-IR (Billerica, MA) unit equipped with a DTGS detector and compared with reference cocrystal and single component crystal spectra. Samples were placed on a ZnSe Attenuated Total Reflectance (ATR) crystal accessory and 64 scans were collected for each sample at a resolution of 4 cm^{-1} over a wavenumber region of 4000-600 cm^{-1}.

Results

Cocrystal solubility dependence on pH

Because CBZ-SAC, CBZ-SLC, and CBZ-4ABA-HYD transformed to CBZ(D) at all pH values studied, cocrystal solubility dependence could not be measured by equilibrium methods in pure solvent. As was demonstrated in the theoretical section, when transformation occurs during solubility measurements, the theoretical cocrystal solubility dependence on pH can be estimated by measuring transition concentration dependence on pH. Table 5.3 shows the experimental coformer and drug concentrations and pH values at the transition concentration between cocrystal and carbamazepine dihydrate (CBZ(D)) for CBZ-SAC, CBZ-SLC, and CBZ-4ABA-HYD. At the transition concentration, CBZ(D) and the respective cocrystal were the solid phases at equilibrium. Results show that SAC and SLC transition concentrations increase with increasing pH. 4ABA transition concentrations approach a minimum at a pH value (pH ~ 3.9) between the two pK_a values of the amphoteric coformer. Table 5.3 indicates that a range of drug concentrations were measured at the transition concentration. Because further studies are needed to determine if the drug concentration is dependent on coformer concentration or ionic strength, the average drug concentration was taken for each cocrystal and is included as a footnote in the table below. It is noted that the average $[R]_{tr}$ values are slightly higher than CBZ(D) solubility in pure water (approximately 0.0005 M).

Table 5.3. Experimental pH values and drug and coformer concentrations measured at the transition concentration where drug and cocrystal are in equilibrium with solution.

CBZ-SAC			
pH	**$[CBZ]_{tr}$ (M)[a]**	**$[SAC]_{tr}$ (M)**	**Solid phases**
1.07	0.00061	0.0024	CBZ(D) and CBZ-SAC
1.10	0.00070	0.0021	
1.17	0.00057	0.0024	
1.98	0.00065	0.0092	
2.08	0.00058	0.0089	
2.13	0.00070	0.0086	
2.54	0.00068	0.028	
2.58	0.00062	0.025	
2.77	0.00074	0.047	
2.80	0.00083	0.030	
2.84	0.00069	0.047	
2.95	0.00090	0.065	

[a]Average $[CBZ]_{tr}$ = 0.00069 (± 0.00003) M

CBZ-SLC			
pH	**$[CBZ]_{tr}$ (M)[b]**	**$[SLC]_{tr}$ (M)**	**Solid phases**
1.04	0.00040	0.0011	CBZ(D) and CBZ-SLC
1.05	0.00053	0.0012	
1.07	0.00058	0.0012	
1.94	0.00063	0.0011	
1.98	0.00058	0.0014	
2.16	0.00054	0.0015	
2.87	0.00058	0.0026	
2.90	0.00060	0.0023	
2.96	0.00059	0.0028	
3.76	0.00057	0.012	
3.78	0.00059	0.012	
3.87	0.00078	0.014	
3.94	0.00090	0.018	

[b]Average $[CBZ]_{tr}$ = 0.00061 (± 0.00003) M

CBZ-4ABA-HYD[1]			
pH	**$[CBZ]_{tr}$ (M)[c]**	**$[4ABA]_{tr}$ (M)**	**Solid phases**
1.08	0.00093	0.138	CBZ(D) and CBZ-4ABA-HYD
1.52	0.00067	0.056	
3.93	0.00060	0.0068	
5.28	0.00057	0.029	

[1]Data courtesy of Neal Huang.

[c]Average $[CBZ]_{tr}$ = 0.00069 (± 0.00008) M

Figure 5.6 shows the pH dependence of $[SAC]_{tr}$, $[SLC]_{tr}$, and $[4ABA]_{tr}$. For CBZ-SAC and CBZ-SLC, cocrystals with a non-ionizable drug and acidic coformer, results show that $[A]_{tr}$ increases with increasing pH (Figures 5.6a,b). The transition concentration dependence on pH for CBZ-4ABA-HYD confirmed the predicted behavior of a cocrystal with a non-ionizable drug and amphoteric coformer. Figure 5.6c shows that the coformer transition concentration ($[4ABA]_{tr}$) is lowest at pH 3.9. The experimental behavior is in good agreement with the predicted trend (solid lines) using equation (22) for CBZ-SAC and CBZ-SLC and equation (27) for CBZ-4ABA-HYD.

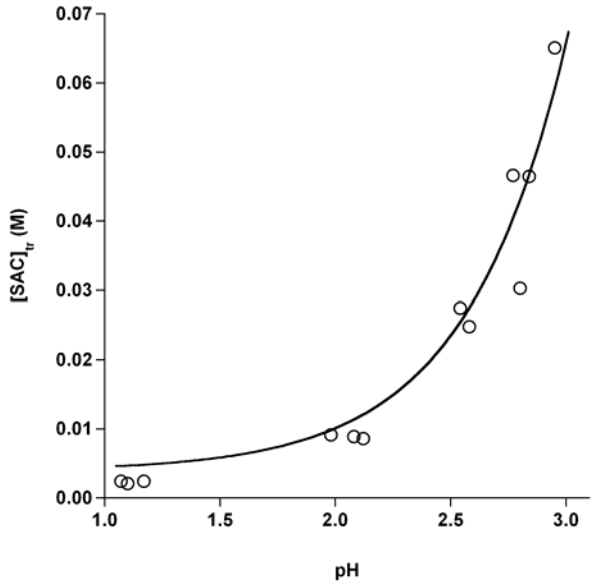

(a)

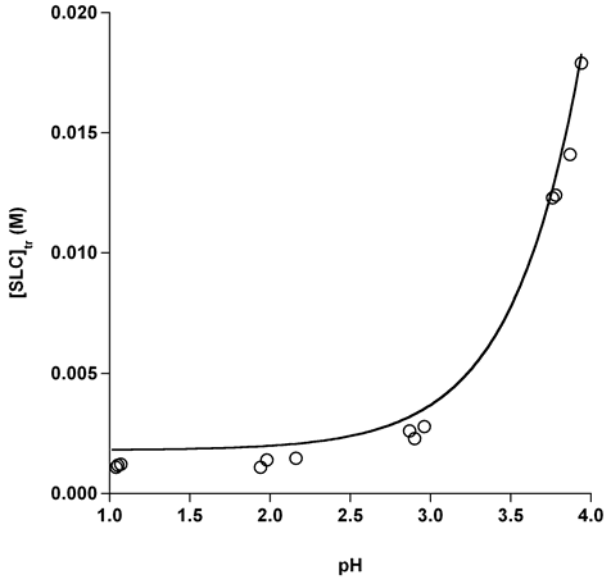

(b)

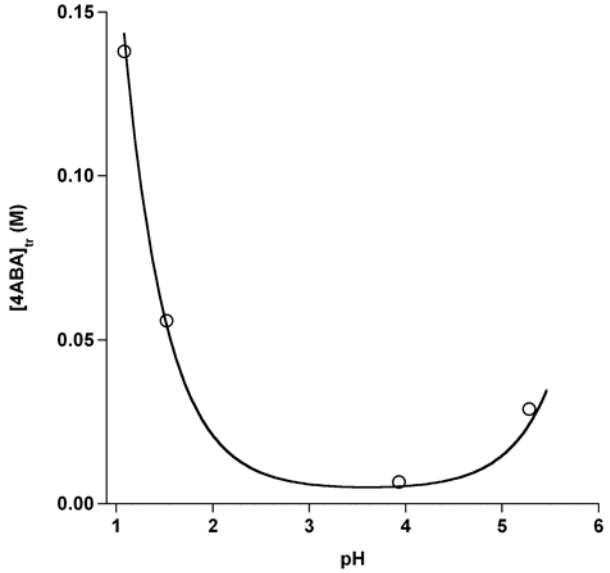

(c)

Figure 5.6. Experimental and predicted coformer transition concentration, A_{tr} and AB_{tr} dependence on pH at 23°C for (a) CBZ-SAC, (b) CBZ-SLC, and (c) CBZ-4ABA-HYD. Curves represent theoretical calculations from equation (22) for $[SAC]_{tr}$ and $[SLC]_{tr}$ and from equation (27) for $[4ABA]_{tr}$.

Cocrystal K_{sp} values were calculated from the measured coformer and average drug transition concentrations. For 1:1 cocrystals with a monoprotic acidic coformer, such as CBZ-SAC or CBZ-SLC, the K_{sp} was estimated from the slope ($K_{sp}/[R]_{tr}$) of a plot of $[A]_{tr}$ vs. $\left(1+\frac{K_a}{[H^+]}\right)$ (Figure 5.7); for 2:1 cocrystals with an amphoteric coformer, such as CBZ-4ABA-HYD, the K_{sp} was estimated from the slope ($K_{sp}/[R]_{tr}^2$) of a plot of $[AB]_{tr}$ vs. $\left(1+\frac{K_{a1,HAB}}{[H^+]}+\frac{[H^+]}{K_{a2,HAB}}\right)$ (Figure 5.8).

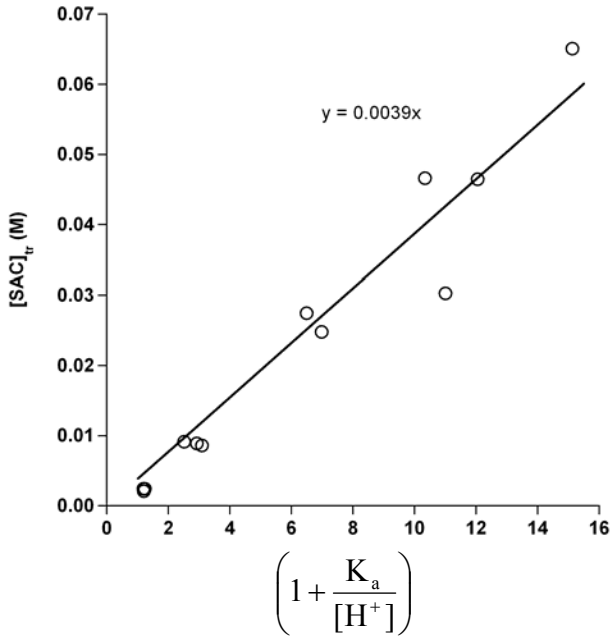

(a)

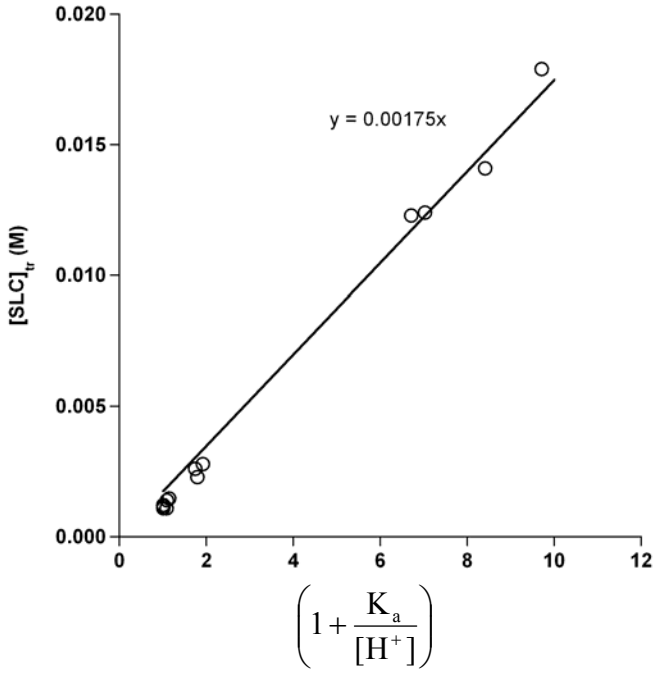

(b)

Figure 5.7. Plots to calculate K_{sp} according to equation 22 for (a) CBZ-SAC and (b) CBZ-SLC. The slope is the $K_{sp}/[R]_{tr}$.

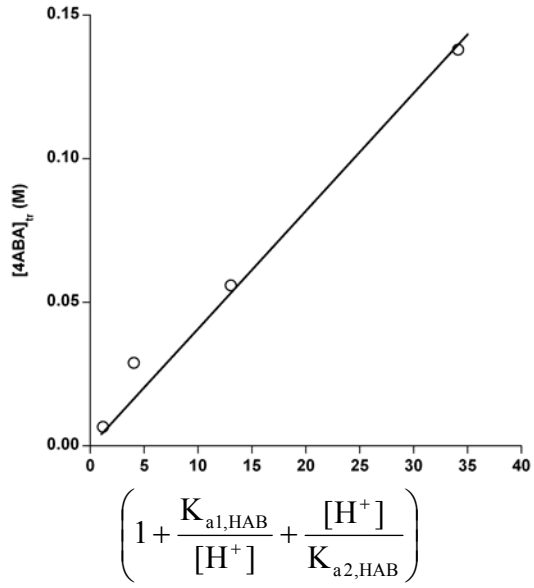

Figure 5.8. Plots to calculate K_{sp} according to equation 27 for CBZ-4ABA-HYD. The slope is the $K_{sp}/([R]_{tr})^2$.

These plots resulted in negative y-intercepts that were not significantly different from zero, and therefore set to intersect the origin. The ratios and the calculated K_{sp} values are included in Table 5.4. The good agreement between the experimental and predicted data in Figure 5.6 and the goodness of fit of the ratio ($K_{sp}/[R]_{tr}$ or $K_{sp}/[R]_{tr}^2$) is indicative that an experiment to measure the transition concentration at a single pH could provide a good first estimate of a cocrystal K_{sp} if time or sample quantity is limited.

Table 5.4. Cocrystal K_{sp} values calculated using transition concentrations in Table 5.3 and equations 22 and 27.

Cocrystal	slope ($K_{sp}/[R]_{tr}$ or $K_{sp}/[R]_{tr}^2$) (± standard error)	R^2	K_{sp} (± standard error)
CBZ-SAC	3.9 (± 0.2) x 10^{-3}	0.94	2.7 (± 0.1) x 10^{-6} M^2
CBZ-SLC	1.75 (± 0.04) x 10^{-3}	0.99	1.13 (± 0.05) x 10^{-6} M^2
CBZ-4ABA-HYD	4.1 (± 0.3) x 10^{-3}	0.98	2.0 (± 0.1) x 10^{-9} M^3

From the experimental and theoretical behavior of A_{tr} or AB_{tr} with pH one can conclude that the solubility of the cocrystal increases with increasing pH for CBZ cocrystals with acidic coformers, SAC or SLC, and has a U shape curve for a cocrystal with an amphoteric coformer, 4ABA. These results also indicate that as the cocrystal solubility increases, higher coformer concentrations would be needed to maintain cocrystal stability.

With a calculated K_{sp}, the solubility dependence on pH can be estimated and compared to CBZ(D) solubility. Figure 5.9 shows the solubility ratio of CBZ-SAC to CBZ(D) and of CBZ-SLC to CBZ(D). Theoretically, CBZ-SAC is approximately 3 – 1,300 times more soluble than CBZ(D) between pH 1 – 7, and CBZ-SLC is approximately 2 – 200 times more soluble than CBZ(D) between pH 1 – 7. While CBZ is nonionizable, its cocrystals can achieve significant solubility increases with pH since

the coformers are ionizable. Cocrystals, however, have limited solubilities. The high cocrystal solubility shown in Figure 5.9 is limited by the solubility of the drug and by solubility of a coformer salt. Salt formation has been observed to occur when the solubility of acidic compounds increases between 3 and 4 log units (Avdeef 2003).

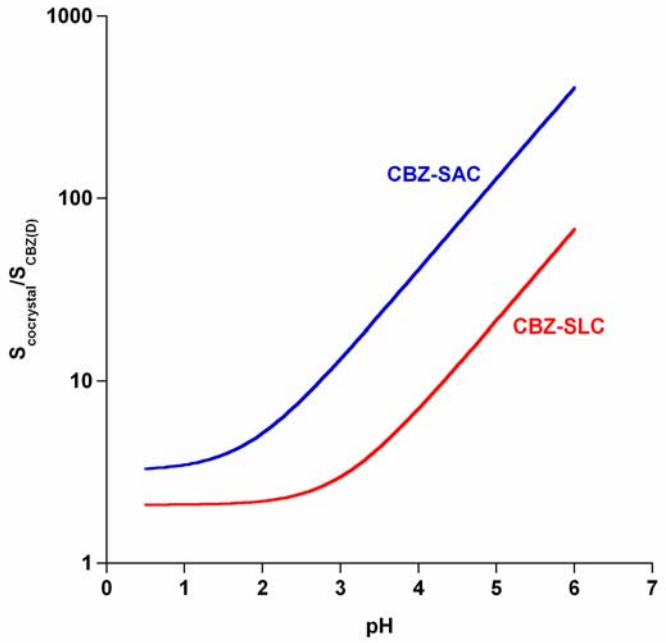

Figure 5.9. Calculated solubility ratio of cocrystal to CBZ(D) as a function of pH based on experimentally measured transition concentrations from pH 1-3 for CBZ-SAC and pH 1-4 for CBZ-SLC.

The CBZ-4ABA-HYD K_{sp} from Table 5.4 was used to calculate the cocrystal solubility dependence on pH (Figure 5.10). When compared to CBZ(D) solubility, the cocrystal is approximately 3 – 13 times more soluble between pH 1 – 7.

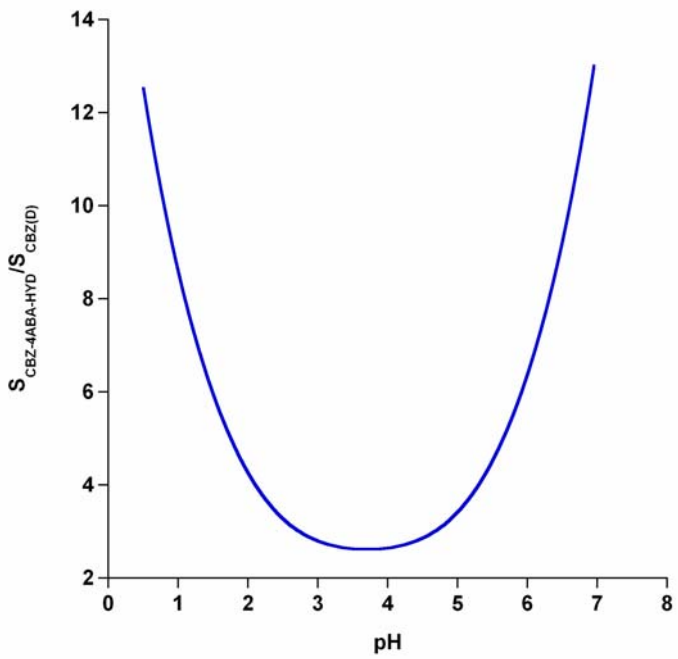

Figure 5.10. Calculated solubility ratio of cocrystal to CBZ(D) as a function of pH based on experimentally measured transition concentrations from pH 1-5 for CBZ-4ABA-HYD.

The transition concentrations from Table 5.3 were used to generate phase solubility diagrams for CBZ-SAC, CBZ-SLC, and CBZ-4ABA-HYD (Figure 5.11), assuming ideal behavior, allowing for the identification of cocrystal and drug stability regions. The solubility curve at each pH was generated using the calculated K_{sp} from the respective transition concentration. Deviations between the predicted and experimental coformer transition concentrations may be the result of the limitations of the assumptions of activities equal to concentrations (Bergstrom, Luthman et al. 2004). Deviations between the predicted and experimental drug transition concentrations is the result of average $[R]_{tr}$ included on the figure as opposed to the individual $[R]_{tr}$ measured at the respective pH. Figure 5.11 indicates that the coformer transition concentrations ($[A]_{tr}$) increase with pH. This increase can be correlated to an increase in solubility with pH, represented by the intersection of the cocrystal solubility curve and the 1:1 stoichiometric

line. As cocrystal solubility increases, the concentration of coformer necessary to maintain cocrystal stability increases. The solubility of each cocrystal is higher than CBZ(D) at all pH values studied, suggesting that phase transformation will be faster as pH of aqueous solutions increase. Cocrystals are predicted to be more soluble than CBZ(D) even at the pH of lowest solubility, i.e., pH 1 for CBZ-SAC and CBZ-SLC and at pH 4 for CBZ-4ABA-HYD.

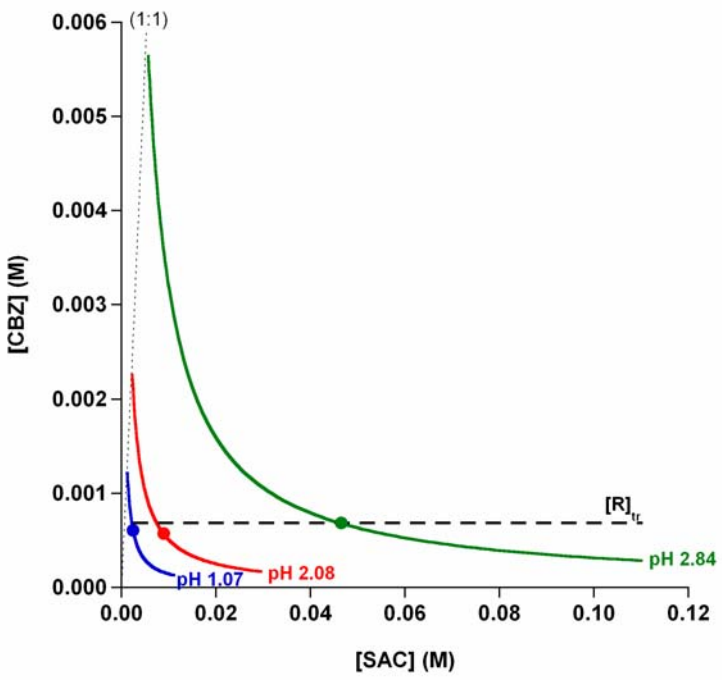

(a)

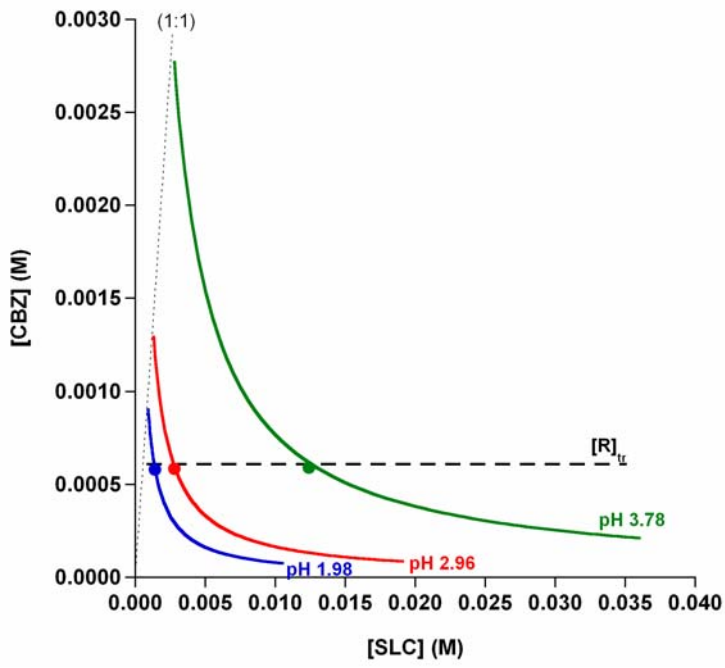

(b)

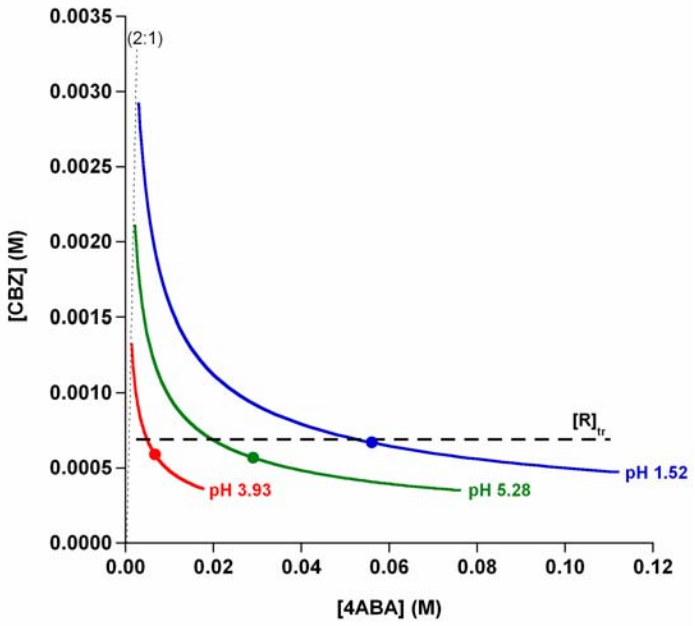

(c)

Figure 5.11. Predicted cocrystal solubility (solid lines) for (a) CBZ-SAC, (b) CBZ-SLC, and (c) CBZ-4ABA-HYD according to equations (22) and (27) using experimentally measured K_{sp} values at each pH and $pK_{a,saccharin} = 1.8$; $pK_{a,salicylic\ acid} = 3.0$; $pK_{a,4\text{-}aminobenzoic\ acid} = 2.6$ and 4.8. Experimentally measured transition concentrations are represented by filled circles. Dashed line represents the average $[R]_{tr}$ measured in the pH range studied for the respective cocrystal. The 1:1 and 2:1 dotted lines represent the stoichiometric solution concentration of cocrystal reactants.

Cocrystal dissolution dependence on pH

The theoretical cocrystal solubility predicted from transition concentrations studies were compared with pH-dependent dissolution behavior. From Figure 5.7, CBZ-SAC solubility was predicted to be approximately 370 times greater at pH 7 than pH 1. The cocrystal solubility was also predicted to be about 3.5 times higher than CBZ(D) at pH 1 and about 1300 times higher pH 7. CBZ-SAC dissolution was faster at pH 7 than pH 1, as indicated by the transformation of CBZ-SAC to CBZ(D) (Figure 5.13), causing the CBZ concentrations measured at pH 7 to be lower than that at pH 1 (Figure 5.12a). As cocrystal dissolves, drug and coformer are released into the dissolution media. Release of coformer (i.e. SAC) from the cocrystal can be indicative of cocrystal dissolution rate when the drug (i.e. CBZ) crystallizes into a more stable form. Based on initial SAC concentrations, CBZ-SAC dissolution was approximately 20 times faster at pH 7 than pH (Figure 5.12b). It should be noted, however, that this increase in dissolution rate is due to acid ionization equilibria and cocrystal to CBZ(D) transformation, both allow the cocrystal to further dissolve. Based on the SAC concentrations, cocrystal dissolution at pH 1 and 7 are approximately 2 and 50 times, respectively, faster than CBZ(D) dissolution (Rodríguez-Hornedo and Murphy 2004). Table 5 summarizes dissolution rates based on CBZ and SAC concentrations.

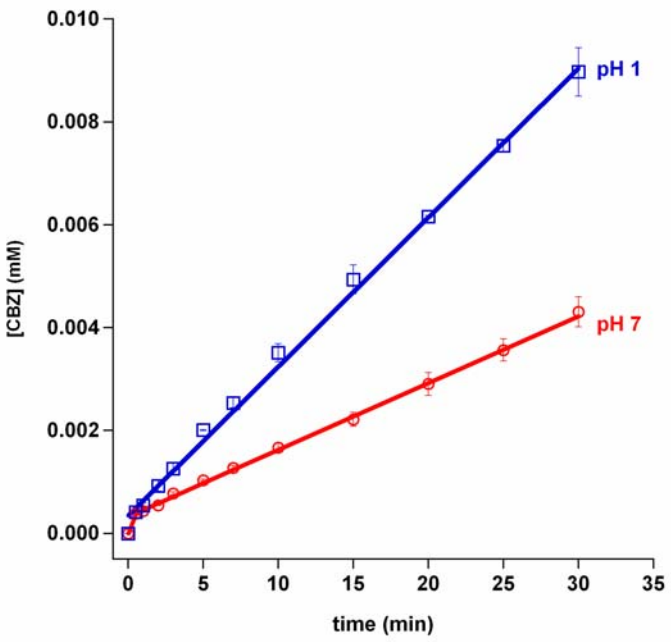

(a)

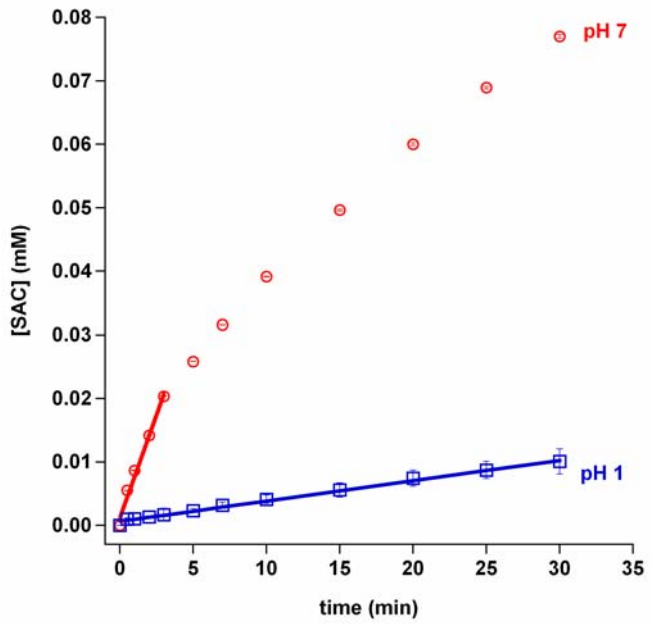

(b)

Figure 5.12. (a) CBZ and (b) SAC concentrations during cocrystal dissolution from a disk at pH 1 (□) and 7 (○) at 23°C, 200rpm. Bars represent standard errors.

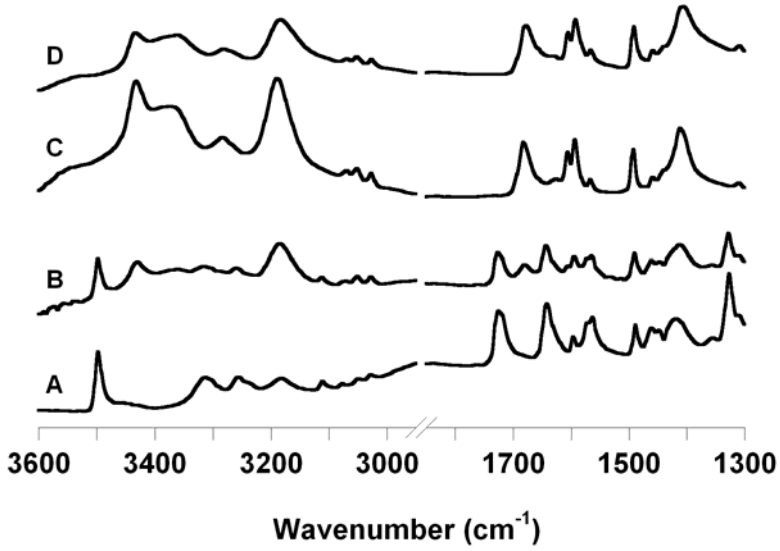

Figure 5.13. FTIR spectra of compressed disk of (A) CBZ-SAC reference, (B) CBZ-SAC post disk dissolution at pH 1, (C) CBZ-SAC post disk dissolution at pH 7, and (D) CBZ dihydrate reference.

Table 5.5. Initial dissolution rates (IDR) from disk dissolution of CBZ-SAC at pH 1 and 7 at 23°C. Solid phase analysis was done by FTIR.

	CBZ IDR[a]		SAC IDR[a]		Solid phase after 30 minutes
pH	(10^{-3} mg/cm^2/min)	(mM/cm^2/min)	(10^{-3} mg/cm^2/min)	(mM/cm^2/min)	
1	(20.6 ± 0.4)	5.8 (± 0.1) x 10^{-4}	(17.7 ± 0.4)	6.4 (± 0.1) x 10^{-4}	CBZ-SAC and CBZ(D)
7	(9.2 ± 0.1)	2.6 (± 0.1) x 10^{-4}	(354 ± 24)	12.9 (± 0.9) x 10^{-3}	CBZ(D)

[a]Values expressed as average ± standard error.

Transformation of cocrystal to CBZ(D) needs to be slowed or inhibited to achieve higher drug concentrations at pH 7. Polyvinylpyrrolidone (PVP) and hydroxypropylcellulose (HPC) polymers have previously been shown to slow CBZ(D) crystallization (Tian, Sandler et al. 2006; Tian, Saville et al. 2007). Raman spectroscopy was used to monitor cocrystal transformation at pH 7 in which excess cocrystal was added to a solution containing polymer. Concentrations of polymer studied included 1%

and 5% PVP-K19 and 1% HPC (data not shown). Preliminary studies showed that 1% HPC was the most effective at slowing CBZ-SAC to CBZ(D) transformation at pH 7. It should be noted that the solubility of CBZ(D) in 1% HPC was approximately 0.7mM compared to 0.5mM in the absence of polymer (data not shown).

Powder dissolution studies were performed using the cocrystal because the increased surface area leads to faster dissolution and higher drug concentrations compared to disk dissolution. Therefore, powder dissolution presented the most challenging case to slow CBZ(D) crystallization. Transformation to CBZ(D) was slowed and thus allowed cocrystal dissolution rate to be estimated from both CBZ and SAC concentrations. Initial cocrystal dissolution was approximately 6 times faster at pH 7 than at pH 1 in 1% HPC (Figure 5.14). Although CBZ-SAC had converted to CBZ(D) after 30 minutes in pH 7 (Figure 5.15), supersaturation was maintained for sufficient time to achieve higher drug concentrations.

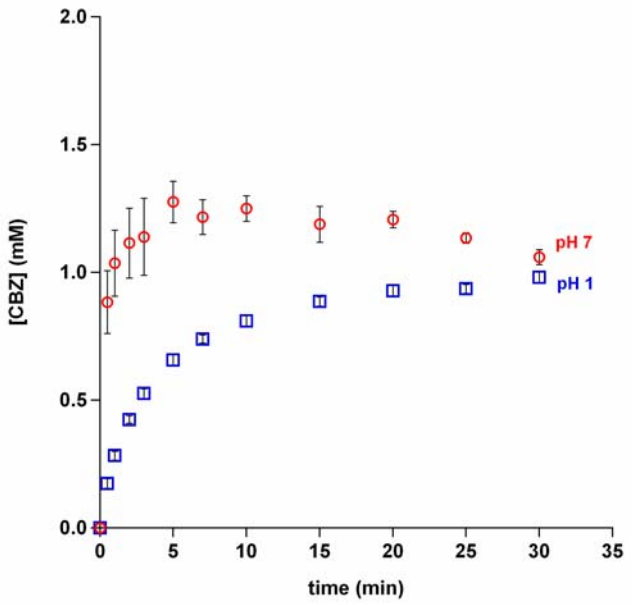

(a)

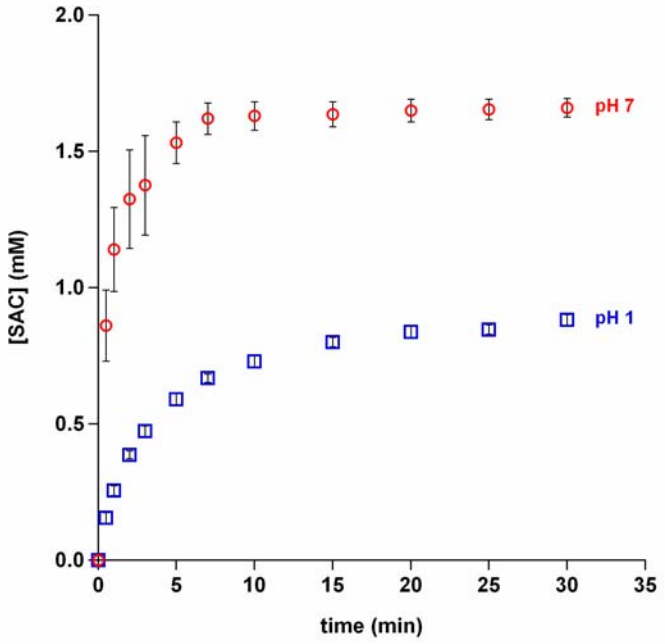

(b)

Figure 5.14. Average (a) CBZ and (b) SAC concentration at pH 1 (□) and 7 (○) as a function of time during powder dissolution of CBZ-SAC in 1% HPC at 23°C, 200rpm. Bars represent standard errors.

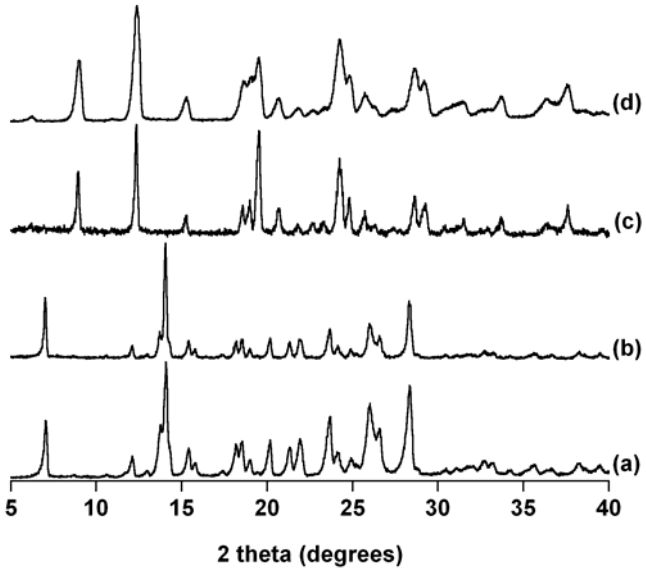

Figure 5.15. XRPD (a) reference CBZ-SAC, (b) after 30 minute powder dissolution pH 1, (c) after 30 minute powder dissolution pH 7, and (d) reference CBZ(D).

CBZ-4ABA-HYD dissolution (data courtesy of Neal Huang) was compared to the predicted solubility dependence on pH for a cocrystal with a non-ionizable drug and amphoteric coformer. The cocrystal proved to have a faster dissolution rate at pH 1 and 7 than at pH 4, as indicated by the transformation to CBZ(D) by FTIR analysis (Figure 5.17) and therefore lower CBZ concentrations from cocrystal dissolution in pH 1 and 7 (Figure 5.16a). Dissolution of CBZ-4ABA-HYD can be inferred by measuring 4ABA concentrations; however, just as with CBZ-SAC, the dissolution rates could be slightly higher. CBZ-4ABA-HYD exhibits 5 and 14 times higher initial disk dissolution rates at pH 1 and pH 7, respectively, than at pH 4 when monitoring 4ABA concentrations (Figure 5.16b). This is consistent with the pH-dependent solubility predicted for a cocrystal with an amphoteric coformer shown in Figure 5.8.

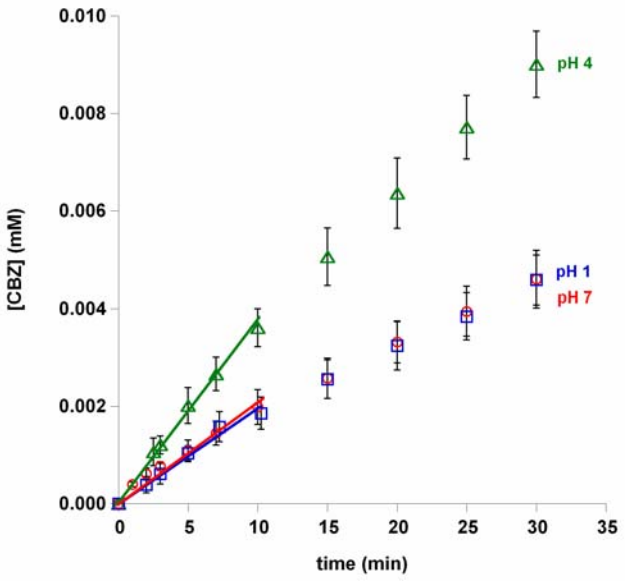

(a)

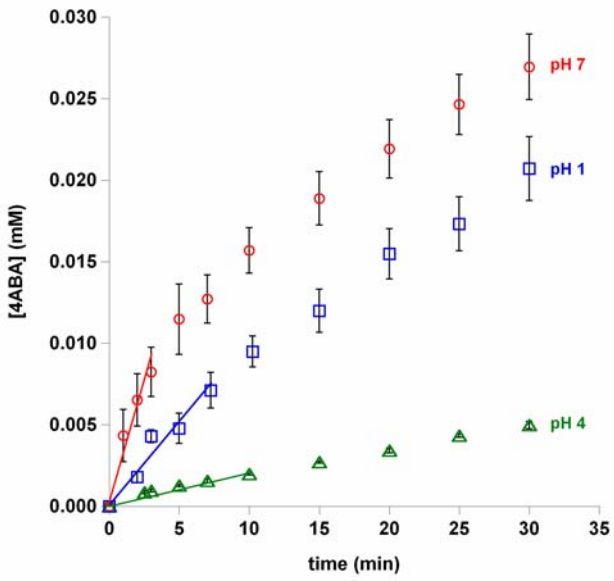

(b)

Figure 5.16. Average (a) CBZ and (b) 4ABA concentrations as a function of time during disk dissolution of CBZ-4ABA-HYD at pH 1 (□), 4 (△), and 7 (○) at 23°C, 200rpm. Bars represent standard error. (Data courtesy of Neal Huang.)

Table 5.6. Initial dissolution rates (IDR) from disk dissolution of CBZ-4ABA-HYD at pH 1, 4, and 7 at 23°C. Solid phase analysis was done by FTIR. (Data courtesy of Neal Huang.)

	CBZ IDR[a]		**4ABA IDR[a]**		**Solid phase after 30 minutes**
pH	(10^{-3} mg/cm^2/min)	(mM/cm^2/min)	(10^{-3} mg/cm^2/min)	(mM/cm^2/min)	
1	(10.4 ± 0.3)	3.8 (± 0.1) x 10^{-4}	(39.7 ± 5.4)	1.9 (± 0.2) x 10^{-3}	CBZ(D)
4	(20.8 ± 0.5)	7.2 (± 0.1) x 10^{-4}	(6.3 ± 0.2)	3.8 (± 0.1) x 10^{-4}	CBZ-4ABA-HYD and CBZ(D)
7	(10.5 ± 0.4)	3.8 (± 0.1) x 10^{-4}	(110.1 ± 4.5)	5.4 (± 0.2) x 10^{-3}	CBZ(D)

[a]Values expressed as average ± standard error.

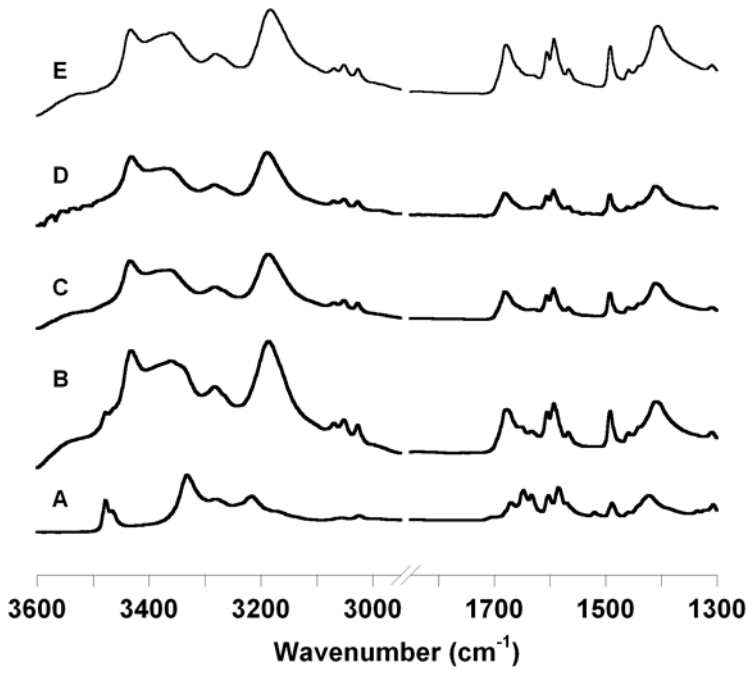

Figure 5.17. FTIR spectra of compressed tablets of (A) CBZ-4ABAHYD reference; CBZ-4ABA-HYD post disk dissolution at (B) pH 4, (C) pH 1, and (D) pH 7; (E) CBZ dihydrate reference.

Conclusions

Cocrystal solubility, stability, and dissolution have been shown to be pH-dependent, even for non-ionizable drugs. Thermodynamic models are presented that describe cocrystal solubility and stability dependence on solubility product, component pK_a and solution pH. The models presented here enable one to generate a complete pH-solubility profile, define stability domains, and estimate cocrystal solubilities that are experimentally inaccessible with a minimum number of experiments. Families of cocrystals exist with the same drug and a variety of coformers which enables one to design a cocrystal with the desired solubility dependence on pH.

Appendix

Included in this appendix are additional models presented in Tables 5.1 and 5.2 that describe cocrystal solubility and transition concentrations. The model for a cocrystal with a zwitterionic drug is presented in full detail in chapter 6. Each model will begin with the necessary equilibrium reactions for the type of ionization and stoichiometry for the cocrystal. All transition concentrations (C_{tr}) presented in this appendix refer to the transition between solid drug and solid cocrystal. This appendix can also be used as a guide for future cocrystals reported in literature if they do not follow the stoichiometries or ionizations presented here.

1:1 cocrystal with non-ionizable API and diprotic acidic ligand

$$R\text{-}H_2A_{solid} \rightleftharpoons R_{soln} + H_2A_{soln}$$

$$K_{sp} = [R][H_2A] \tag{1}$$

$$H_2A \rightleftharpoons HA^- + H^+$$

$$K_{a1,H_2A} = \frac{[H^+][HA]}{[H_2A]} \tag{2}$$

$$HA^- \rightleftharpoons A^{2-} + H^+$$

$$K_{a2,H_2A} = \frac{[H^-][A^{2-}]}{[HA^-]} \tag{3}$$

Mass balance on $[A]_T$:

$$[A]_T = [H_2A] + [HA^-] + [A^{2-}] \tag{4}$$

Using equilibrium constants to substitute into equation (4):

$$[A]_T = \frac{K_{sp}}{[R]}\left(1 + \frac{K_{a1,H_2A}}{[H^+]} + \frac{K_{a1,H_2A}K_{a2,H_2A}}{[H^+]^2}\right) \tag{5}$$

Mass balance on $[R]_T$:

$$[R]_T = [R] \tag{6}$$

Substituting equation (6) into equation (5):

$$[A]_T = \frac{K_{sp}}{[R]_T}\left(1 + \frac{K_{a1,H_2A}}{[H^+]} + \frac{K_{a1,H_2A}K_{a2,H_2A}}{[H^+]^2}\right) \tag{7}$$

For a 1:1 cocrystal, $S_{cocrystal} = [A]_T = [R]_T$

$$S_{cocrystal} = \sqrt{K_{sp}\left(1 + \frac{K_{a1,H_2A}}{[H^+]} + \frac{K_{a1,H_2A}K_{a2,H_2A}}{[H^+]^2}\right)} \tag{8}$$

Equation (7) can be rewritten specifically at the transition concentration, C_{tr}, as:

$$[A]_{tr} = \frac{K_{sp}}{[R]_{tr}}\left(1 + \frac{K_{a1,H_2A}}{[H^+]} + \frac{K_{a1,H_2A}K_{a2,H_2A}}{[H^+]^2}\right) \tag{9}$$

2:1 cocrystal with non-ionizable API and diprotic acidic ligand

$R_2\text{-}H_2A_{solid} \rightleftharpoons 2R_{soln} + H_2A_{soln}$

$$K_{sp} = [R]^2[H_2A] \tag{10}$$

$H_2A \rightleftharpoons HA^- + H^+$

$$K_{a1,H_2A} = \frac{[H^+][HA]}{[H_2A]} \tag{11}$$

$HA^- \rightleftharpoons A^{2-} + H^+$

$$K_{a2,H_2A} = \frac{[H^-][A^{2-}]}{[HA^-]} \tag{12}$$

Mass balance on $[A]_T$:

$$[A]_T = [H_2A] + [HA^-] + [A^{2-}] \tag{13}$$

Using equilibrium constants to substitute into equation (13):

$$[A]_T = \frac{K_{sp}}{[R]^2}\left(1 + \frac{K_{a1,H_2A}}{[H^+]} + \frac{K_{a1,H_2A}K_{a2,H_2A}}{[H^+]^2}\right) \quad (14)$$

Mass balance on $[R]_T$:

$$[R]_T = [R] \quad (15)$$

Substituting equation (15) into equation (14):

$$[A]_T = \frac{K_{sp}}{[R]_T^2}\left(1 + \frac{K_{a1,H_2A}}{[H^+]} + \frac{K_{a1,H_2A}K_{a2,H_2A}}{[H^+]^2}\right) \quad (16)$$

For a 2:1 cocrystal, $S_{cocrystal} = [A]_T = \frac{1}{2}[R]_T$

$$S_{cocrystal} = \sqrt[3]{\frac{K_{sp}}{4}\left(1 + \frac{K_{a1,H_2A}}{[H+]} + \frac{K_{a1,H_2A}K_{a2,H_2A}}{[H+]^2}\right)} \quad (17)$$

Equation (16) can be rewritten specifically at the transition concentration, C_{tr}, as:

$$[A]_{tr} = \frac{K_{sp}}{[R]_{tr}^2}\left(1 + \frac{K_{a1,H_2A}}{[H^+]} + \frac{K_{a1,H_2A}K_{a2,H_2A}}{[H^+]^2}\right) \quad (18)$$

2:1 cocrystal with non-ionizable API and amphoteric ligand

R_2-HAB $\rightleftharpoons$ 2R + HAB

$$K_{sp} = [R]^2[HAB] \quad (19)$$

HAB $\rightleftharpoons$ $A^-B + H^+$

$$K_{a1,HAB} = \frac{[A^-B][H^+]}{[HAB]} \quad (20)$$

$HABH^+$ $\rightleftharpoons$ HAB + H^+

$$K_{a2,HAB} = \frac{[HAB][H^+]}{[HABH^+]} \quad (21)$$

Mass balance on $[AB]_T$:

$$[AB]_T = [HAB] + [A^-B] + [HABH^+] \quad (22)$$

Using equilibrium constants to substitute into equation (22):

$$[AB]_T = \frac{K_{sp}}{[R]^2}\left(1 + \frac{K_{a1,HAB}}{[H^+]} + \frac{[H^+]}{K_{a2,HAB}}\right) \quad (23)$$

Mass balance on $[R]_T$:

$$[R]_T = [R] \quad (24)$$

Substituting equation (24) into equation (23):

$$[AB]_T = \frac{K_{sp}}{[R]_T^2}\left(1 + \frac{K_{a1,HAB}}{[H^+]} + \frac{[H^+]}{K_{a2,HAB}}\right) \quad (25)$$

For a 2:1 cocrystal, $S_{cocrystal} = [A]_T = \frac{1}{2}[R]_T$, and therefore, equation (25) can be rewritten as:

$$S_{cocrystal} = \sqrt[3]{\frac{K_{sp}}{4}\left(1 + \frac{K_{a1,HAB}}{[H^+]} + \frac{[H^+]}{K_{a2,HAB}}\right)} \quad (26)$$

Equation (25) can be rewritten specifically at the transition concentration, C_{tr}, as:

$$[AB]_{tr} = \frac{K_{sp}}{[R]_{tr}^2}\left(1 + \frac{K_{a1,H_2A}}{[H^+]} + \frac{[H^+]}{K_{a2,HAB}}\right) \quad (27)$$

1:1 cocrystal with basic API and acidic ligand

$B\text{-}HA_{solid} \rightleftharpoons B_{soln} + HA_{soln}$

$$K_{sp} = [B][HA] \quad (28)$$

$$HA \rightleftharpoons A^- + H^+$$

$$K_{a,HA} = \frac{[H^+][A^-]}{[HA]} \tag{29}$$

$$BH^+ \rightleftharpoons B + H^+$$

$$K_{a,B} = \frac{[H^+][B]}{[BH^+]} \tag{30}$$

Mass balance on $[A]_T$:

$$[A]_T = [HA] + [A^-] \tag{31}$$

Using equilibrium constants to substitute into equation (31):

$$[A]_T = \frac{K_{sp}}{[B]}\left(1 + \frac{K_{a,HA}}{[H^+]}\right) \tag{32}$$

Mass balance on $[B]_T$:

$$[B]_T = [B] + [BH^+] \tag{33}$$

$$[B]_T = [B]\left(1 + \frac{[H^+]}{K_{a,B}}\right) \tag{34}$$

$$[B] = \frac{[B]_T}{\left(1 + \frac{[H^+]}{K_{a,B}}\right)} \tag{35}$$

Substituting equation (35) into equation (32):

$$[A]_T = \frac{K_{sp}}{[B]_T}\left(1 + \frac{[H^+]}{K_{a,B}}\right)\left(1 + \frac{K_{a,HA}}{[H^+]}\right) \tag{36}$$

For a 1:1 cocrystal, $S_{cocrystal} = [A]_T = [B]_T$

$$S_{cocrystal} = \sqrt{K_{sp}\left(1 + \frac{K_{a,HA}}{[H^+]}\right)\left(1 + \frac{[H^+]}{K_{a,B}}\right)} \tag{37}$$

Equation (36) can be rewritten specifically at the transition concentration, C_{tr}, as:

$$[A]_{tr} = \frac{K_{sp}}{[B]_{tr}}\left(1+\frac{[H^+]}{K_{a,B}}\right)\left(1+\frac{K_{a,HA}}{[H^+]}\right) \tag{38}$$

Because, $[B]_{tr} = S_B$ at the transition concentration, $[B]_{tr}$ is expressed as:

$$[B]_{tr} = [B]_o\left(1+\frac{[H_+]}{K_{a,2}}\right) \tag{39}$$

Therefore, equation (38) is rearranged to give:

$$[A]_{tr} = \frac{K_{sp}}{[B]_o}\left(1+\frac{K_{a,1}}{[H^+]}\right) \tag{40}$$

2:1 cocrystal with basic API and diprotic acidic ligand

$B_2\text{-}H_2A_{solid} \rightleftharpoons 2B_{soln} + H_2A_{soln}$

$$K_{sp} = [B]^2[HA] \tag{41}$$

$H_2A \rightleftharpoons HA^- + H^+$

$$K_{a1,H_2A} = \frac{[H^+][HA^-]}{[H_2A]} \tag{42}$$

$HA^- \rightleftharpoons A^{2-} + H^+$

$$K_{a2,H_2A} = \frac{[H^+][A^{2-}]}{[HA^-]} \tag{43}$$

$BH^+ \rightleftharpoons B + H^+$

$$K_{a,B} = \frac{[H^+][B]}{[BH^+]} \tag{44}$$

Mass balance on $[A]_T$:

$$[A]_T = [H_2A] + [HA^-] + [A^{2-}] \tag{45}$$

Using equilibrium constants to substitute into equation (44):

$$[A]_T = \frac{K_{sp}}{[B]^2}\left(1 + \frac{K_{a1,H_2A}}{[H^+]} + \frac{K_{a1,H_2A}K_{a2,H_2A}}{[H^+]^2}\right) \tag{46}$$

Mass balance on $[B]_T$:

$$[B]_T = [B] + [BH^+] \tag{47}$$

$$[B]_T = [B]\left(1 + \frac{[H^+]}{K_{a,B}}\right) \tag{48}$$

$$[B] = \frac{[B]_T}{\left(1 + \frac{[H^+]}{K_{a,B}}\right)} \tag{49}$$

Substituting equation (49) into equation (46):

$$[A]_T = \frac{K_{sp}}{[B]_T^2}\left(1 + \frac{[H^+]}{K_{a,B}}\right)^2\left(1 + \frac{K_{a1,H_2A}}{[H^+]} + \frac{K_{a1,H_2A}K_{a2,H_2A}}{[H^+]^2}\right) \tag{50}$$

For a 2:1 cocrystal, $S_{cocrystal} = [A]_T = \frac{1}{2}[B]_T$, and therefore, equation (50) can be rewritten as:

$$S_{cocrystal} = \sqrt[3]{\frac{K_{sp}}{4}\left(1 + \frac{K_{a,1}}{[H^+]} + \frac{K_{a1,H_2A}K_{a2,H_2A}}{[H^+]^2}\right)\left(1 + \frac{[H^+]}{K_{a,B}}\right)^2} \tag{51}$$

Equation (50) can be rewritten specifically at the transition concentration, C_{tr}, as:

$$[A]_{tr} = \frac{K_{sp}}{[B]_{tr}^2}\left(1 + \frac{[H^+]}{K_{a,B}}\right)^2\left(1 + \frac{K_{a1,H_2A}}{[H^+]} + \frac{K_{a1,H_2A}K_{a2,H_2A}}{[H^+]^2}\right) \tag{52}$$

Because $[B]_{tr} = S_B$ at the transition concentration, $[B]_{tr}$ is expressed as:

$$[B]_{tr} = [B]_o\left(1+\frac{[H_+]}{K_{a,B}}\right) \tag{53}$$

Therefore, equation (52) is rearranged to give:

$$[A]_{tr} = \frac{K_{sp}}{[B]_o^2}\left(1+\frac{K_{a1,H_2A}}{[H^+]}+\frac{K_{a1,H_2A}K_{a2,H_2A}}{[H^+]^2}\right) \tag{54}$$

1:1 cocrystal with amphoteric API and acidic ligand

$HAB\text{-}HX_{solid} \rightleftharpoons HAB_{soln} + HX_{soln}$

$$K_{sp} = [HAB][HX] \tag{55}$$

$HAB \rightleftharpoons {}^{-}AB + H^+$

$$K_{a1,HAB} = \frac{[H^+][^{-}AB]}{[HAB]} \tag{56}$$

$HABH^+ \rightleftharpoons HAB + H^+$

$$K_{a2,HAB} = \frac{[H^+][HAB]}{[HABH^+]} \tag{57}$$

$HX \rightleftharpoons X^- + H^+$

$$K_{a,HX} = \frac{[H^+][X^-]}{[HX]} \tag{58}$$

Mass balance on $[AB]_T$:

$$[AB]_T = [HAB] + [^{-}AB] + [HABH^+] \tag{59}$$

Using equilibrium constants to substitute into equation (59):

$$[AB]_T = \frac{K_{sp}}{[HX]}\left(1+\frac{K_{a1,HAB}}{[H^+]}+\frac{[H^+]}{K_{a2,HAB}}\right) \tag{60}$$

Mass balance on $[X]_T$:

$$[X]_T = [HX] + [X^-] \tag{61}$$

$$[X]_T = [HX]\left(1 + \frac{K_{a,HX}}{[H^+]}\right) \tag{62}$$

$$[HX] = \frac{[X]_T}{\left(1 + \frac{K_{a,HX}}{[H^+]}\right)} \tag{63}$$

Substituting equation (63) into equation (60):

$$[AB]_T = \frac{K_{sp}}{[X]_T}\left(1 + \frac{K_{a,HX}}{[H^+]}\right)\left(1 + \frac{K_{a1,HAB}}{[H^+]} + \frac{[H^+]}{K_{a2,HAB}}\right) \tag{64}$$

For a 1:1 cocrystal, $S_{cocrystal} = [AB]_T = [X]_T$

$$S_{cocrystal} = \sqrt{K_{sp}\left(1 + \frac{K_{a,HX}}{[H^+]}\right)\left(1 + \frac{K_{a1,HAB}}{[H^+]} + \frac{[H^+]}{K_{a2,HAB}}\right)} \tag{65}$$

Equation (64) can be rewritten specifically at the transition concentration, C_{tr}, as:

$$[AB]_{tr} = \frac{K_{sp}}{[X]_{tr}}\left(1 + \frac{K_{a,HX}}{[H^+]}\right)\left(1 + \frac{K_{a1,HAB}}{[H^+]} + \frac{[H^+]}{K_{a2,HAB}}\right) \tag{66}$$

Because, $[AB]_{tr} = S_{AB}$ at the transition concentration, $[AB]_{tr}$ is expressed as:

$$[AB]_{tr} = [AB]_o\left(1 + \frac{K_{a1,HAB}}{[H^+]} + \frac{[H^+]}{K_{a2,HAB}}\right) \tag{67}$$

Therefore, equation (66) is rearranged to give:

$$[X]_{tr} = \frac{K_{sp}}{[AB]_o}\left(1 + \frac{K_{a,HX}}{[H^+]}\right) \tag{68}$$

References

Avdeef, A. (2003). *Absorption and Drug Development: Solubility, Permeability, and Charge State*. New York, John Wiley & Sons.

Bak, A., A. Gore, et al. (2008). "The co-crystal approach to improve the exposure of a water insoluble compound: AMG 517 sorbic acid cocrystal characterization and pharmacokinetics." *Journal of Pharmaceutical Sciences* **97**: 3942-3956.

Bergstrom, C., K. Luthman, et al. (2004). "Accuracy of calculated pH-dependent aqueous drug solubility." *European Journal of Pharmaceutical Sciences* **22**: 387-398.

Childs, S. L., L. J. Chyall, et al. (2004). "Crystal Engineering Approach to Forming Cocrystals of Amine Hydrochlorides with Organic Acids. Molecular Complexes of Fluoxetine Hydrochloride with Benzoic, Succinic, and Fumaric Acids." *Journal of the American Chemical Society* **126**: 13335-13342.

Childs, S. L. and K. I. Hardcastle (2007). "Cocrystals of piroxicam with carboxylic acids." *Crystal Growth & Design* **7**: 1291-1304.

Childs, S. L., N. Rodríguez-Hornedo, et al. (2008). "Screening strategies based on solubility and solution composition generate pharmaceutically acceptable cocrystals of carbamazepine." *Crystal Engineering Communications* **10**: 856-864.

Fleischman, S. G., S. S. Kuduva, et al. (2003). "Crystal Engineering of the Composition of Pharmaceutical Phases: Multiple-Component Crystalline Solids Involving Carbamazepine." *Crystal Growth & Design* **3**: 909-919.

Good, D. J. and N. Rodríguez-Hornedo (2008). "True solubility advantage of cocrystals: measurement, relationships, and pharmaceutical implications." *Crystal Growth & Design* (in press).

Hickey, M. B., M. L. Peterson, et al. (2006). "Performance comparison of a co-crystal of carbamazepine with marketed product." *European Journal of Pharmaceutical Sciences* **67**: 112-119.

Howard, J. R. and P. L. Gould (1987). "Drug Release from Thermosetting Fatty Vehicles Filled into Hard Gelatin Capsules." *Drug Development and Industrial Pharmacy* **13**: 1031-1045.

Jayasankar, A., L. S. Reddy, et al. (2008). "The Role of Cocrystal and Solution Chemistry on the Formation and Stability of Cocrystals with Different Stoichiometry." *Crystal Growth & Design* (in press).

Lukacs, M., G. Barcsa, et al. (1998). "The effects of pH, ionic strength and buffer concentration of mobile phase on RF of acidic compounds in ion-pair TLC." *Chromatographia* **48**: 511-516.

McNamara, D. P., S. L. Childs, et al. (2006). "Use of a glutaric acid cocrystal to improve oral bioavailability of a low solubility API." *Pharmaceutical Research* **23**: 1888-1897.

Nehm, S., B. Rodríguez-Spong, et al. (2006). "Phase Solubility Diagrams of Cocrystals Are Explained by Solubility Product and Solution Complexation." *Crystal Growth & Design* **6**: 592-600.

Nehm, S., K. F. Seefeldt, et al. (2005). "Phase Diagrams to Predict Solubility and Crystallization of Cocrystals." *The AAPS Journal* **7**: Abstract W4235.

Reddy, L. S., S. J. Bethune, et al. (2009). "Cocrystals and Salts of Gabapentin: pH dependent cocrystal stability and solubility." *Crystal Growth & Design* **9**: 378-385.

Remenar, J. F., S. L. Morissette, et al. (2003). "Crystal Engineering of Novel Cocrystals of a Triazole Drug with 1,4-Dicarboxylic Acids." *Journal of the American Chemical Society* **125**: 8456-8457.

Rodríguez-Hornedo, N. and D. Murphy (2004). "Surfactant-facilitated crystallization of dihydrate carbamazepine during dissolution of anhydrous polymorph." *Journal of Pharmaceutical Sciences* **93**: 449-460.

Serajuddin, A. T. M. (2007). "Salt formation to improve drug solubility." *Advanced Drug Delivery Reviews* **59**: 603-616.

Shiraki, K., N. Takata, et al. (2008). "Dissolution Improvement and the Mechanism of the Improvement from Cocrystallization of Poorly Water-soluble Compounds." *Pharmaceutical Research* **25**: 2581-2592.

Tian, F., N. Sandler, et al. (2006). "Visualizing the conversion of carbamazepine in aqueous suspension with and without the presence of excipients: A single crystal study using SEM and Raman microscopy." *European Journal of Pharmaceutics and Biopharmaceutics* **64**: 326-335.

Tian, F., D. J. Saville, et al. (2007). "The influence of various excipients on the conversion kinetics of carbamazepine polymorphs in aqueous suspension." *Journal of Pharmacy and Pharmacology* **59**: 193-210.

Trask, A. V., W. D. S. Motherwell, et al. (2005). "Pharmaceutical Cocrystallization: Engineering a Remedy for Caffeine Hydration." *Crystal Growth & Design* **5**: 1013-1021.

Williamson, D. S., D. L. Nagel, et al. (1987). "Effect of pH and ions on the electronic structure of saccharin." *Food and Chemical Toxicology* **25**: 211-218.

Yalkowsky, S. H. (1999). *Solubility and Solubilization in Aqueous Media*. New York, Oxford University Press.

CHAPTER SIX

PH-DEPENDENT SOLUBILITY OF GABAPENTIN-3-HYDROXYBENZOIC ACID COCRYSTAL

Introduction

A series of gabapentin (GBP) cocrystals and salts were discovered using the reaction crystallization method (Reddy, Bethune et al. 2009). Thirteen carboxylic acids were chosen as coformers. Table 6.1 includes the five multi-component crystals for which their crystal structure was solved.

Table 6.1. New multi-component crystals of gabapentin obtained by reaction crystallization with various carboxylic acid coformers.

Coformer	Multi-component crystal	Stoichiometry
3-hydroxybenzoic acid	cocrystal	1:1
4-hydroxybenzoic acid	disordered	1:1
salicylic acid	salt	1:1
1-hydroxy-2-naphthoic acid	salt	1:1
RS-mandelic acid	salt	1:1

This brief chapter discusses the pH-dependent solubility of the 1:1 gabapentin-3-hydroxybenzoic acid (GBP-3HBA) cocrystal. This cocrystal represents a unique case in that gabapentin exists as a zwitterion in the crystal structure which is reflected in the following model.

A zwitterionic drug, such as gabapentin, is expressed as $^{-}ABH^{+}$, and the diprotic coformer is expressed as H_2X. The pK_a values for gabapentin are 3.68 for the COO^{-} group and 10.70 for the NH_3^{+} group (O'Neil, Smith et al. 2001). The pK_a values for 3-hydroxybenzoic acid are 4.06 for the carboxylic acid group and 9.92 for the hydroxyl group (Serjeant and Dempsey 1979). The equilibrium reactions for cocrystal dissociation and respective reactant ionizations (assuming no complexation in solution) are as follow:

$$^{-}ABH^{+}H_2X_{solid} \rightleftharpoons {}^{-}ABH^{+}_{soln} + H_2X_{soln}$$

$$K_{sp} = [^{-}ABH^{+}][H_2X] \quad (1)$$

$$HABH^{+} \rightleftharpoons {}^{-}ABH^{+} + H^{+}$$

$$K_{a1,^{-}ABH^{+}} = \frac{[^{-}ABH^{+}][H^{+}]}{[HABH^{+}]} \quad (2)$$

$$^{-}ABH^{+} \rightleftharpoons {}^{-}AB + H^{+}$$

$$K_{a2,^{-}ABH^{+}} = \frac{[^{-}AB][H^{+}]}{[^{-}ABH^{+}]} \quad (3)$$

$$H_2X \rightleftharpoons HX^{-} + H^{+}$$

$$K_{a1,H_2X} = \frac{[HX^{-}][H^{+}]}{[H_2X]} \quad (4)$$

$$HX^{-} \rightleftharpoons X^{2-} + H^{+}$$

$$K_{a2,H_2X} = \frac{[X^{2-}][H^{+}]}{[HX^{-}]} \quad (5)$$

where K_{sp} is the cocrystal solubility product and $K_{a1,^{-}ABH^{+}}$, $K_{a2,^{-}ABH^{+}}$, K_{a1,H_2X}, and K_{a2,H_2X} are ionization constants of reactants. The total drug concentration or analytical concentration is the sum of all the ionized species and is given by

$$[AB]_T = [^{-}ABH^{+}] + [HABH^{+}] + [^{-}AB] \quad (6)$$

and total coformer concentration is a sum of ionized (HX^{-}, X^{2-}) and unionized (H_2X) species

$$[X]_T = [H_2X] + [HX^{-}] + [X^{2-}] \quad (7)$$

Substituting the equilibrium constants from equations (1), (2), and (3) into equation (6) gives

$$[AB]_T = \frac{K_{sp}}{[H_2X]}\left(1 + \frac{[H^+]}{K_{a1,^{-}ABH^{+}}} + \frac{K_{a2,^{-}ABH^{+}}}{[H^+]}\right) \quad (8)$$

Rewriting equation (7) to express $[H_2X]$ in terms of $[X]_T$ results in:

$$[H_2X] = \frac{[X]_T}{\left(1 + \frac{K_{a1,H_2X}}{[H^+]} + \frac{K_{a1,H_2X}K_{a2,H_2X}}{[H^+]^2}\right)} \quad (9)$$

Substituting equation (9) into equation (8) gives the total drug concentration

$$[AB]_T = \frac{K_{sp}}{[X]_T}\left(1 + \frac{[H^+]}{K_{a1,^{-}ABH^{+}}} + \frac{K_{a2,^{-}ABH^{+}}}{[H^+]}\right)\left(1 + \frac{K_{a1,H_2X}}{[H^+]} + \frac{K_{a1,H_2X}, K_{a2,H_2X}}{[H^+]^2}\right) \quad (10)$$

For a 1:1 cocrystal, cocrystal solubility equals total drug or total coformer concentration:

$S_{cocrystal} = [AB]_T = [X]_T$

Therefore, cocrystal solubility is expressed as:

$$S_{cocrystal} = \sqrt{K_{sp}\left(1 + \frac{[H^+]}{K_{a1,^{-}ABH^{+}}} + \frac{K_{a2,^{-}ABH^{+}}}{[H^+]}\right)\left(1 + \frac{K_{a1,H_2X}}{[H^+]} + \frac{K_{a1,H_2X}K_{a2,H_2X}}{[H^+]^2}\right)} \quad (11)$$

Equation (11) indicates solubility of a cocrystal with a zwitterionic drug and acidic coformer is dependent on K_{sp}, pK_a values of both cocrystal components, and solution pH. If K_{sp} is known, one can calculate the solubility of cocrystal ($S_{cocrystal}$) at any given pH. Alternatively, if cocrystal solubility is know at given pH, K_{sp} can be calculated from equation (11).

Because cocrystal and drug stability are critical to predict transformations during all stages of drug development, the solubility product is important to generate a phase solubility diagram (PSD) which can reveal the regions of stability for single and multiple component crystals. For cocrystals that incongruently dissolve and will convert to either single component in pure solvent, calculating the solubility product can be done in two ways: (1) measuring cocrystal solubility dependence on coformer concentration under conditions which the cocrystal is the thermodynamically stable phase, or (2) measuring the transition concentration at a single (or multiple) pH value(s) for aqueous solutions or organic solvents, providing the cocrystal K_{sp} in the respective solvents. Method 1 has been proven for carbamazepine-succinic acid (Childs, Rodríguez-Hornedo et al. 2008) in water, carbamazepine-4-aminobenzoic acid in ethanol (Jayasankar, Reddy et al. 2008), and carbamzepine-nicotinamide in ethanol (Nehm, Rodríguez-Spong et al. 2006). Method 2 has been proven for a variety of carbamazepine, theophylline, and caffeine cocrystals (Good and Rodríguez-Hornedo 2008).

For cocrystals that congruently dissolve over a particular pH range, conversion to single component will not occur in pure solvent. Therefore, measuring solubility dependence on pH can directly lead to the K_{sp} using equation (11). This is the method employed for the GBP-3HBA.

Materials and Methods

Gabapentin and 3-hydroxybenzoic acid were purchased from Spectrum Chemicals and Adrich Chemicals, respectively. The reaction crystallization method was used to synthesize GBP-3HBA. Solubility studies were performed by slurrying excess GBP-3HBA in water at room temperature. Solution pH was adjusted by adding either 1M hydrochloric acid or 1M sodium hydroxide. Time points were taken at 72 and 96 hours to confirm that equilibrium was attained. Resulting solids were isolated and analyzed by XRPD. Aliquots were diluted approximately 500-1000 times to be analyzed by HPLC. Because GBP-3HBA is a 1:1 cocrystal, solubility of the cocrystal is equal to either the gabapentin or 3-hydroxybenzoic acid concentration. HPLC was used to analyze 3-hydroxybenzoic acid solution concentration with a Waters system (Bedford, MA) equipped with a photodiode array UV/Vis detector. A 45% water/55% methanol with 0.1% trifluoroacetic acid mobile phase was used to flow at 1mL/min through an Atlantis C18 column (Waters, Bedford, MA). 3-hydroxybenzoic acid was analyzed at 272nm.

Results and Discussion

The solubility of GBP-3HBA was measured as a function of pH (Table 6.2). The solubility was also measured at pH 2.6, but conversion from the cocrystal to 3-hydroxybenzoic acid occurred, so this measurement was not used in the following analysis. This indicates though that the stability of the coformer is important to consider in addition to the drug and cocrystal. No conversion occurred at other pH values studied.

Table 6.2. pH-dependent solubility of gabapentin-3-hydroxybenzoic acid

pH	solubility (M)
4.0	0.117
4.9	0.307
5.3	0.579
5.7	0.797

Figure 6.1 shows how the K_{sp} for GBP-3HBA was calculated. If transformation does not occur and equilibrium solubility measurements can be taken for a cocrystal, the K_{sp} can be calculated from convenient solubility experiments using equation 11. The intercept was not statistically significant from zero, so therefore the plot was forced through the origin. The K_{sp} for GBP-3HBA was estimated to be 0.0145 (±0.0009) M^2.

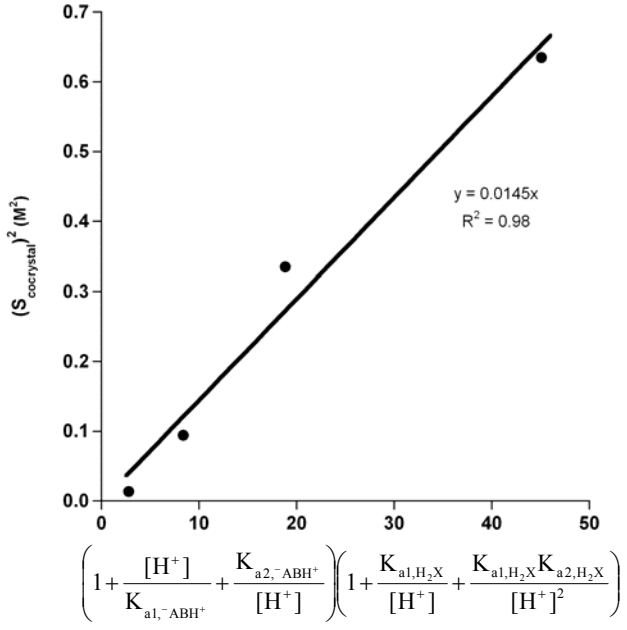

Figure 6.1. Calculation of gabapentin-3HBA cocrystal K_{sp} according to equation (11) using measured cocrystal solubility as a function of pH. Slope is the K_{sp}.

Figure 6.2 shows GBP-3HBA solubility as a function of pH including the predicted solubility curve using the K_{sp} from Figure 6.1. Figure 6.2 shows that the experimentally measured solubilities of gabapentin-3HBA cocrystal are in good agreement with the predicted solubility from equation 11. The model predicts a minimum cocrystal solubility at a pH between the two pK_a values of the components (3.68 and 4.06).

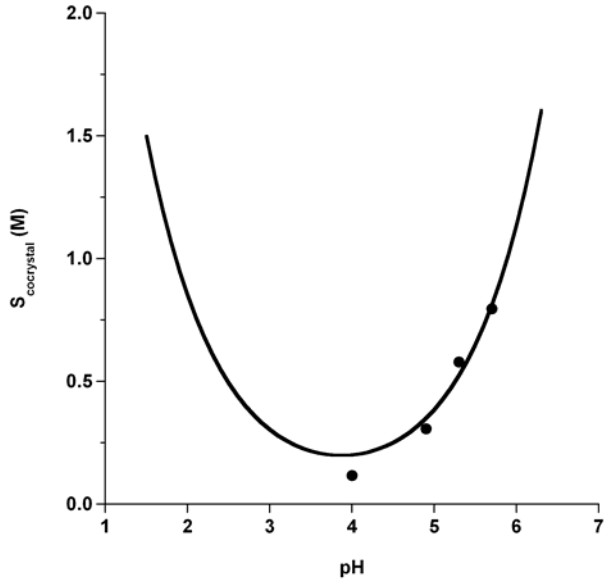

Figure 6.2. GBP-3HBA solubility dependence on pH. Symbols represent experimental data from Table 6.1. Predicted solubility curve has been generated using the K_{sp} from Figure 6.1.

A solubility-pH plot for all three phases (cocrystal, gabapentin, and 3HBA) is valuable to predict phase stability and transformations. Because accurate values of 3-hydroxybenzoic acid and gabapentin solubility dependence on pH could not be obtained from literature, the solubility of each species was calculated at a single pH. Gabapentin solubility was approximately 150 mg/mL (0.88 M) at pH 7.3. 3-hydroxybenzoic acid solubility was approximately 8 mg/mL (0.06 M) at pH 2.8. The Henderson-Hasselbalch

relationship was used to calculate the intrinsic solubility of each species, and from this, their solubility dependence on pH was calculated. Figure 6.3 shows the pH-dependent solubility for all three phases. Solid lines represent the pH range over which the respective component is predicted to be thermodynamically stable. Dashed lines represent component solubility and pH ranges over which the respective component may transform to the most thermodynamically stable phase.

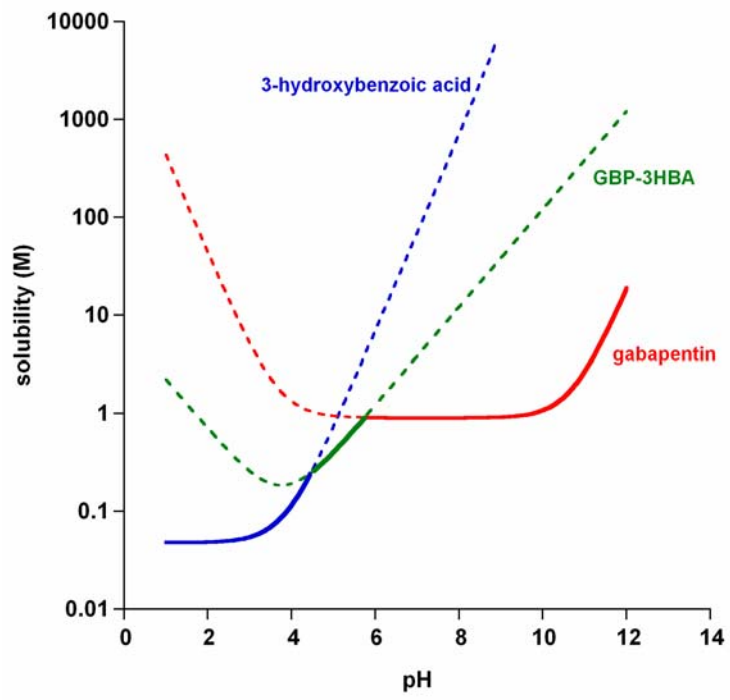

Figure 6.3. pH-dependent solubility of GBP-3HBA cocrystal and the individual components of drug and coformer.

The cocrystal solubility and component solubilities plotted in Figure 6.3 provide reasonable estimates of the cocrystal stability. Gabapentin-3HBA cocrystal is predicted to be the most thermodynamically stable phase between pH 4.7 and 5.8, however solubility studies indicated that the cocrystal was stable at pH 4.0. The lack of agreement

at pH 4.0 between predicted and experimental solubility and stability may be due to slow transformation kinetics or transformation levels below the detection limit of XRPD. The role of solute activity on the accuracy of predicted solubilities using the Henderson-Hasselbalch equation has not been considered in this study but has been reported to be important in the case of cationic drugs (Bergstrom, Luthman et al. 2004).

Because cocrystal is the most thermodynamically stable phase between pH 4.7 and 5.8, gabapentin-3HBA can be synthesized from aqueous solutions in this pH range. At pH values higher than 5.8, the solution pH was determined by solute concentrations and could not be controlled independently. Therefore, experimental solubility measurements are not reported at pH values higher than 5.8.

Conclusions

A theoretical model describing cocrystal solubility dependence on pH and pK_a has been presented for a unique cocrystal type. Gabapentin-3-hydroxybenzoic acid is a 1:1 cocrystal in which gabapentin exists as a zwitterion in the crystal structure but the coformer remains unionized. pH-dependent solubility experiments between approximately pH 4 and 5.7 allowed for the estimation of the cocrystal solubility product. Cocrystal solubility was also compared to gabapentin and 3-hdyroxybenzoic acid solubility, which revealed regions of stability for the single and multi-component species.

References

Bergstrom, C., K. Luthman, et al. (2004). "Accuracy of calculated pH-dependent aqueous drug solubility." *European Journal of Pharmaceutical Sciences* **22**: 387-398.

Childs, S. L., N. Rodríguez-Hornedo, et al. (2008). "Screening strategies based on solubility and solution composition generate pharmaceutically acceptable cocrystals of carbamazepine." *Crystal Engineering Communications* **10**: 856-864.

Good, D. J. and N. Rodríguez-Hornedo (2008). "True solubility advantage of cocrystals: measurement, relationships, and pharmaceutical implications." *Crystal Growth & Design* (in press).

Jayasankar, A., L. S. Reddy, et al. (2008). "The Role of Cocrystal and Solution Chemistry on the Formation and Stability of Cocrystals with Different Stoichiometry." *Crystal Growth & Design* (in press).

Nehm, S., B. Rodríguez-Spong, et al. (2006). "Phase Solubility Diagrams of Cocrystals Are Explained by Solubility Product and Solution Complexation." *Crystal Growth & Design* **6**: 592-600.

O'Neil, M., A. Smith, et al., Eds. (2001). *The Merck Index, 13th edition*, Merck & Co. Inc.

Reddy, L. S., S. J. Bethune, et al. (2009). "Cocrystals and Salts of Gabapentin: pH dependent cocrystal stability and solubility." *Crystal Growth & Design* (published online Dec 2008).

Serjeant, E. P. and B. Dempsey (1979). *Ionization Constants of Organic Acids in Aqueous Solution*. Oxford, Pergamon.

CHAPTER SEVEN

CONCLUSIONS AND FUTURE WORK

This dissertation has focused on the thermodynamic and kinetic parameters that explain crystallization and solubility of cocrystals. The specific objectives of this research were (1) to develop theoretical models that explain cocrystal solubility through cocrystal and solution chemistry, (2) to predict solubility and stability behavior of cocrystals and to direct transformations to or from cocrystal, (3) to develop an efficient and scalable cocrystal synthesis method that could also be used for cocrystal screening, and (4) to develop theoretical models that predict pH-dependent solubility and stability of cocrystals.

Carbamazepine-nicotinamide and carbamazepine-saccharin solubility decreased with increasing coformer concentration in organic solvents, demonstrating that cocrystals follow solubility product behavior. Overall cocrystal solubility increased in the presence of solution complexation. Both solubility product and complexation constants were measured from solubility studies. Graphical representation of the cocrystal solubility dependence on coformer concentration can serve as a diagnostic tool for the stoichiometry of solution complexes. For a 1:1 cocrystal solubility is increased by a constant value, the product of K_{sp} and K_{11} when there is 1:1 solution complexation, and cocrystal solubility goes through a minimum value when there are 1:1 and 1:2 solution complexes. Other carbamazepine cocrystals currently studied in our lab have

demonstrated this minimum value, suggesting that higher order complexes exist in solution. A 1:1 solution complex formed between carbamazepine and nicotinamide in 2-propanol and ethyl acetate and between carbamazepine and saccharin in 2-propanol. Complex formation was shown to be related to solubility of components. Complexation was observed in solvents in which individual components had lower solubilities than in solvents in which complexation was not observed. Therefore, higher solubilities may favor solute-solvent interactions whereas lower solubilities may favor solute-solute interactions, leading to complex formation.

Solution-mediated methods for cocrystal synthesis have the risk of crystallizing the single component phases and often a very large number of solvents and experimental conditions need to be tested. A reaction crystallization method is presented in this thesis and is based on theoretical solubility models. Cocrystal and drug solubility diagrams reveal conditions of undersaturation, saturation, and supersaturation with respect to cocrystal and/or single component crystalline phases. While crystallization will occur in supersaturated conditions, dissolution will occur in undersaturated conditions. Therefore supersaturation with respect to only cocrystal can be generated by the effect of cocrystal components on decreasing the solubility of the molecular complex to be crystallized. This new method has been successfully used in the synthesis of cocrystals, including carbamazepine, sulfadimidine, caffeine, theophylline, gabapentin, and itraconazole.

Because many cocrystal components are ionizable, the effects of pH on cocrystal solubility and stability were studied. Many cocrystals are more soluble than the single component drug, particularly at higher pH values when the drug is non-ionizable and the coformer is acidic. Therefore, measuring equilibrium solubility dependence on pH

cannot be achieved due to phase transformations. The transition concentration represents an equilibrium point on the phase diagram in which cocrystal solubility equals drug solubility. Measuring the transition concentration dependence on pH allowed for the calculation of the cocrystal solubility dependence on pH in pure solvent. Carbamazepine-saccharin, carbamazepine-salicylic acid, and carbamazepine-4-aminobenzoic acid cocrystals were more soluble than carbamazepine dihydrate at all pH values studied. Therefore, cocrystal solubility dependence on pH was estimated from measuring the transition concentration dependence on pH. Another cocrystal, gabapentin-3-hydroxybenzoic acid, was less soluble than the single components within a particular pH range which allowed for direct measurements of equilibrium solubility. Experimental transition concentrations or solubility measurements followed predicted trends based on the type of cocrystal studied (i.e. cocrystal stoichiometry and ionization properties of components).

Theoretical models have also been presented for a variety of cocrystals with different stoichiometries and ionization properties. Although the first goal was to impart pH-dependent solubility and dissolution to a non-ionizable drug, and therefore three carbamazepine cocrystals were chosen to study, additional studies to confirm some of the other models would be a pragmatic future project. For example, itraconazole can achieve higher solubilities and faster dissolution rates at low pH values since it is a weak base. However, a cocrystal of itraconazole with an acidic ligand such as tartaric acid, succinic acid, or malic acid could theoretically achieve high solubilities and fast dissolution rates at low and high pH values and a minimum solubility between the pK_a values of the components.

If the solubility of a cocrystal can increase the concentration of drug in solution, possible phase transformations not only need to be predicted but also prevented. A study was done to show that supersaturation could be maintained during carbamazepine-saccharin powder dissolution at pH 7 in the presence of 1% HPC. Future work surrounding the use of polymers to sustain drug concentrations needs to be explored. Other polymers, such as hydroxypropylmethylcellulose, have been shown to slow the transformation of drugs throughout the literature, particularly carbamazepine. Current studies are ongoing to determine which polymers can slow transformations from cocrystal to single component drug for a variety of cocrystals and to study the interactions between the polymer and drug molecules.

Theoretical models that predict cocrystal solubility as a function of either complexation or ionization are presented in this thesis. A logical next step is to develop models that that incorporate both solution complexation and ionization.

If a cocrystal is to be selected for pharmaceutical development, bioavailability studies need to be performed. Three cocrystals have been reported in the literature where higher plasma concentrations were achieved in dogs and rats when the cocrystal was dosed compared to the single component drug. This thesis has shown that high theoretical cocrystal solubilities can be achieved which may ultimately lead to increases in bioavailability. Formulations should be developed that can maintain supersaturation to achieve desired blood levels. Also, if a cocrystal is to make it successfully to market, a robust synthesis method needs to be employed to perform large-scale manufacturing. The reaction crystallization method is theoretically based and has been proven to be a reliable method for cocrystal synthesis, yet it still needs to be tested on much larger

scales. Over the past five years, research surrounding cocrystals has revealed that they can be used to tailor pharmaceutical properties. Large families of cocrystals being designed and continued research may enable one to select a cocrystal with desired pharmaceutical properties.